Università degli Studi di Milano

Department of Biomedical Sciences for Health

PhD course in Integrated Biomedical Research

XXXI cycle

PhD thesis

Computed tomography and magnetic resonance imaging for the study of congenital heart diseases

PhD thesis by:

Marco ALÌ

R11265

Advisor: Prof. Francesco SARDANELLI

Co-Advisor: Dr. Francesco SECCHI

“Niente nella vita va temuto, dev’essere solamente compreso.

Ora è tempo di comprendere di più, così possiamo temere di meno.”

MARIE CURIE

Acknowledgements

First and foremost, I would like to thank Prof. Francesco Sardanelli and Dr. Francesco Secchi, who have been my mentors during these years; their teachings go way beyond the research. It was a pleasure to be their disciple.

Secondly, I would like to thank my colleagues. The results achieved during these years were also possible thanks to them. We have lived many experiences together, and with many of them we have become more than colleagues, we have become friends.

Finally, my biggest thank goes to my parents. This thesis is dedicated to my mother and my father, without which today I would not be here.

Contents

List of figures

List of tables

List of abbreviations

AAS	Ascending aortic strain
ACCESS CV	Academic Research Organization Consortium for Continuing Evaluation of Scientific Studies – Cardiovascular
BMI	Body mass index
BT	Blood-threshold
CAs	Competitive athletes
CCT	Cardiac computed tomography
CHD	Congenital heart disease
CMR	Cardiac magnetic resonance
CNR	Contrast-to-noise ratio
CoR	Coefficient of repeatability
CT	Computed tomography
CVD	Cardiovascular disease
DLP	Dose length product
DPG	2,3-diphosphoglycerate
ECG	Electrocardiographically
ED	Effective dose
EDVI	End diastolic volume index
EF	Ejection fraction
ESVI	End systolic volume index
FC	Fontan circulation
FUH	Functional univentricular heart
HCM	Hypertrophic cardiomyopathy
ICMJE	International Committee of Medical Journal Editors
IHD	Ischemic heart disease
IQR	Interquartile range
JAMA	Journal of the American Medical Association
MR	Magnetic resonance
MRS	Magnetic resonance spectroscopy
NEJM	New England Journal of Medicine
NIH	National Institutes of Health
PC	Phase contrast
PCr	Phosphocreatine

PDE	Phosphodiester
PME	Phosphomonoester
ROI	Region of interest
SD	Standard deviation
SNR	Signal-to-noise ratio
SV	Stroke volume
TE	Echo time
ToF	Tetralogy of Fallot
TPM	Trabeculae and papillary muscles
TR	Repetition time
VENC	Velocity encoding
YODA	The Yale University Open Data Access
γATP	γ-adenosine triphosphate

Summary

Background

Cardiovascular disease (CVD) is a leading cause of morbidity and mortality worldwide causing in only Europe 3.9 million deaths corresponding the 45% of total deaths [1]. In particular, among CVD, the congenital heart disease (CHD) is one of the most serious heart defect with an incidence of 8 per 1,000 live births [2].

Purpose

In recent years, the role of imaging techniques in the diagnosis and follow-up of these patients has become increasingly important due to their progressive technological advancement. This doctoral thesis shows the results that we achieved in the use of cardiac computed tomography (CCT) and cardiac magnetic resonance (CMR) examination in patients with CHD.

Section I – Cardiac computed tomography in CHD patients

In this chapter, we propose a study showing the possibility to obtain an impressively low ionizing dose reduction in pediatric CHD patients. Indeed, because the CCT can give valuable anatomic information on CHD in children but implies radiation exposure in subjects who are more radiosensitive than adult patients and that have a longer lifetime to develop stochastic effects from radiation, is very important to perform high-quality but low-dose examinations in this kind of patients. Thus, we evaluated a total of 100 pediatric CCT performed using 80, 100, or 120 kVp, showing that a high-quality pediatric CT can be performed using a 64-slice scanner, with a radiation effective dose close to 2 mSv in about 50% of the cases [3].

Section II – Heart and great vessels CMR evaluation

In this section, are shown four studies focused on the use of CMR as a non-invasive imaging tool for the morpho-functional evaluation of heart and great vessels in patients with CHD. Concerning the study of heart dysfunction we published one paper on patients with non-obstructive hypertrophic cardiomyopathy (HCM) [4] and another one on patients with functional univentricular heart (FUH)

[5]; while regarding the study of great vessels we focused on the evaluation of the aortic strain [6] and flow measurement [7] in patients with different CVD, including CHD.

The 2% HCM patients have a left ventricle wall thickness that reaches 13-15 mm, overlapped with those measured in mild forms of HCM. This overlap makes clinically relevant to differentiate athlete's heart from mild forms of non-obstructive HCM. Thus, we decide to assess the left ventricle wall thickness and the myocardial metabolism of HCM patients compared to competitive athletes (CAs) using the magnetic resonance spectroscopy (MRS). We demonstrated that at the ^{1}H-MRS there is a significant increase in myocardial lipids in HCM patients compared to competitive athletes, leading to the fact that it may be used as an additional final phase of a CMR protocol including standard morphologic and functional imaging in the differential diagnosis between HCM and athlete's heart [4].

Starting from the results of an our previous study [8] showing that the inclusion of the hypoplastic chamber during the segmentation of cine images of FC patients may result in a less accurate measurement of the ejection fraction, we decided to validated a blood-threshold (BT) segmentation method for CMR cine images in FUH patients. Thus, we successfully validated in a pool of 44 FUH patients the use of a BT technique for the segmentation of cine images observing that a high intra- and inter-reader reproducibility for the assessment of ventricular stroke volume (SV) and an excellent agreement with aortic flow values used as a benchmark. [5].

Arterial stiffness is one of the earliest manifestations of adverse structural and functional changes within the vessel wall. When the aorta is considered, stiffness is a main determinant of age-related systolic and pulse pressure increase, a major predictor of stroke and myocardial infarction, and has been associated with heart failure [9]. Previous authors showed that ascending aortic strain (AAS) measured at CMR is markedly decreased before the fifth decade of life and that can be considered as an early manifestation of vascular aging [10]. Our aim was to evaluate the AAS in 1,027 consecutive patients with different types of CVD who underwent CMR , showing that differences in age, gender, and cardiovascular disease independently affect ascending aorta strain; in particular the lower

ascending aorta strain observed in tetralogy of Fallot (ToF) fosters its assessment during follow-up in adulthood [6].

Blood flow measurements are based on the segmentation of a vessel contour that may be performed manually or, more typically, semi-automatically, with the use of computer software likely impacting on measurement reproducibility. Reader experience may play a role as well. Thus, we aimed to estimate the intra- and inter-reader reproducibility of blood flow CMR measurements through the ascending aorta and main pulmonary artery in 50 patients affected with CHD or with aortic and/or pulmonary valve disease; also investigating the impact on reproducibility of the reader's experience with CMR. Our results showed a good-to-excellent reproducibility for all variables except the backward flow of the ascending aorta, with a limited impact of operator's training [7].

Section III – To share or not to share our trial data?

In clinical research, spontaneous data sharing is not yet as common as it is in other fields such as genetics, astronomy or physics [11]. However, the concept of data sharing has been suggested for many reasons, including the patient-centred nature of medical research and healthcare and the expectation that knowledge from existing data should be maximized to benefit all stakeholders. Although a transition to data sharing is a process that will take time and planning, those who adopt the principles and practices of open science will likely benefit from it [12, 13]. In addition, the emergence of data sharing as a potential requirement by some agencies and journals warrants attention by the imaging community. Indeed, from July 1st, 2018 the International Committee of Medical Journal Editors (ICMJE) will require a data sharing statement as a condition of consideration for publication of clinical trials [14].

Thus, considering the amount of results that we collected in these three years of my PhD program, we asked ourselves about the potential advantages and disadvantages in sharing our source data with the scientific world. Our conclusions, enclosed in a paper published this year on European Radiology [15], have been discussed in this section.

Conclusions

Both imaging modalities have limitations and advantages. CMR can evaluate heart function and vessel flow but require a long acquisition time and in same patients a long sedation time. CCT has a very high spatial resolution and short acquisition time but implies ionizing radiation exposure.

This PhD thesis confirms the crucial role of CMR in functional analysis and the relevant possibilities of x-ray dose reduction in CCT, leading the foundations for future studies on the application of imaging techniques in the diagnosis and prognosis of CVD.

Section I

–

Cardiac computed tomography in CHD patients

High-quality low-dose cardiovascular computed tomography (CCT) in pediatric patients using a 64-slice scanner

Introduction

In the setting of CHD, noninvasive imaging techniques such as echocardiography, CMR, and CCT play a crucial role in the visualization of cardiovascular structures [16].

Echocardiography, being a ubiquitous and radiation free technique, represents the first approach for patients having or suspected to have CHD, but it has limitations in defining complex anatomy and reliable imaging of coronary arteries, especially in older children who have a poor acoustic window [16, 17]. CMR is considered the standard of reference for evaluation of ventricular volumes and valve regurgitation but it still usually requires relatively long imaging times and sedation or anesthesia in children aged<8 years as well as in developmentally delayed patients of all ages [18–20]. CCT and invasive angiography expose patients to ionization radiation, with potentially more dangerous effects in younger patients. A previous study demonstrated that the radiation exposure from diagnostic catheterization is substantially higher than that from CCT in a pediatric population [16].

In recent years, CCT technology has advanced rapidly. It now provides improved spatial and temporal resolution. Electrocardiographically (ECG)-gated coronary CCT can now be routinely obtained in pediatric patients with a radiation dose as low as 1.2 mSv using dual-source CCT technology [21]. Unfortunately, these scanners are still available in few centers. On the other hand, in order to reduce radiation exposure keeping a good image quality, radiologists can apply tailored protocols for CCT in pediatric patients even using 64slice scanners which are currently a kind of ‘‘standard’’ technology in radiology department.

Thus, our aim was to estimate radiation dose and image quality in pediatric CCT using a 64-slice scanner.

Material and methods

Patient population

Ethics Committee approval was obtained for this retrospective study. A total of 100 CCT exams of patients aged <18 years, performed between January 2010 and December 2016 at our Institution, were retrospectively evaluated. Disease distribution in the study population is summarized in Table 1.

Table 1: disease distribution in the study population

Disease	Patients (n)
Known or suspected coronary abnormality	
Anomalous origins	18
Coronary fistula	6
Complex congenital heart disease	
Tetralogy of Fallot	20
Transposition of great arteries	10
Truncus arteriosus	4
Aortic disease	
Stent evaluation in coarctation	18
Interrupted or hypoplastic arch	2
Pulmonary artery disease	
Pulmonary artery stenosis with stent	11
Subvalvar pulmonary stenosis	3
Major aorto-pulmonary collateral arteries in pulmonary atresia	3
Total	100

Image acquisition

At our department, all CCT studies, including those performed in pediatric patients, are performed under the direct responsibility of a cardiovascular radiologist. To minimize technical errors, technicians are carefully instructed by the radiologist on a case-by-case basis.

The CCT examinations were performed on a 64-slice computed tomography (CT) scanner (Somatom 64, Siemens Healthcare, Erlangen, Germany). Patients aged less than 3 years needed sedation. The administration of sedative drugs happened shortly before the CT exam. The anesthesiologist monitored the patient conditions during the procedure and evaluated the patient status after the exam. Midazolam was administered intravenously (dose of 0.1–1.1mg/kg), orally (dose of

0.5–0.6mg/ kg), or intramuscularly (only in one patient, dose of 0.2mg/kg). The administration route of ketamine was intravenous (dose of 0.9–1.9mg/kg) or intramuscular (dose of 3.3–5.4mg/kg). Propofol was intravenously administered at a dose of 0.5–2.4mg/kg. The variability of the administered doses depended on age, comorbidities, and known drug response of the patient.

A tailored CCT protocol was performed according to the clinical question. In the majority of patients (n=80), the unenhanced scan was waived to reduce the radiation dose. A bolus of contrast material of 5–60mL (Iopamiro 370, Bracco Imaging S.p.A., Milan, Italy) followed by saline solution in the range of 10–60mL was intravenously injected by means of a power injector (Empower CTA, EZEM, Westbury, NY, USA) at a flow rate of 1.5–3.0mL/s according to the patient's characteristics and the clinical question.

When investigating cardiac anatomy or coronary arteries, a test-bolus technique was used. A time Attenuation curve was obtained by measuring the enhancement within a region of interest (ROI) positioned in an ascending aorta or in the pulmonary trunk according to the clinical question. The contrast arrival time was determined from the time to peak enhancement and was used to estimate the scan delay for a full-bolus diagnostic CCT [22].

To acquire an angiogram, we used the bolus tracking technique, based on real-time monitoring of the main bolus during injection to acquire a series of dynamic low-dose monitoring scans at the level of the vessel of interest. The trigger threshold inside the ROI was set at 100 HU above the baseline. The delay between each monitoring scan acquisition was 1.25s. As soon as the threshold was reached, the table moved to the cranial start position. During this interval the contrast material concentration increased to the desired level of enhancement [23].

The CCT were either performed without ECG synchronization or using a prospective or a retrospective ECG-gating depending on the patient's heart rate and rhythm and on whether an evaluation of myocardial function was indicated [24]. Tube voltage was set at 80, 100, or 120kVp; tube current was set between 36 and 100mAs, according to body size. The gantry rotation time was 0.33s; pitch was 0.2–0.5. The reconstruction parameters were set as follows: section thickness=0.75mm; reconstruction interval=0.45mm; matrix size=512–512; and field of view=250mm.

Two-dimensional images were then transferred to a workstation (Multimodality, Siemens Healthcare, Erlangen, Germany) for obtaining off-line three-dimensional reconstructions.

Radiation exposure

The dose length product (DLP) was retrieved for each patient. The effective dose (ED) in mSv was calculated as DLP*k. The conversion factor for the chest, k (measured in mSv/mGy/cm), varied with age and was estimated from the International Commission on Radiological Protection publication 103 recommendation [25, 26]. The ED was then evaluated for four patient age groups (newborns<1 year, 1–5 years, 6–10 years, and 11–17 years), and according the tube voltage used (kVp).

Image quality assessment

Signal-to-noise ratio (SNR) and contrast-to-noise ratio (CNR) were calculated for each scan using the following formulas: $SNR=HU_{left\ ventricle}/SD_{air}$; $CNR= [(HU_{left\ ventricle} - HU_{myocardium})/SD_{air}]$. Assessment of subjective image quality was independently performed by two observers with eight and four years of experience in cardiovascular imaging. Image analysis was performed individually and image series were evaluated in a random order. Scans were classified using a three-level scale (3=very good; 2=good; and 1=poor). The two readers agreed on the following criteria:

- images were judged as very good when all structures were well visualized without artifacts;
- images were judged as good when almost all structures were well visualized even though some artifacts were visible;
- images were judged as poor when the vascular structures were not well visualized due to the presence of large artifacts.

Statistical analysis

Statistical analyses were performed using statistical software (SPSS for Windows v.21.0, SPSS Inc., Chicago, IL). Parametric variables were expressed as mean and standard deviation (SD), whereas non-parametric variables were expressed as median and interquartile ranges (IQR). Overall comparisons

among groups were performed using the Kruskal–Wallis test; the paired post-hoc analysis of the two groups was performed using the Mann–Whitney U test. A P value<0.05 was considered as significant.

The inter-observer agreement about the image quality qualitative assessment was evaluated using the Cohen k, with the following interpretation of the k values: <0.20=slight agreement; 0.21–0.40=fair agreement; 0.41–0.60=moderate agreement; 0.61–0.80=substantial agreement; 0.81–1.0=almost perfect agreement [27].

Results

Study population

The study population included 100 patients (63 boys, 37 girls), aged 6.9±5.4 years (mean±SD). The most common primary indications for CCT were complex CHD (n=34), pulmonary arteries abnormalities (n=22), and coronary arteries abnormalities (n=24). A detailed list of indications is provided in Table 1.

Radiation exposure

The overall median ED was 1.3 mSv (IQR=0.8–2.7mSv). Concerning the subgroup analysis, the median ED was 1.0 mSv (IQR= 0.6–1.4mSv) for exams performed at 80 kVp, 1.9 mSv (1.1–3.5mSv) for exams performed at 100 kVp, and 5.1mSv (3.6–6.0) for exams performed at 120 kVp (*P* <0.001). Post-hoc analysis is reported in Table 2.

Table 2: effective dose by tube voltage

	Effective dose (mSv)	*P* value
80 kVp (n = 49)	1.0 (0.6–1.4)	<0.001
100 kVp (n = 35)	1.9 (1.1–3.5)	
120 kVp (n = 16)	5.1 (3.6–6.0)	
80 kVp vs. 100 kVp		<0.001
80 kVp vs. 120 kVp		<0.001
100 kVp vs. 120 kVp		0.003

Examples of CCT images obtained at 80, 100, and 120kVp are shown in Figs. 1–4. Comparing not ECG-triggered, prospectively ECGtriggered, and retrospectively ECG-gated examinations, median

ED were 1.1 (0.6–3.1) mSv, 1.3 (1.0– 1.8) mSv and 1.7 (1.3–3.5) mSv, respectively (P <0.036). Post-hoc analysis is reported in Table 3.

Table 3: effective dose for not ECG-synchronized examinations, prospectively ECG-triggered examinations, and retrospectively ECG-gated examinations

	Effective dose (mSv)	*P* value
A		
Not ECG-synchronized (n = 55)	1.1 (0.6–3.1)	0.036
B		
Prospective ECG-triggering (n = 25)	1.3 (1.0–1.8)	
C		
Retrospective ECG-gating (n = 20)	1.7 (1.3–3.5)	
A vs. B		0.347
A vs. C		0.022
B vs. C		0.027

Data of effective dose are medians and interquartile ranges in parentheses. The Kruskal–Wallis test was used for the overall comparison while the Mann–Whitney U test was used for the post-hoc analysis.

Finally, a significantly different ED was also found among the age groups (P <0.001). Post-hoc analysis is reported in Table 4.

Table 4: effective dose by patient age

	Effective dose (mSv)	*P* value
A		
Newborn (n = 15)	1.0 (0.5–1.3)	<0.001
B		
1–5 years (n = 25)	0.8 (0.6–1.2)	
C		
6–10 years (n = 27)	1.6 (1.1–2.4)	
D		
11–17 years (n = 33)	3.4 (1.5–5.1)	
A vs. B		0.639
A vs. C		0.038
A vs. D		0.020
B vs. C		0.003
B vs. D		<0.001
C vs. D		0.081

Data of effective dose are medians and interquartile ranges in parentheses. The Kruskal–Wallis test was used for the overall comparison while the Mann–Whitney U test was used for the post-hoc analysis.

Figure 1: Cardiac CT of a one-month-old new born with a double outlet right ventricle

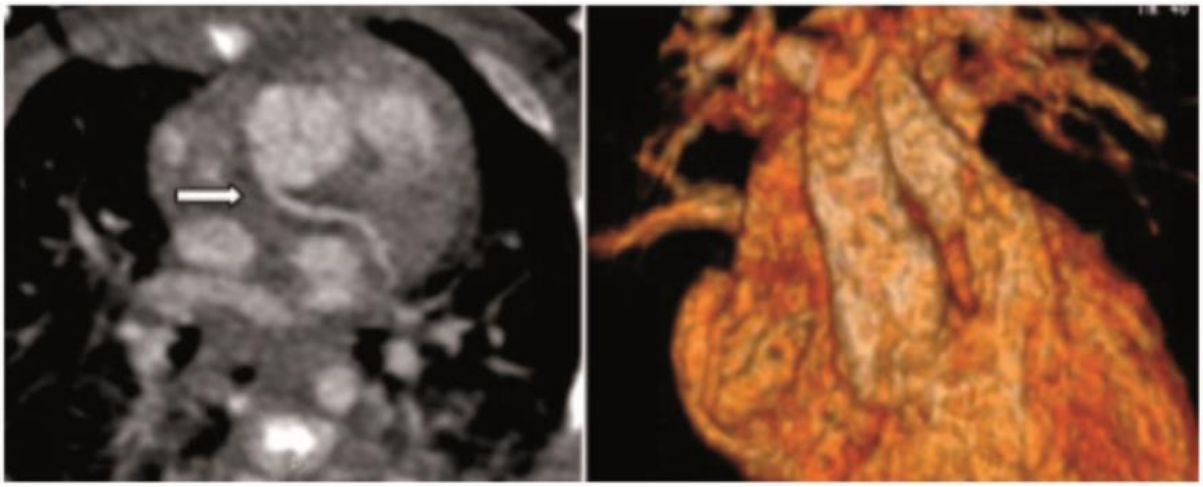

Prospectively ECG-triggered scan for the definition of coronary and intra-cardiac anatomy was performed. Effective dose was 0.3 mSv using 80 kVp. On the left panel, the abnormal origin of left main coronary artery is shown. On the right panel, a 3D reconstruction of great vessels anatomy is shown (double outlet right ventricle)

Figure 2: Cardiac CT of a two-year-old with tetralogy of Fallot with sub-pulmonary stenosis surgically treated

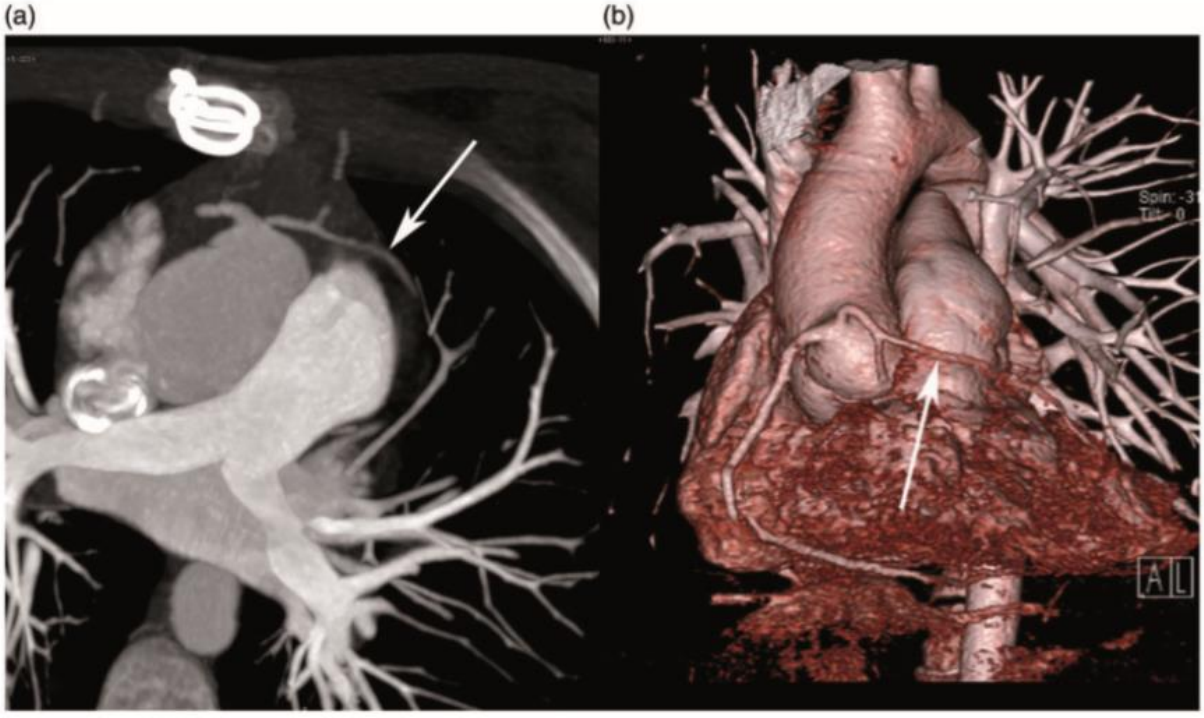

Retrospectively ECG-triggered scan for the definition of coronary and intra-cardiac anatomy was performed before a new surgical procedure. Effective dose was 1.1 mSv using 80 kVp. Anomalous left coronary origin from right sinus passed anterior of right ventricle outflow tract is shown (arrows).

Figure 3: cardiac CT of an eight-year-old girl with tetralogy of Fallot treated with a pulmonary conduit

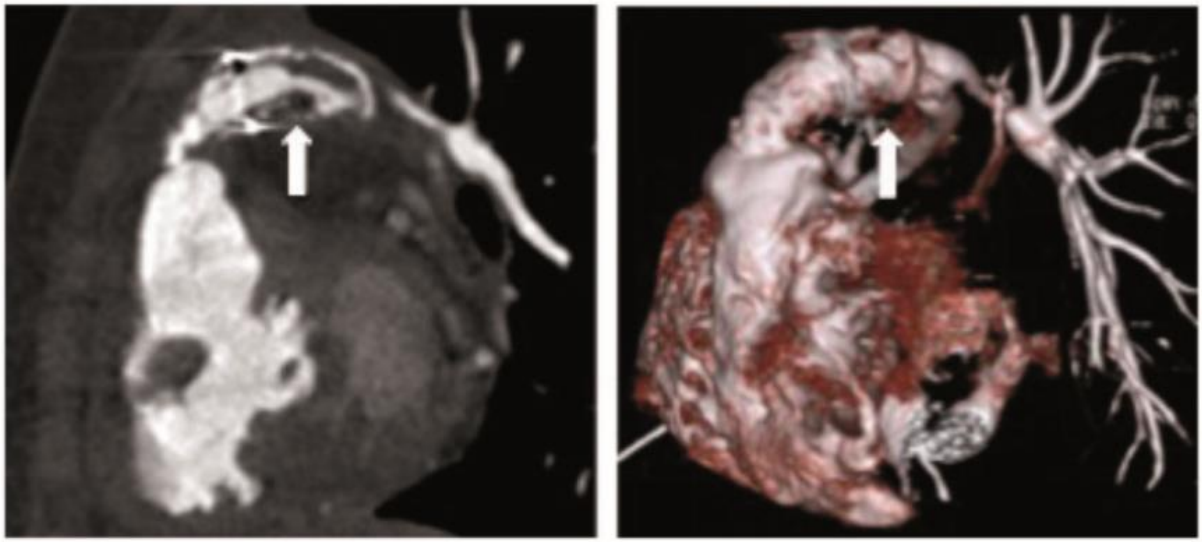

An angiographic not ECG-triggered scan was performed for evaluating pulmonary stents. Effective dose was 1.1 mSv using 100 kVp. On the left panel, a thrombosis of the pulmonary conduit due to endocarditis is shown. On the right panel, a 3D reconstruction of pulmonary conduit and pulmonary arteries is shown.

Figure 4: cardiac CT of a 14-year-old girl with tetralogy of Fallot and pulmonary stenosis.

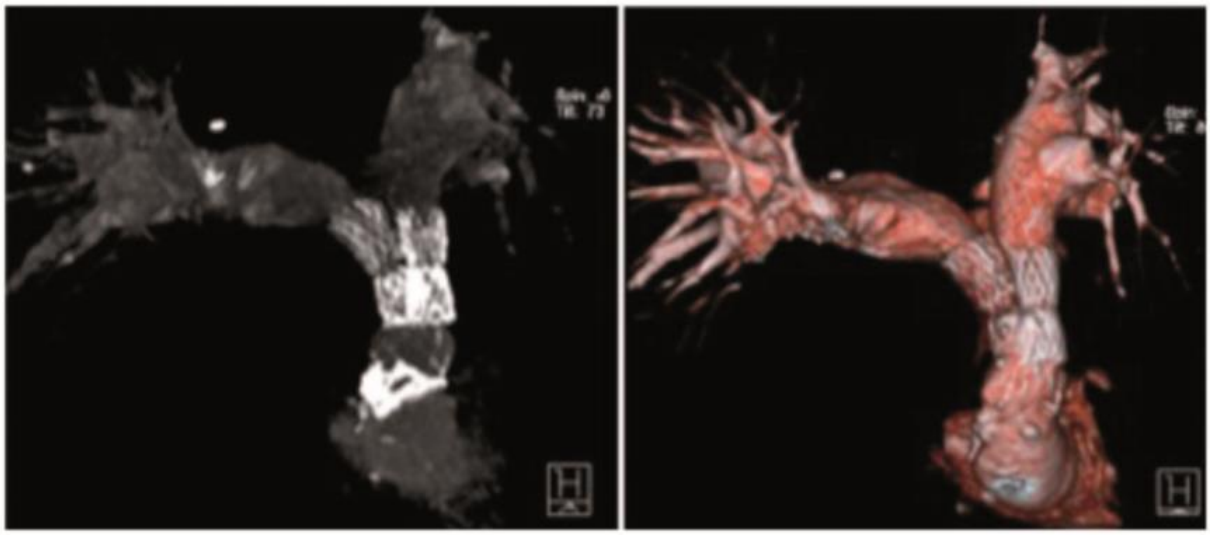

An angiographic not ECG-triggered scan was performed to evaluate pulmonary stents. The effective dose was 2 mSv using 120kVp. On the left panel, a maximum intensity projection of both stents is shown. On the right panel, a 3D reconstruction of pulmonary arteries is shown.

Image quality

Overall, the image quality was judged by the first reader (most expert) to be very good in 56 examinations (56%), good in 39 (39%), and poor in five (5%). The agreement between the two readers was almost perfect (k=0.880). A non-significant difference in terms of subjective image quality was found, both overall and among the three groups of kilovoltage used (P =0.296). In terms of objective image quality, the SNR was 30.6 (IQR=23.4–33.6), 29.4 (IQR=23.7–34.8), and 24.7 (IQR=19.4–34.3), at 120, 100, and 80 kVp, respectively (P =0.486). The median CNR was 21.0 (IQR=14.8–24.4), 19.1 (IQR=15.6–23.9), and 25.3 (IQR=19.4–33.4), at 120, 100 and 80 kVp, respectively (P =0.336). There were not significant differences according to SNR and CNR in the different age-group patients. In particular, the median of SNR was 30.5 (IQR=22.5– 36.6), 25.2 (IQR=15.1–30.9), 24.9 (IQR=20.6–41.1), and 24.4 (IQR=20.7–30.9) in newborn, 1–5, 6–10, and 11–17 age groups, respectively (P =0.227). The mean CNR was 19.4 (IQR=24.8–23.5), 20.1 (IQR=10.8–20.9), 23.3 (IQR=13.7–41.1), and 18.4 (IQR=10.7–20.8) in newborn, 1–5, 6–10, and 11–17 age groups, respectively (P =0.101).

Discussion

In this study, we assessed radiation exposure and image quality of 64-slice CCT in a consecutive series of 100 pediatric patients. Using a tailored dose-saving protocol with careful radiologist's supervision of technical performance, the overall median ED was limited to 1.3 mSv, including both prospective and retrospective ECG-triggering. Image quality was very good or good in 95/100 patients. Of note, the inter-observer reproducibility for the qualitative evaluation of image quality was almost perfect.

Our results can be favorably compared with those obtained by other authors. Tsai et al. [28] described an average ED for pediatric CCT of 2.6, 2.1, and 2.0 mSv for 16-, 64-, and 128-slice CCT, respectively, using a prospectively triggered acquisition. Conversely, the dose estimated in other studies was 6.8 mSv [25] or 12 mSv [29] using a 64-slice scan with retrospective ECG-gating.

In recent years, the advent of new generation scanners implied a drastic decrease in radiation exposure, also in the pediatric setting. The study published by Han et al. [20] analyzed a cohort of 70

pediatric patients and found an average ED of 1.7 mSv for retrospectively ECG-gated CCT and 0.9 mSv for prospectively ECG-triggered CCT. These findings highlighted the increasing role of CCT in the pediatric setting, in particular as a tool that allows to avoid diagnostic angiography or to limit or overcoming the diagnostic phase of interventional angiography. In fact, Lee et al. [30] demonstrated that in a population of 14 neonates with complex CHD referred for diagnostic cardiac catheterization after initial assessment with echocardiography and CCT, none of them required additional diagnostic imaging. This is a goal in terms of reduction of radiation dose considering the 13.4 mSv that are required on average for a diagnostic catheterization [16].

Our study showed that using a ‘‘standard’’ 64-slice scanner high-quality images can be obtained with a relatively low radiation exposure, fulfilling the diagnostic aim of the examination. This is an important clinical finding considering that 64-slice CT units remain the most available type of CT scanner in the majority of radiology departments [31–33].

Rapid technological development resulted in accelerated technical and functional obsolescence of imaging equipment, creating a need for renewal [34]. A dramatic change in this scenario, in the current era of ‘‘spending review’’ by public health systems, is not expected.

Thus, implementing CCT dose-saving protocols on 64-slice scanners should be considered as mandatory, especially in the pediatric population. Importantly, since no differences were found in terms of SNR and CNR among the different tube voltages used (120, 100, or 80 kVp), our experience suggests that an 80-kVp protocol could be adequate to image most pediatric patients.

The results in terms of CNR deserve a particular comment. Although the difference among the groups was not statistically significant, probably due to the small sample size combined with data distribution, a higher CNR at the lowest tube voltage (80 kVp) was observed (median 25.3 vs. 21.0 for 120kVp and 19.1 for 100kVp). This possible increase in CNR could be explained with the higher contrast effect of the iodinated contrast material at lower voltages [35]. Notably, the agreement in image quality evaluation between the two observers was not conditioned by the voltage used.

The approach here presented (tailored protocols under strict control by the cardiovascular radiologist) could be generally applied also to late-generation CT scanners, allowing for a lower and

lower dose exposure, in particular in the pediatric population. All these results are inverting the traditional way of thinking about the comparison between CCT and CMR in pediatric patients. Most probably, CMR will no longer be an easy winner because of being radiation-free. As radiation doses go lower and lower, towards 0.1–0.2 mSv, examination time and need for sedation, spatial resolution as well as image quality related to movement artifacts can play in favor of CCT. In addition, when considering the probability of multiple CMR examinations, the potential gadolinium accumulation in the brain should be taken into account [35].

The results of this study should be interpreted in view of its limitations. First, we should consider the retrospective study design. However, we included the whole consecutive series of pediatric patients who underwent CCT at our institution in the study period (starting from the installation of the 64-slice unit). Thus, the study reports what happened in real clinical life. Second, the number of patients is rather small as CMR is still preferred in the evaluation of CHD patients.

In conclusion, CCT is a valuable imaging modality when evaluating pediatric patients with a large spectrum of known or suspected cardiovascular abnormalities. Using dose-saving techniques, CCT protocols tailored to the pediatric population allowed for performing high-quality CCT in children with a relatively low radiation exposure also using a ‘‘standard’’ 64-slices scanner.

Section II

–

Heart and great vessels

CMR evaluation

^{1}H and ^{31}P myocardial magnetic resonance spectroscopy in non-obstructive hypertrophic cardiomyopathy patients and competitive athletes

Introduction

HCM is the most common genetic cardiac disease with a prevalence of 0.2% [36]. In half the cases, the transmission is autosomal dominant with incomplete penetration [37, 38]. The most common mutations involve sarcomere proteins, particularly C-binding myosin protein, the heavy beta-myosin chain and troponin T [39]. This disease is characterized by hypertrophy of the left ventricle, mostly asymmetric, and is usually located at the basal portion of the septum [40]. Diastolic dysfunction and outflow tract obstruction of the left ventricle may be present, causing major clinical manifestations such as angina, dyspnea, dizziness and syncope [41, 42]. In approximately 30% of HCM patients, ventricular hypertrophy is moderate without obstruction of the outflow tract of the left ventricle, both at rest and under stress and, therefore, the disease is silent [43]. In this form, the clinical onset can be the sudden death induced by rhythm disorders. Indeed, HCM was reported to be responsible for 35% of sudden deaths in young athletes [44, 45].

Competitive athletes with intense and regular training exercise usually develop cardiovascular changes leading to a reversible para physiological myocardial hypertrophy known as athlete's heart. This condition shows symmetrical and homogeneous hypertrophy, with variations in the wall thickness smaller than 2 mm [46]. In 2% of such athletes, the left ventricle wall thickness reaches 13–15 mm [47], with a distribution partially overlapped with those measured in mild forms of HCM, especially mutations of troponin T [48]. Thus, it is clinically relevant to differentiate between athlete's heart and mild forms of non-obstructive HCM.

MRS is a non-invasive diagnostic technique allowing for the in vivo evaluation of myocardial metabolism [49, 50] by measuring the signal intensity of ^{31}P or ^{1}H. In particular, with ^{31}P-MRS, the ratio between phosphocreatine (PCr) and γ-adenosine triphosphate (γATP) may be measured, representing an index of the myocardial energy reserve [38, 51–53]. On the other side, ^{1}H-MRS allows

for estimating the total creatine (Cr) (sum of PCr and Cr) [54, 55], which is associated with myocardial contractility [56, 57]; moreover, myocardial lipids may be measured using ^{1}H-MRS [58, 59].

The aim of this study was to evaluate the left ventricle function in patients affected by HCM compared with that of competitive athletes and to assess the myocardial metabolism using ^{31}P-MRS and ^{1}H-MRS in the two populations.

Materials and methods

Study design and inclusion criteria

This prospective cross-sectional study was approved by the local ethics committee and each subject signed a written informed consent. Inclusion criteria were as follows: patients aged 18 years or more with a known diagnosis of non-obstructive HCM, defined as asymmetric hypertrophy of the left ventricle, with the typical patchy pattern with local distribution of late gadolinium enhancement [47, 48]; competitive athletes aged 18 years or more, in good health, without any reported cardiovascular symptoms and with intense exercise training in the month prior to the enrollment, quantified in at least 10h per week. Exclusion criteria were contraindications to magnetic resonance such as pacemakers/defibrillators, intracranial ferromagnetic vascular clips, intraocular metal fragments, or severe claustrophobia.

Magnetic resonance imaging

Each enrolled subject underwent a 1.5-T magnetic resonance (Magnetom Sonata Maestro Class, Siemens Medical Solutions, Erlangen, Germany), including a morphologic and functional imaging study, with the patient in the supine position.

The imaging protocol included balanced steady-state free precession sequences (true fast imaging with steady-state free precession, true-FISP) using a four-channel surface phased-array coil in the short axis plane covering the entire heart. Technical parameters were as follows: ECG-gating; TR/TE 4.0/1.5 ms; flip angle 80°; slice thickness 8 mm; temporal resolution 45 ms; field of view 300 × 400

mm2; matrix 119 × 256; 30 phases in breath-hold at end expiration. The kinetic study was processed by manual segmentation using Syngo Argus software (version VE32B, Siemens Medical Solutions, Erlangen, Germany) by a radiologist with a 7-year experience in CMR imaging.

For each subject, the following imaging-derived variables were measured for the left ventricle: end diastolic thickness of the septum; end diastolic thickness of the posterior wall; mass index (i.e., normalized to the body surface area); end diastolic volume index (EDVI); end systolic volume index (ESVI); ejection fraction (EF); stroke volume; and ventricular end diastolic diameter. We have also calculated an asymmetry index, defined as the left ventricle septal-to-posterior wall thickness ratio.

^{1}H MRS

After morphologic and functional imaging, hydrogen containing metabolites were measured in a single voxel of 10 × 20 × 40 mm3 within the interventricular septum. A point-resolved spectroscopy sequence (ECG synchronization; diaphragm navigator; acquisition in the end systolic phase; TR/TE 2000/90 ms; flip angle 90°; number of excitations 150; suppression of the water signal; supine position) was performed using the same four-channel surface phased-array coil used for imaging.

A physicist with 8-year experience in MRS processed all spectra using the jMRUI software that implements the AMARES (Advanced Method for Accurate, Robust, and Efficient Spectral) algorithm quantitation [60]. Preprocessing steps were: apodization (3 Hz), manual or automatic phase correction and subtraction of the baseline with the polynomial method. The area of the two peaks attributable to Cr (3.0 and 3.9 ppm) and the that of the two peaks attributable to lipids (0.9 and 1.3 ppm) were measured and corrected for decay using T2 values published in the literature [61, 62]. The total Cr as well as the total fat was obtained summing up the two relevant components. Data were presented as arbitrary units (au).

^{31}P MRS

Myocardial phosphates were measured through ^{31}P-MRS using a dedicated surface coil tuned for ^{31}P and with the patient in the prone position. On the basis of repeated low-resolution scout images, we placed a grid of volumes of interest so as to guarantee at least one voxel within the anterior ventricular

junction, trying to minimize contamination by ventricular blood. Then, we acquired a multivoxel chemical shift imaging sequence for a single slice (nuclear Overhauser enhancement technique; ECG synchronization for acquisition in the end diastolic phase; repetition time/echo time (TR/ TE) = 800/2.3 ms; flip angle 90°; grid size 8 × 8×60 mm^3; field of view 300 × 300 mm^2; free breathing).

Pre-processing included: exponential filter, zero-filling from 1024 to 2048 points, Fourier transform, frequency and phase correction and subtraction of the baseline with the polynomial method. All spectra were processed by the same physicist using Spectroscopy-Argus software (version VE32B, Siemens Medical Solutions, Erlangen, Germany). The area under the peak of the following metabolites was measured: PCr at 0 ppm; phosphomonoester (PME) at 5.4 and 6.3 ppm; inorganic phosphate (Pi) at 3.7 and 5.2 ppm; phosphodiester (PDE) at 2–3 ppm; γATP at 16.3 ppm. Moreover, we identified the 2,3-diphosphoglycerate (DPG), contained in red blood cells, at about 5.5 ppm, used to correct data for the blood contamination. To this end, we subtracted 11% and 19% of 2,3-DPG from γATP and PDE, respectively, as already described [63]. The signals of γATP, PCr, PDE and Pi were corrected for decay using T2 values published in the literature [64]. Finally, we calculated the following ratios: PCr/γATP; PDE/γATP; 2,3-DPG/γATP; PME/PCr; and Pi/PCr [64]. Data were reported in au.

Statistical analysis

Statistical analysis was performed using non-parametric methods, more appropriate for small samples [65]. Differences between the two groups of subjects were evaluated with the Mann–Whitney U test or the χ^2 test, while bivariate correlations were estimated using the Spearman correlation coefficient.

Statistical analysis was performed using SPSS v.17.0 (IBM SPSS Inc., Chicago, IL, USA). Continuous variables were reported as median and IQR and P values <0.050 were considered statistically significant.

Results

Population characteristics

A total of 22 subjects were enrolled, whose characteristics are reported in Table 5. There were 7 HCM patients and 15 competitive athletes. In particular, athletes were nine bikers and six professional volleyball players with a median weekly training of 10h (IQR 10–14h). The median body mass index (BMI) in HCM patients (25 kg/m^2; IQR 24–29 kg/m^2) was higher (P = 0.041) than that of athletes (22 kg/m^2; IQR 20–23 kg/m^2). Moreover, HCM patients were older than athletes [56 years (IQR 45–62 years) versus 41 years (IQR 35–42 years), P = 0.009].

The mean total duration of magnetic resonance (MR) examinations was approximately 40 min: 20 min for imaging, 5 min for ^{1}H-MRS, and 15 min for ^{31}P-MRS. Processing required 5 min.

Table 5: distribution of demographics of the study population

	Competitive athletes	HCM patients	*P*
N (male/female)	15 (11/4)	7 (6/1)	0.297*
Age (years)[a]	41 (35–42)	56 (45–62)	0.009$
Body mass index (kg/m^2)[a]	22 (20–23)	25 (24–29)	0.041$
Weekly training (h)[a]	10 (10–14)	–	–

HCM hypertrophic cardiomyopathy

* χ^2 test. $ Mann–Whitney U test

[a] Data are presented as median and interquartile range in brackets

Morphology and function

The distribution and comparison of morphologic and functional characteristics of the left ventricle in the two groups are shown in Table 6. Of note, HCM patients showed a lower stroke volume than athletes [74 ml (IQR 72–86 ml) versus 111 ml (IQR 102–142 ml), P = 0.008], but an equivalent ejection fraction [68% (IQR 55–73%) versus 68% (IQR 65–69%), P = 1.000]. Moreover, HCM patients showed a much larger asymmetry index than athletes [2.0 (IQR 1.6–2.3) versus 1.1 (IQR 1.0–1.3), P =0.022]. Figure 5 shows examples of an athlete and a HCM patient.

Table 6: functional and morphologic variables of the left ventricle in the two groups

	Competitive athletes	HCM patients	*P**
End diastolic volume index (ml/m^2)	95 (85–102)	73 (58–76)	0.029
End systolic volume index (ml/m^2)	30 (28–32)	20 (16–34)	0.274
Stroke volume (ml)	111 (102–142)	74 (72–86)	0.008
Ejection fraction (%)	68 (65–69)	68 (55–73)	1.000
Left ventricle mass index (g/m^2)	72 (66–83)	81 (76–111)	0.052
Interventricular septal thickness (mm)	10 (10–11)	18 (15–21)	0.003
Posterior wall thickness (mm)	8 (7–10)	9 (7–11)	0.520
Asymmetry index	1.1 (1.0–1.3)	2.0 (1.6–2.3)	0.022
Left ventricle diameter (mm)	55 (52–56)	50 (48–52)	0.258

Data are presented as medians and interquartile range in brackets
HCM hypertrophic cardiomyopathy. * Mann–Whitney U test

Figure 5: Cardiac magnetic resonance images in diastolic phase of a mid-ventricular short axis section of an athlete (a) and a hypertrophic cardiomyopathy patient (b). Note that the septal thickness of the patient is greater than that of the athlete

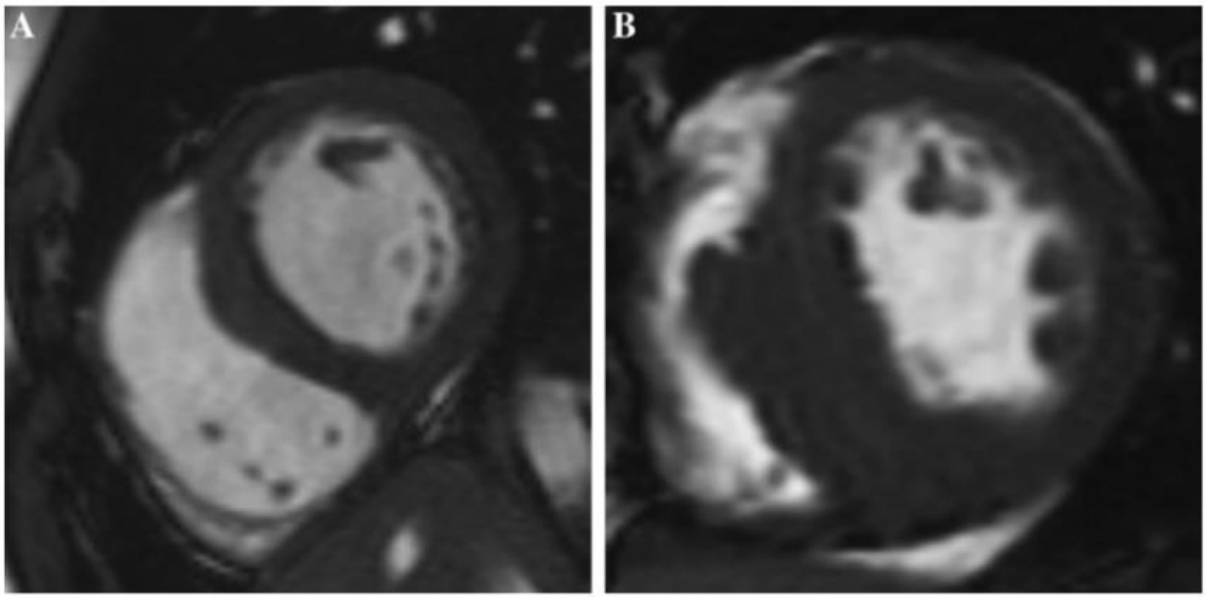

^{1}H-MRS

The ^{1}H-MRS spectrum of one athlete had too low signal to-noise ratio that prevented its analysis. The distribution of the variables measured using ^{1}H-MRS in the two groups and their comparison are shown in Table 7. Importantly, the lipid resonance at 1.3 ppm greatly differed between patients and athletes with a much higher content in HCM patients [554 au (IQR 121–2377 au)] than in competitive athletes [0 au (IQR 0–67 au)] (P = 0.020); similarly for the total lipid content [763 au (IQR 155–1994 au) versus 35 au (IQR 0–183 au), P = 0.046]. Figure 6 shows an example of a hydrogen spectrum of a competitive athlete and a HCM patient.

Table 7: distribution and comparison of metabolites measured by ^{1}H-MRS in the two groups of subjects

	Competitive athletes[a]	HCM patients[a]	*P**
Creatine at 3.0 ppm	19 (6–33)	0 (0–32)	0.799
Creatine at 3.9 ppm	55 (26–71)	43 (12–93)	0.799
Total creatine	58 (42–110)	95 (24–185)	0.447
Lipids at 0.9 ppm	0 (0–60)	125 (0–275)	0.397
Lipids at 1.3 ppm	0 (0–67)	554 (121–2377)	0.020
Total lipids	35 (0–183)	763 (155–1994)	0.046

HCM hypertrophic cardiomyopathy. *Mann–Whitney U test. [a] Data are presented as median and interquartile range in brackets

Figure 6: example of a hydrogen spectrum obtained

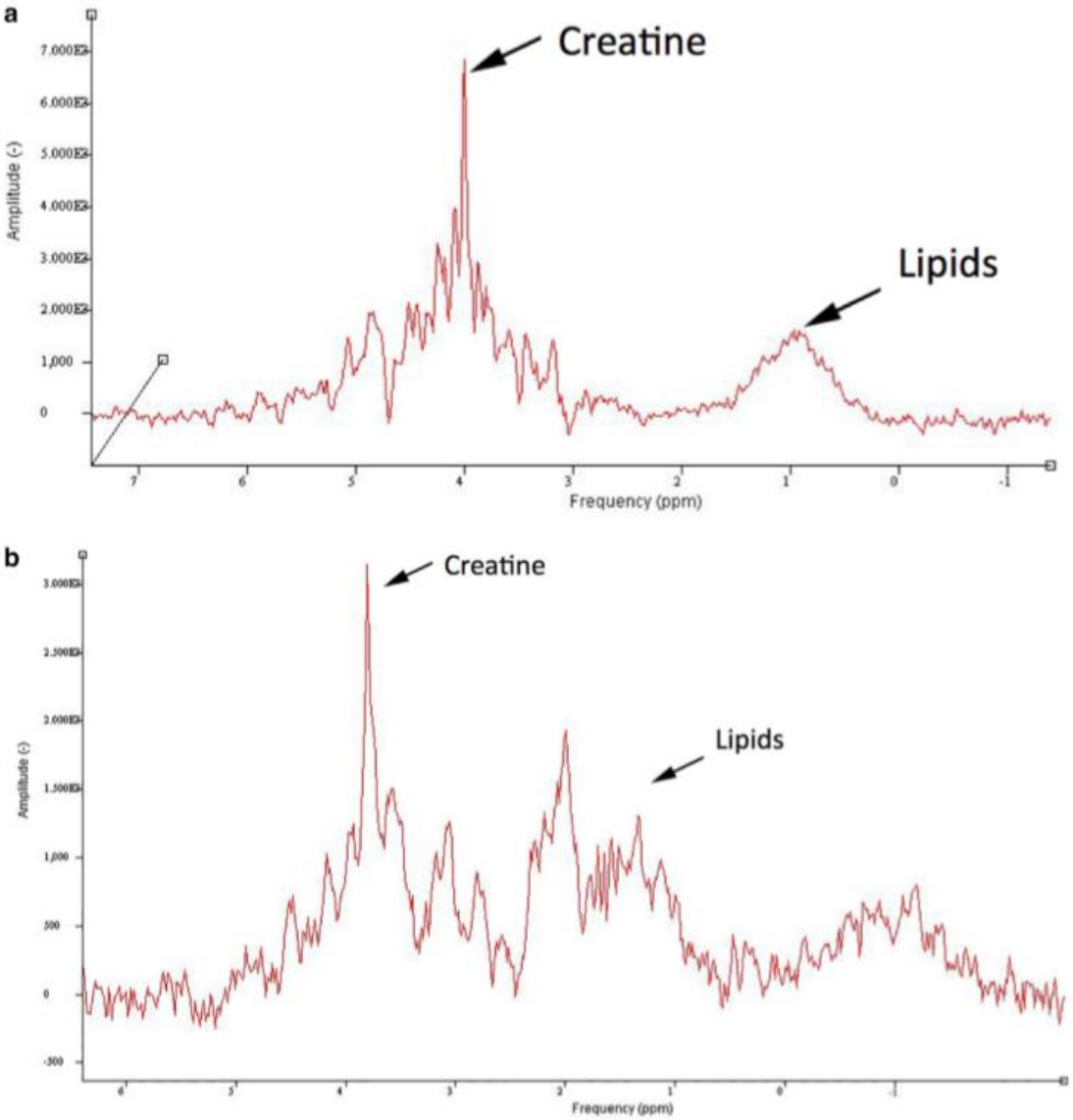

Hydrogen spectrum obtained in an athlete (a) and a hypertrophic cardiomyopathy patient (b). Note that the lipid peak is higher in the patient than in the athlete.

^{31}P MRS

Data from ^{31}P-MRS were not available for two HCM patients due to examination interruption for claustrophobia (in one case) or to low signal-to-noise ratio probably related to patient movement (in the other case). The distribution of the phosphate content in the two groups and their comparison are shown in Table 8.

No differences between patients and athletes were noted in terms of PCr [22 au (IQR 9–25 au) versus 29 au (IQR 20–36 au), P =0.168] and PCr/γATP [4 (IQR 2–5) versus 5 (IQR 4–6), P =0.230]. Vice versa, a significant difference between patients and athletes was noted in terms of 2,3-DPG/γATP [0.2 (IQR 0.0–0.2) versus 0.5 (IQR 0.3–0.7), P =0.008]. Figure 7 shows examples of ^{31}P-MRS spectra of an athlete and a HCM patient.

Table 8: distribution and comparison of phosphate content between the two groups of subjects

	Competitive athletes[a]	HCM patients[a]	*P**
PCr	29 (20–36)	22 (9–25)	0.168
γATP	6 (4–6)	5 (5–6)	0.735
PCr/γATP	5 (4–6)	4 (2–5)	0.230
PDE	7 (4–9)	5 (5–10)	0.612
PME	0.2 (0.0–0.3)	0.4 (0.4–1.8)	0.081
Pi	0.4 (0.0–1.3)	0.4 (0.4–1.7)	0.395
Pi/PCr	0.03 (0.00–004)	0.02 (0.01–0.22)	0.445
PME/PCr	0.01 (0.00–0.01)	0.02 (0.01–0.20)	0.142
PDE/γATP	1.1 (0.6–1.8)	1.1 (0.8–1.7)	0.866
2,3-DPG/γATP	0.5 (0.3–0.7)	0.2 (0.0–0.2)	0.008

HCM, hypertrophic cardiomyopathy; PCr, phosphocreatine; γATP, γ-adenosine triphosphate; PDE, phosphodiester; PME, phosphomonoester; Pi, inorganic phosphate; 2,3-DPG, 2,3-diphosphoglycerate; * Mann–Whitney U test a Data are presented as median and interquartile range in brackets. The content of metabolites is presented in arbitrary units

Figure 7: examples of ^{31}P-MRS spectra

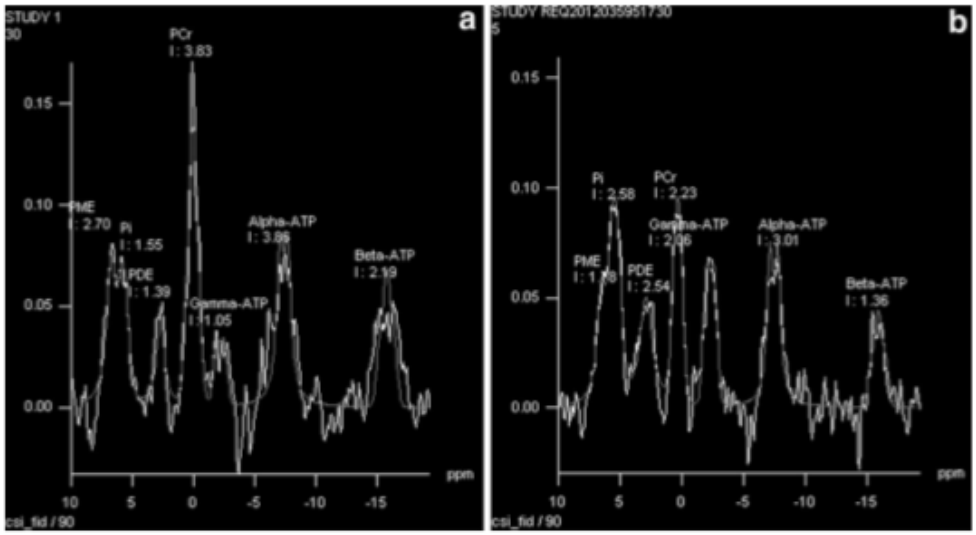

^{31}P-MRS spectra in an athlete (a) and a hypertrophic cardiomyopathy patient (b). PCr, phosphocreatine; ATP, adenosine triphosphate; PDE, phosphodiester; Pi, inorganic phosphate; PME, phosphomonoester. Note that PCr/gamma-ATP ratio is reduced in the HCM patient

Bivariate correlation analysis

As reported in Tables 2, 3, and 4, the variables found to be significantly different in the two groups at bivariate analysis were: age, BMI, stroke volume, EDVI, left ventricular mass index, interventricular septal thickness, asymmetry index, 2,3-DPG/γATP, lipids at 1.3 ppm and total lipids. BMI did not correlate with either lipid resonances at 1.3 ppm (r = 0.318, P = 0.184) or total lipids (r = 0.421, P = 0.065).

Discussion

The main finding of this study is that ^{1}H-MRS, performed in only 5 min after a standard C MR examination, enabled detecting increased intramyocardial lipids in HCM patients in comparison with competitive athletes. These results are somewhat new and may open a perspective for future studies aimed at using

^{1}H-MRS in the differential diagnosis between HCM and athlete's heart. This study adds a new potential biomarker to the well-known differences in the left ventricle remodeling and function.

Causes for the accumulation of intramyocardial lipids in early stages of HCM need to be clarified and a thorough explanation is currently not available. Nonetheless, we can hypothesize that the combined effect of lipid deposition superimposed on fibrosis might help to identify individuals at higher risk of arrhythmias. One study showed that increased myocardial triglycerides in healthy subject are positively correlated to the cardiac volumes [66]. However, to our knowledge, pathologic studies demonstrated only fibrosis infiltration and not fat infiltration in HCM patients [67, 68]. Only patients affected with generalized lipodystrophy were proven to present with left ventricle hypertrophy associated with myocardial steatosis [69]. Other authors showed that overweight and obese women show increase of myocardial triglyceride associated with reduction in cardiopulmonary fitness [70]. Similar results were obtained in patients affected by type-2 diabetes [71, 72].

In our study, the phosphate metabolism of athlete's heart was preserved and the PCr/γATP ratio was in the range of normal values [49], as expected [73]. In advanced HCM, this ratio is known to be reduced resulting in heart failure [42]. The ^{31}P-MRS analysis also showed a significant difference between the two groups in terms of 2,3-DPG/ γATP, with a lower value in HCM patients than in athletes. Considering that γATP alone was not significantly different in the two groups, an increase of 2,3-DPG may explain the difference in 2,3-DPG/γATP. The reason for this phenomenon could lay in the contamination of the blood pool in the voxel in subjects with a small septum. The variation of PME/PCr and Pi/PCr between the two groups was not significant, in line with the literature [64]. Notably, a not significant difference was observed in terms of PCr/γATP, as an indicator of energy metabolism. This may be due to the normal value of septal thickness in our athlete's population, without any overt athlete's heart condition.

As a potential clinical application of our study, we highlight that while ^{1}H-MRS required only five additional minutes, the ^{31}P-MRS protocol required the extraction of the patient from the magnet, the change of the coil and a new patient positioning in an uncomfortable prone position. This means that the clinical feasibility of cardiac ^{1}H-MRS is much higher than that of cardiac ^{31}P-MRS. Moreover, ^{31}P-MRS is no longer available commercially for 1.5-T MR units. It is offered only for 3-T units,

whose results for cardiac imaging were reported to be not clearly better than those obtained with 1.5-T units in terms of image quality [74].

Morphologic and functional imaging data, EDVI and stroke volume, were significantly lower in HCM patients than in athletes, confirming the typical geometric pattern of the disease on one side and the heart adaptation to the intense sport activity on the other, as already reported [41]. A significant increase in left ventricle mass and septal thickness was found in HCM patients compared to athletes, as expected [41]. Interestingly, indexes of systolic function were not significantly different in the two groups, a finding that appears consistent with a relatively early stage of nonobstructive HCM patients.

This study has limitations. First, the number of subjects studied was small and bikers and volley players are different in terms of exercise (low static moderate dynamic for volley; high static and dynamic for cycling), leading to potential differences in cardiac metabolic activity. However, subgroup analysis was not possible due to the lack of statistical power. Second, the higher BMI and age in HCM patients may represent a source of bias, so that we cannot exclude that they can explain the difference in lipid content; however, bivariate correlation analysis between lipids and BMI did not show any significant correlation. Third, we did not calculate the concentrations of metabolites using internal or external references. However, the area under the peak as we used in this work can be considered a valid quantitative approach, utilized in cardiac [63, 75] and non-cardiac studies [76]. Fourth, due to the enrollment criteria, we were not able to test for differences among various underlying etiologies of HCM or specific HCM gene mutations. Fifth, ethical issues prevented from performing late gadolinium enhancement in athletes.

In conclusion, we found a significant increase in myocardial lipids in HCM patients compared to competitive athletes at ^{1}H-MRS. Myocardial ^{1}H-MRS may be an additional final phase of a CMR protocol including standard morphologic and functional imaging in the differential diagnosis between HCM and athlete's heart. Prospective larger studies are needed to confirm this preliminary unexplained, but intriguing observation.

Blood-threshold CMR volume analysis of functional univentricular heart

Introduction

The definition of univentricular heart has evolved from a narrow anatomical focus to a comprehensive view of heterogeneous conditions that ultimately result in a FUH [1–3]. A total cavo-pulmonary connection or Fontan circulation (FC) is the surgical approach of FUH [1, 4–6]. Constant advances in cardiac magnetic resonance CMR techniques and equipment in the last decade now grant adequate anatomical detail in addition to the accurate and not operator-dependent functional assessment of ventricular chambers (main and accessory), cardiac valves, and intra- or extracardiac shunts and conduits. Furthermore, the functional evaluation of FC performed by CMR does not require the use of intravenous contrast material. The possibility of using non-contrast radiation-free CMR restricts the use of computed tomography in circumstances that require a detailed anatomical assessment [7–10]. In addition, contrast-enhanced CMR could allow the detection of the myocardial fibrotic evolution, an evaluation still not clinically feasible with computed tomography [11]. Non-invasive imaging techniques play a major role in the follow-up of patients with FC. In particular, CMR is emerging as the leading modality for pre-/post-surgical assessment of congenital heart disease CHD as well as for early diagnosis of cardiac and systemic complications, clarifying cardiovascular anatomy and physiology [7, 12–15]. Several studies have progressively asserted the correlation between the prognosis of patients with FC and their ventricular size and function calculated with analysis and segmentation of CMR images, showing it to be equally or more accurate than echocardiographic assessment and distinctly more reproducible [8, 16, 17]. In literature, there is limited experience regarding the volume analysis of FC patients. A study [18] showed that the inclusion of the hypoplastic chamber during the segmentation of cine images of FC patients has no effect on the quantification of cardiac volumes, but may result in a less accurate measurement of the ejection fraction.

The aim of our study is to validate the BT segmentation algorithm in CMR cine images for the evaluation of cardiac function in patients with FUH.

Materials and methods

Study population

The ethics committee approval was obtained for this retrospective study (Ethics Committee of the University Hospital San Raffaele; protocol code UH_01; approved on July 14th, 2016). A total of 70 CMR examinations of patients with FUC performed at our institution between March 2008 and March 2015 were initially considered. The inclusion criteria for the re-assessment of the images were: (1) complete acquisition of cardiac volume with cine images; (2) acquisition of through-plane images of flow in the ascending aorta; and (3) the absence of atrial–ventricular valve insufficiency. Therefore, 15 examinations were excluded, and a total of 55 examinations, belonging to 44 patients (7 patients were scanned 2 times and 2 patients 3 times), were included. In case of repeated examinations on the same patient, the time interval was at least 12 months. The 44 patients included 30 males and 14 females, with a mean age and its corresponding SD at the first examination of 25 ± 8 years (mean ± SD). The youngest patient was 7-year-old at the time of examination, and the oldest patient was 41-year-old.

Image acquisition

All CMR examinations were performed with a 1.5-T unit (Magnetom Sonata Maestro Class or Magnetom Aera, Siemens Medical Solutions) with 40- or 45-mT/m gradient power, respectively, using a 4- or 18-channel surface phased-array coil placed over the thorax and with the patient in a supine position. The image acquisition was gated to the ECG signal to produce a cine sequence throughout the systole and diastole and to avoid cardiac artifacts. Each CMR study included a complete set of short-axis (from base to apex) cine images, using an ECG-triggered steady-state free precession pulse sequence acquired with the following technical parameters: TR/TE = 4.0/1.5 ms; flip angle 80°; slice thickness 8 mm; time resolution 45 ms; mean acquisition time 14 ± 4 s (mean ± SD); number of phases 30. Phase contrast (PC) through-plane sequences were used for blood flow quantification [19]. Images perpendicular to the ascending aorta were obtained (1 cm distal to the

sinotubular junction). A breath-hold turbo spoiled gradient echo sequence (fast low-angle shot) was performed for phase velocity mapping with the following technical parameters: TR/TE 4.0/3.2 ms; slice thickness 5 mm; velocity encoding (VENC) from 150 ms to 350 ms; time resolution 41 ms; mean acquisition time 15 ± 4 s. Initially, we acquired the PC sequence with a VENC of 150 ms. In the presence of aliasing, we modified the VENC adding 50 ms for each new sequence, step by step up to the complete disappearance of the aliasing artifact. The PC through-plane sequences produced two sets of images: the magnitude image and the phase-velocity map, the former to provide details on the anatomy and identify the boundaries of the vessel and the latter for blood flow estimation [20].

Image assessment

Two independent radiologists, R1 and R2, with comparable experience (about 4 years) performed the segmentation of cardiac and flow images using MEDIS QMass 7.6 and QFlow 5.6 (Medis Medical Imaging Systems, Leiden, The Netherlands) [21, 22]. For the segmentation of cardiac images, in each session both readers independently manually traced the epicardial contour of the FUH both in the end-diastolic and end-systolic phases. Thus, the blood-threshold technique (Mass-K mode) was applied using a 50% BT and the EDVI, ESVI, SV, EF, and cardiac mass values were calculated in a totally automated way. For the segmentation of flow images of the ascending aorta, in each session each one of the two readers positioned a region of interest on the vessel boundary of a selected slice. Subsequently, each reader propagated the segmentation through the remaining slices, the software proposed an automated adjustment, and the reader was allowed to manually correct the adjusted contours. For each session, forward flow and backward flow measurements were obtained.

Statistical analysis

Data were reported as mean ± SD or median and IQR according to normal distribution or non-normal distribution, respectively. The Wilcoxon test and Spearman correlation were used to compare and correlate the median value of SV and aortic forward flow, respectively. The Bland–Altman method

was used to estimate the intra- and inter-reader reproducibility. The intra-reader reproducibility was performed only for R1 with at least a 10-day interval between the two sessions. The coefficient of repeatability (CoR) was calculated as 1.96 × SD of differences of the two datasets. Reproducibility was reported as complement to 100% of the ratio between the CoR and the mean. Bias (mean of the differences of the two datasets) and 95% limits of agreement (bias ± 2 SD) were plotted as well.

Results

The image analysis was feasible in all patients and no artifacts prevented readers from performing the segmentation. Fifty-five examinations were analyzed. No clinically relevant aortic regurgitation was found. The median value of the SV and aortic forward flow were 57.7 ml (IQR 47.9–75.6 ml) and 57.4 ml (IQR 48.9–80.4 ml), respectively. We found no significant difference (P = 0.123), but a significant correlation (r = 0.789, P < 0.001) between mean SV and aortic forward flow. All ventricle and aortic functional parameters are shown in Table 9.

Table 9: ventricle and aortic functional parameters

EDVI (ml/m^2)	63.7 (51.9–82.2)
ESVI (ml/m^2)	26.8 (21.3–46.0)
SV (ml)	57.7 (47.9–75.6)
EF (%)	51.3 (43.4–60.0)
Mass index (g/m^2)	89.2 (73.2–131.4)
Aortic forward flow (ml/heart beat)	57.4 (48.9–80.4)
Aortic backward flow (ml/heart beat)	1.9 (0.5–3.9)

Data reported as median (interquartile interval) EDVI, end-diastolic volume index; ESVI, end-systolic volume index; SV, stroke volume; EF, ejection fraction.

The bias between the SV values measured by R1 was 0.12 ml, accompanied by a CoR of 8.1 ml, corresponding to an intra-reader reproducibility of 86%. The bias was − 0.1 ml, accompanied by a CoR of 2 ml corresponding to a reproducibility of 96%. The inter-reader analysis of SV showed a CoR of 8.63 ml over a bias of − 1.9 ml, corresponding to an inter-reader reproducibility of 85%. The same data for the aortic forward flow were 2.12 ml over a mean difference of 0.24 ml, corresponding to an inter-reader reproducibility of 96%. Bland–Altman plots for intra- and inter-reader reproducibility are

shown in Figs. 8a, b and 9a, b, respectively. An example of segmentation of cine CMR images with the BT technique is shown in Fig. 10.

Figure 8: Bland-Altman plots of intra-reader reproducibility

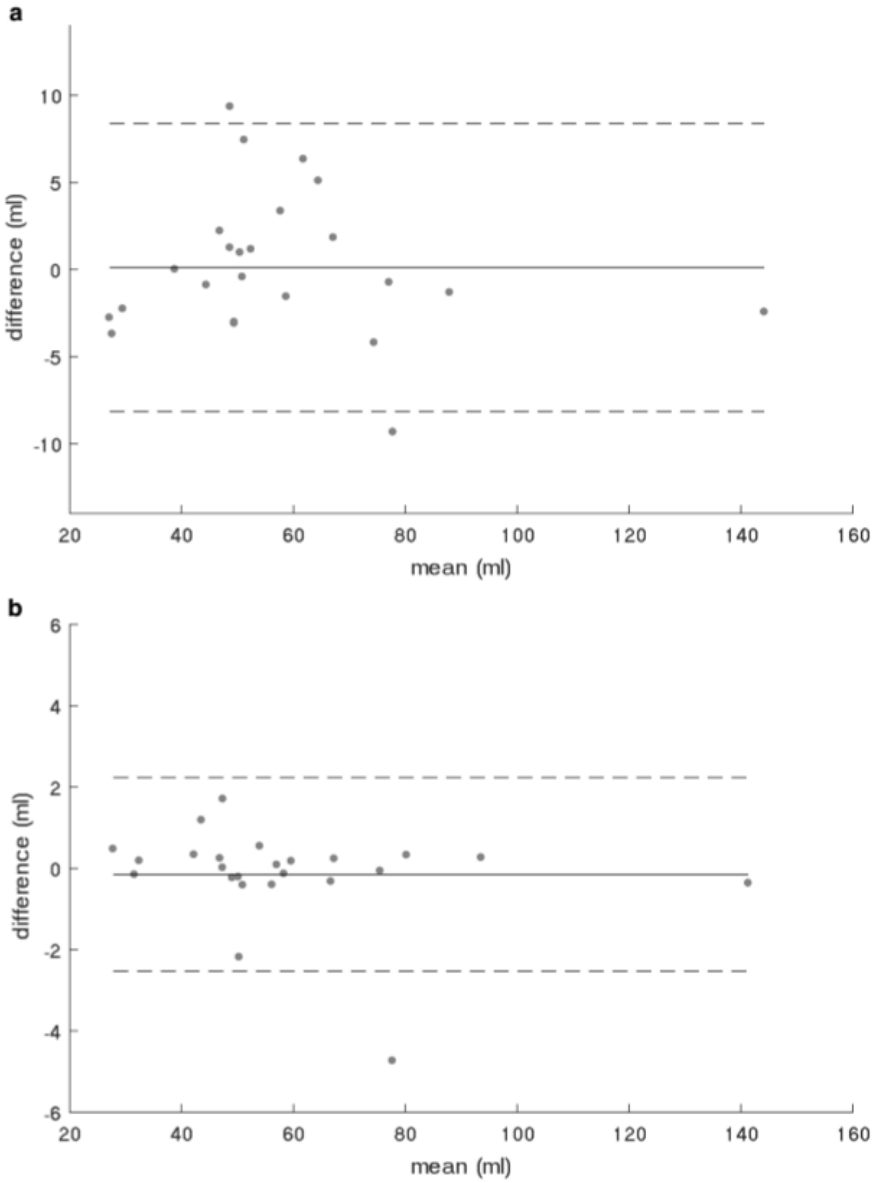

Bland–Altman plot for intra-reader reproducibility of stroke volume measurement (a); Bland–Altman plot for aortic forward flow measurement (b).

Figure 9: Bland-Altman plots of inter-reader reproducibility

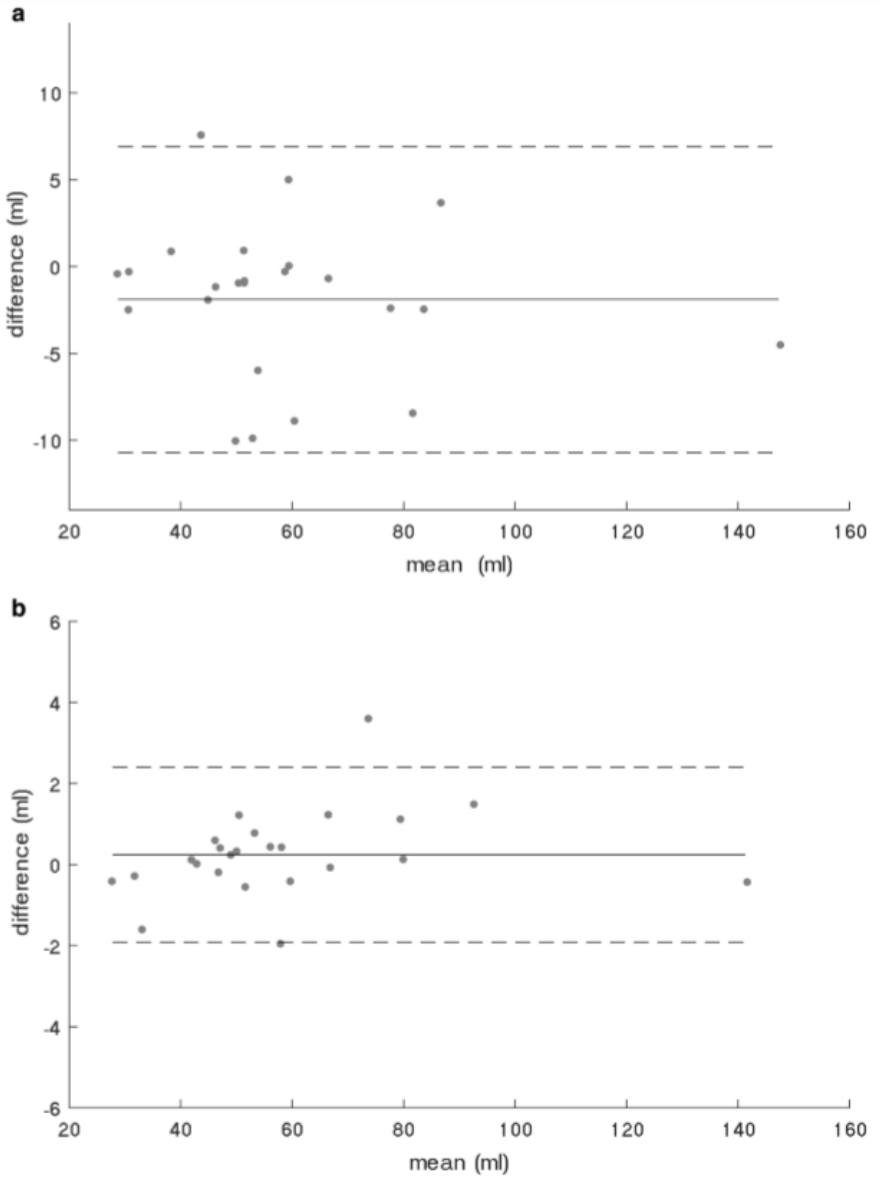

Bland–Altman plot for inter-reader reproducibility of stroke volume measurement (a); Bland–Altman plot for aortic forward flow measurement (b).

Discussion

In CMR, ventricular volume and function assessment is achieved through the segmentation of cine images. This post-processing technique, initially exclusively manually performed by trained readers, implies the recognition of the difference between the blood pool in the ventricular cavity, of other anatomical structures normally in the ventricular chamber such as trabeculae and papillary muscles (TPM) as well as of the ventricular walls. Manual tracing of contours for the ventricular walls and

TPM by an experienced reader still constitutes the most widely validated and employed approach. However, in the last decade, several studies have validated techniques that, while less time-efficient than a fully automated solution, have tried to address the numerous limitations of the fully automated approach and provided a solid method, well-balanced in terms of cost-effectiveness analysis, to obtain a proper estimate of the ventricular volume and mass with minimal manual input [22–25]. One of these limitations is the unreliable allocation of TPM to the myocardial mass or to the blood pool. TPM allocation was shown to substantially influence the accuracy of ventricular volume and mass assessment. In some recent automatic software, there is the possibility to exclude TPM from the blood pool [26–28]. However, in particular conditions such as FUH, the delineation of hyper trabeculations remains difficult.

A BT technique such as the Mass-K Mode algorithm can serve as a time-saving and accurate solution to this clinical issue. In this technique, after the reader has manually traced only the epicardial contours on the end-systolic and end-diastolic phases of the cine images, the software calculates a blood percentage for each pixel inside the contoured area, considering the different signal intensity of the blood and myocardium. After visual inspection, the reader can freely alter, in any slice and phase, the default BT value of signal intensity discrimination. Moreover, semi-automated detection of the epicardial margin can be used, requiring only small manual adjustments on good quality images, further curtailing the time required for the post-processing stage [29].

The Mass-K Mode algorithm has been validated for clinical routine application, showing both accurate and reproducible evaluation of ventricular mass and volume and reduced time of analysis, by Jaspers et al. [29] on phantoms and on 12 patients with normal cardiac anatomy and function and more recently by Varga-Szemes et al. [25] on 137 patients with a broad range of cardiac diseases not including CHD.

The results of our study validate the use of this BT technique in patients with an abnormal cardiac anatomy, such as the one that is found in patients with FC. In the absence of other reference tools to validate ventricular volume assessments, we choose to use aortic flow measurements as an independent benchmark for SV, since previous studies showed it to be a solid and reproducible

standard. Of note, we found no significant difference and a significant correlation between the two values [30–32].

Figure 10: example of segmentation of short-axis cine images with blood-threshold technique

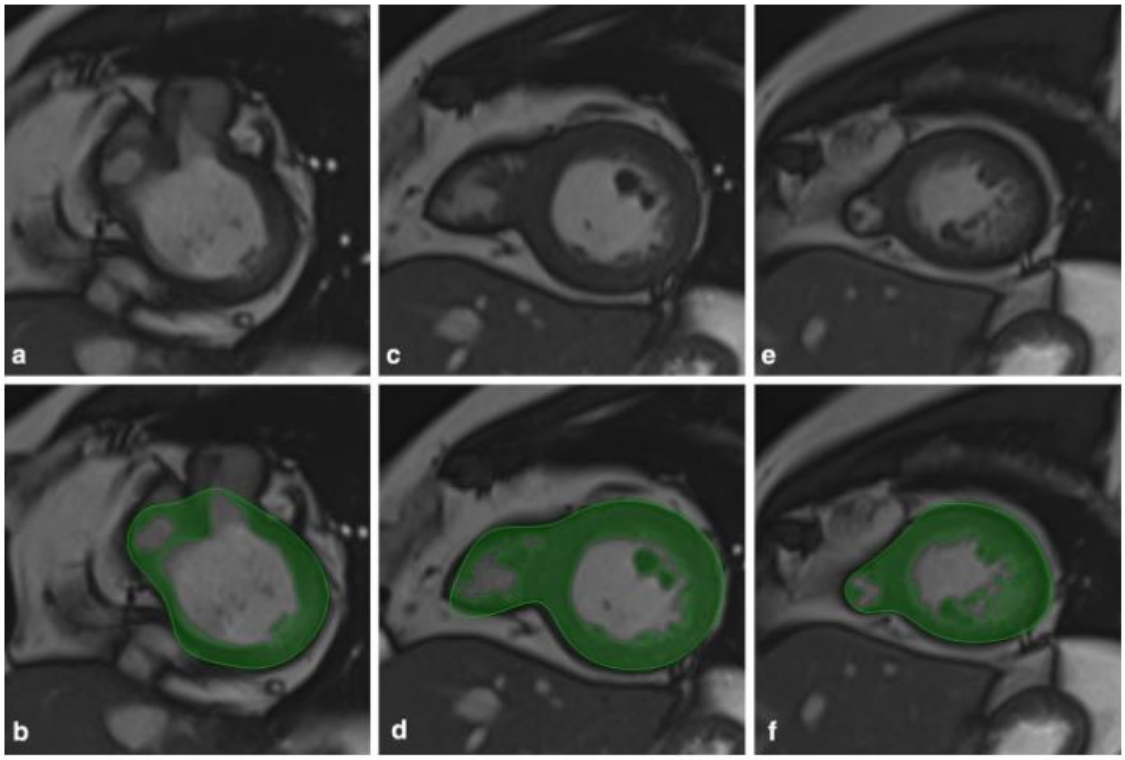

a, c, e Short-axis slices of cine images from base to apex without the blood-threshold mode.
b, d, f The same images after manual epicardial volume analysis with blood-threshold mode activation.

In addition, a greater level of automation and a lesser need of manual adjustments granted by the use of the BT technique and the semi-automated recognition of epicardial contours and aortic walls account for the excellent inter- and intra-reader reproducibility of both SV and aortic flow volume (85 and 96%, respectively).

Our study has limitations. First, it is a retrospective study on a relatively small number of subjects and it is based on a single-center historical series of FC patients; however, FUV patients are a very small population and usually referred to a single center. Second, it is possible that, due to the retrospective design of our study, even small differences in the acquisition parameters, reasonably likely to happen in the absence of a standardized CMR acquisition protocol, may have negatively influenced the quality of cine images and therefore the performance of the BT technique. Third, the

study lacks an independent reference standard, though the aortic flow analysis may be considered substantially independent of the cardiac cine study. Fourth, both readers were equally experienced (about 4 years); further studies are required to investigate reproducibility between readers with different levels of experience.

Finally, we should consider the possibility of obtaining the same volume analysis with different software; this new function could be integrated in future software to be used in FUH patients. To summarize, we successfully validated the use of a BT technique for the segmentation of cine images in patients with FC. We observed a high intra- and inter-reader reproducibility for the assessment of ventricular SV and excellent agreement with aortic flow values used as a benchmark.

Strain of ascending aorta on cardiac magnetic resonance in 1027 patients: Relation with age, gender, and cardiovascular disease

Introduction

Arterial stiffness is one of the earliest manifestations of adverse structural and functional changes within the vessel wall. When the aorta is considered, stiffness is a main determinant of age-related systolic and pulse pressure increase, a major predictor of stroke and myocardial infarction, and has been associated with heart failure [9, 77, 78]. Pulse wave velocity measured by applanation tonometry is a well-known functional method to non-invasively quantify aortic stiffness providing an average measure of stiffness over a certain vessel length. Conversely, strain, compliance, and distensibility are local markers of arterial elasticity, which can be measured using MR imaging, allowing the detection of more subtle changes in regional stiffness [79].

The use of MR imaging has several advantages over ultrasound imaging including three-dimensional visualization that allows to place the imaging plane perpendicular to the vessel with a high reproducibility. Thus, aortic distensibility can be measured as a change in two dimensional vessel perimeter or area instead of one-dimensional vessel diameter [79]. Previous authors showed that AAS measured with cardiac CMR is markedly decreased before the fifth decade of life and that can be considered as an early manifestation of vascular aging [10]. AAS was also shown to be independently correlated with coronary atherosclerosis and coronary calcium content [80] as well as to be an independent predictor of progression toward hypertension in non-hypertensive subjects [81].

Our aim was to evaluate the AAS in a large consecutive series of patients who underwent CMR, comparing age classes, gender, and different types of CVD, also including subjects with normal CMR examinations.

Materials and methods

Study design and population

The local Ethics Committee approved this retrospective study (Ethics Committee of the University Hospital San Raffaele; protocol code AS01; approved on April 7th, 2016) and informed consent was waived. Patients were selected from a database of CMR studies performed between September 2008 and August 2014 at the Radiology unit of the IRCCS Policlinico San Donato, San Donato Milanese, Italy. CMR examinations with an image quality that impairs AAS evaluation were excluded from analysis. Moreover, in the case of multiple CMR examinations in the same patient, only the first one was included.

Image acquisition

We retrospectively selected images acquired with two different 1.5 T machines. Magnetom Sonata Maestro Class (Siemens, Erlangen, Germany), was used to perform the studies from September 2008 to March 2014 (n =1294); subsequent studies (n= 69) were performed using Magnetom Aera (Siemens, Erlangen, Germany). Retrospectively ECG-gated breath-hold two-dimensional phase-contrast gradient recalled echo sequences with a through-plane velocity encoding gradient ranging from 150 to 350 cm/s were performed on a transverse plane above the aortic bulb. Sequence parameters were as follows: repetition time 49.75 ms, echo time 3.1 ms, flip angle 30° for Magnetom Sonata; 37.12 ms, 2.47 ms, 20° for Magnetom Aera. Parallel imaging with acceleration factor 2 and retrospective ECG-gating with 30 phases per cycle (with repetition time dependent on the R-R interval) were set on both machines.

Image analysis

Image post-processing was performed using Argus Flow software (Syngo Argus Flow, version 4.02, Siemens, Erlangen, Germany). Magnitude images were used to semi-automatically segment aortic contours in each cardiac phase. During the segmentation process, an expert cardiac radiologist with 2–7 years of experience in CMR selected the frame with the optimal contrast between aortic lumen and

aortic wall. Then, the operator traced in the same frame the aortic contour, which was automatically propagated in all frames of the cardiac cycle and manually corrected when necessary.

The AAS was calculated as defined by Redheuil et al. [5], namely:

$$AAS = \frac{A_{max} - A_{min}}{A_{min}}$$

where A_{max} and A_{min} represent respectively the maximum and minimum aortic cross-sectional area measured during a single cardiac cycle.

Statistical analysis

The Shapiro-Wilk test was employed to assess normality of data distribution. Due to non-normal data distribution, descriptive statistics are provided as median and corresponding IQR values. To evaluate the influence of age, gender, and CVD on the AAS values, we performed a three-way ANOVA test. The log-transformation of the data was obtained to reach the condition of normal distribution needed to perform the tree-way ANOVA. Age was categorized into 7 age bins (0–9, 10–19, 20–29, 30–39, 40–49, 50–59 and ≥60 years). Moreover, post-hoc tests for CVD and age bin factors were performed.

After this global analysis, the statistical differences in AAS values were analyzed in the larger subgroups, namely: subjects with normal CMR (i.e. unremarkable examination in subjects examined to exclude cardiac abnormalities), patients with ToF, and patients with ischemic heart disease (IHD). Taking into account only these types of CVD, the evaluation of AAS changes over all the selected age bins was not possible, due to the different age distribution of subjects affected by congenital (ToF) and age-related (IHD) CVD. Therefore, statistical inference on AAS trends over age was evaluated comparing ToF and IHD subjects only with normal CMR subjects. To this aim, the Mann-Whitney U tests was used for each age bin. On the other hand, to evaluate the influence of gender and CVD on AAS values, a two-way ANOVA was performed. Also, in this case, log-transformation of the data was obtained to perform multivariate analysis. Finally, age was considered as a continuous variable and correlation between age and AAS values was estimated using Spearman correlation coefficient.

Statistical significance level was set to $P < 0.050$ and the analysis was performed using SPSS (IBM Corporation, New York, NY, United States).

Results

A total of 1363 CMRs were retrieved; among them, 42 examinations were excluded due to an insufficient image quality. Moreover, in order to create homogenous CVD categories, we excluded disease subgroups composed of less than 10 subjects. For this reason, other 294 cases were excluded from the analyzed sample.

The final number of analyzed patients was 1027. Among them, 726 were men (median age 37 years, IQR18–60) and 301 were women (median age 34 years, IQR 16–54), with borderline significance between genders ($P = 0.051$). Fig. 11 shows age distribution between genders.

Figure 11: age distribution in the analysed sample

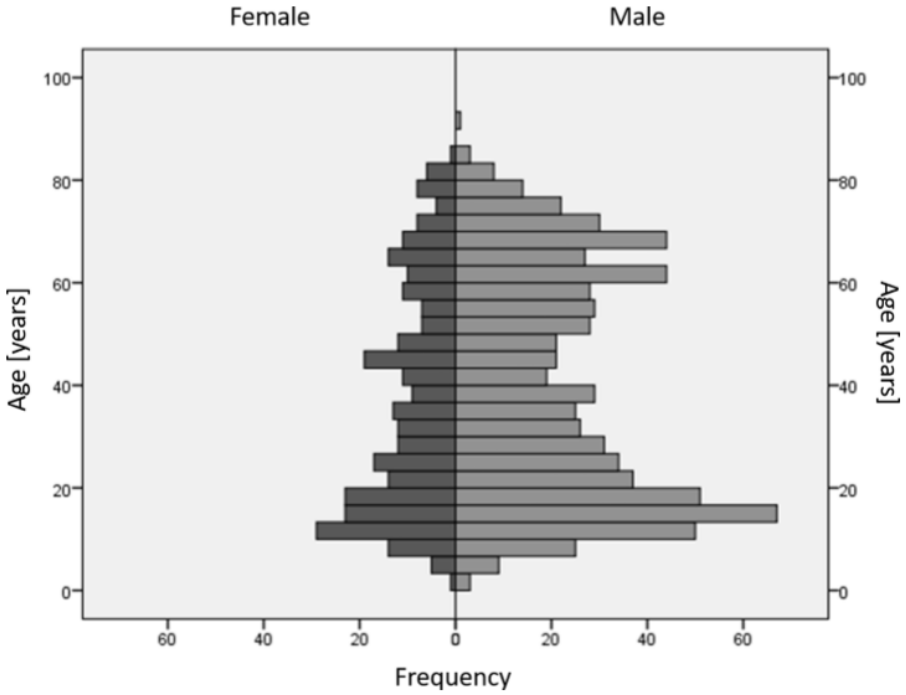

Histograms representing age distribution among different genders in the 1027 analyzed patients.

Taking into account all the analyzed subjects, the median AAS value was 0.25 (IQR 0.17–0.38). Shapiro Wilks test showed that AAS data were not normally distributed ($P < 0.001$) The AAS resulted inversely correlated with age ($\rho = -0.51$, $P < 0.001$). Moreover, women showed a significantly ($P =$

0.006) higher AAS (median 0.28, IQR 0.20–0.41) compared to men (median 0.24, IQR 0.16–0.36). The results of the three-way ANOVA are shown in Table 10.

Table 10: output of ANOVA analysis

Source	Type III Sum of Squares	df	Mean Square	F	p-value
Age bin	19.170	6	3.195	14.295	**0.000**
Gender	1.670	1	1.670	7.470	**0.006**
CVD	16.400	18	0.911	4.076	**0.000**
CVD * Age bin	20.899	89	0.235	1.051	0.360
CVD * Gender	4.011	18	0.223	0.997	0.460
Gender * Age bin	0.463	6	0.077	0.346	0.913
CVD * Gender * Age bin	10.075	51	0.198	0.884	0.703
Error	187.071	837	0.224		
Total	2272.154	1027			
Corrected Total	348.130	1026			

Output of the three-way ANOVA analysis that takes into account the effect of age, gender and cardiovascular disease on ascending aortic strain values. Data shows that all the three variables (age, gender and CVD) are independently associated to AAS. Statistically significant p-values are highlighted in bold.
CVD: cardiovascular disease; df: degrees of freedom.

Post-hoc analysis showed significant differences in AAS among all the age bins except for those between 30 and 49 years of age. Fig. 12 shows the AAS trend over decades of age, while results of post-hoc test for different CVD type sand their corresponding descriptive statistics are presented in Table 11.

Figure 12: ascending aortic strain over age

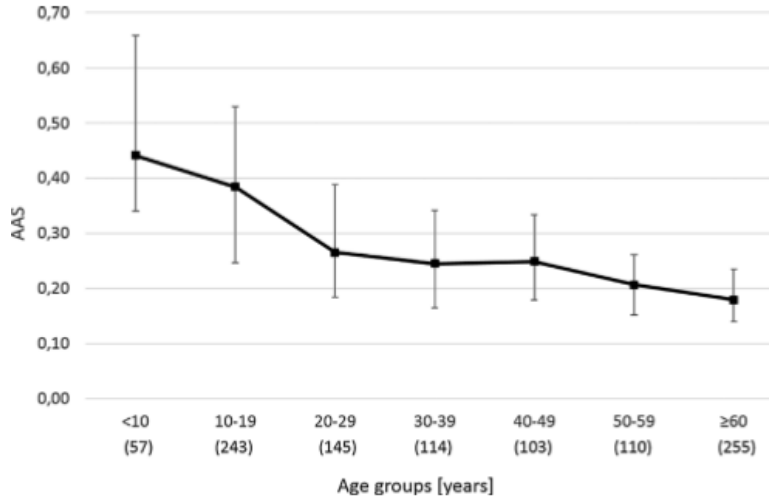

Ascending aortic strain (AAS) values over decades of age in the analyzed sample of 1027 consecutive subjects. For each age subgroup the number of included subjects is reported between brackets

Of the total of 1027 cases, the major subgroups were represented by 192 subjects with normal CMR (128 men, 64 women; median age 36 years, IQR 18–51), 166 patients affected with IHD (132 men, 34 women, median age 64 years, IQR 58–71), and 92 patients affected with ToF (57 men, 35 women; median age 25 years, IQR 14–40). In all the three subgroups, there was no significant difference in terms of age between men and women (normal CMR, P =0.997; IHD, P = 0.658, ToF: P = 0.361).

Table 11: post hoc tests performed on different cardiovascular disease subgroups

CVD (number of subjects)	Median	Q_1	Q_3	*p-value*
Normal CMR (192)	0.30	0.22	0.41	
Tetralogy of Fallot (92)	0.30	0.16	0.39	**< 0.001**
Transposition of the great arteries (61)	0.25	0.18	0.36	**0.006**
Post Melody valve implantation (39)	0.20	0.13	0.31	**< 0.001**
Fontan procedure (23)	0.23	0.16	0.34	**0.007**
Bicuspid aortic valve (45)	0.36	0.23	0.61	0.047
Pulmonary insufficiency (70)	0.30	0.18	0.57	0.334
Aortic insufficiency (33)	0.30	0.18	0.42	0.487
Aortic valve stenosis (15)	0.64	0.32	0.90	**< 0.001**
Pulmonary valve stenosis (22)	0.26	0.15	0.39	0.088
Ross procedure (10)	0.13	0.09	0.22	**< 0.001**
Ascending aortic dilatation (58)	0.18	0.13	0.26	**< 0.001**
Ascending aortic aneurysm (19)	0.14	0.10	0.20	**< 0.001**
Aortic coarctation (66)	0.41	0.32	0.57	**< 0.001**
Ischemic heart disease (166)	0.18	0.14	0.26	**< 0.001**
Dilated cardiomyopathy (34)	0.22	0.19	0.30	**0.001**
Hypertrophic cardiomyopathy (31)	0.25	0.19	0.34	0.058
Surgical ventricular restoration (32)	0.22	0.16	0.26	**< 0.001**
Left ventricular hypertrophy (19)	0.28	0.18	0.32	0.060

In this table are shown only post hoc tests performed between subjects with normal cardiac magnetic resonance and patients with different diseases. Statistically significant p-values are highlighted in bold.
CMR: cardiac magnetic resonance; CVD: cardiovascular disease.

Multivariate analysis performed on the subsample composed by these three major subgroups showed significant differences in AAS values between genders (P = 0.002) and among CVD subgroups (P < 0.001), without interaction between CVD subgroups and genders (P =0.119). In general, median AAS values were higher in women than in men, as can be seen in the boxplot represented in Fig. 13. However, post-hoc analysis showed a significant difference in AAS between men and women only for ToF patients (P = 0.008). Moreover, men with ToF showed a significantly

lower AAS when compared with men with normal CMR (P =0.005). In the other two subgroups, this difference appeared to be not significant within the analyzed sample. No significant difference was found between genders in subjects with normal CMR (P = 0.728). In IHD patients, AAS was significantly lower compared to that of normal CMR subjects (men: P < 0.001, women: P =0.016), without significant difference between genders (P =0.732). In subjects with normal CMR, the analysis of AAS trend over age showed an inverse correlation with age both in men (ρ= −0.53, P < 0.001) and women (ρ= −0.54, P < 0.001); AAS decreased with age also in IHD patients (ρ= −0.16, P =0.039), this correlation remaining significant in women (ρ= −0.40, P = 0.021) but not in men (ρ= −0.11, P =0.224). Evaluating AAS over decades of age, men with IHD had an AAS significantly lower than that of normal CMR subjects only between 50 and 59 years of age (P = 0.019). No significant differences were found between women affected with IHD and women with normal CMR for all age bins.

Figure 13: subgroup analysis

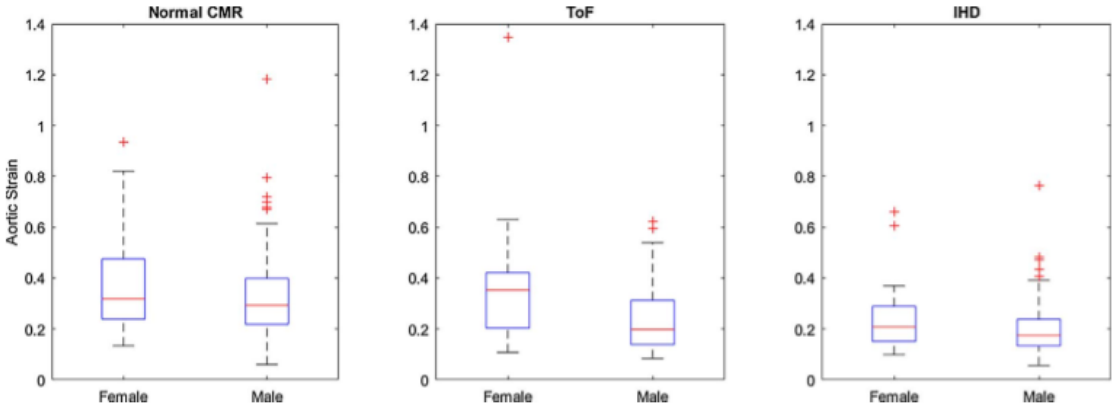

Three boxplots that represents ascending aortic strain values in normal cardiac magnetic resonance (CMR) subjects, patients with tetralogy of Fallot (ToF) and ischemic heart disease (IHD), subdivided by gender

Also, in ToF patients the AAS decreased with age, significantly in men (ρ= −0.66, P < 0.001), not significantly in women (ρ= −0.28, P = 0.106). Moreover, men affected with ToF belonging to the 20–49 age range had AAS values significantly lower than men with normal CMR (20–29 years, P = 0.002; 30–39 years, P = 0.011; 40–49 years, P < 0.001); after 50 years of age, this difference was not significant. On the other hand, women affected by ToF did not show significantly lower AAS values

for all the age bins when compared to normal CMR women. Fig. 14 shows the age-related changes of AAS over decades of age for all the above-mentioned subgroups.

Figure 14: ascending aortic strain over age in subgroup analysis

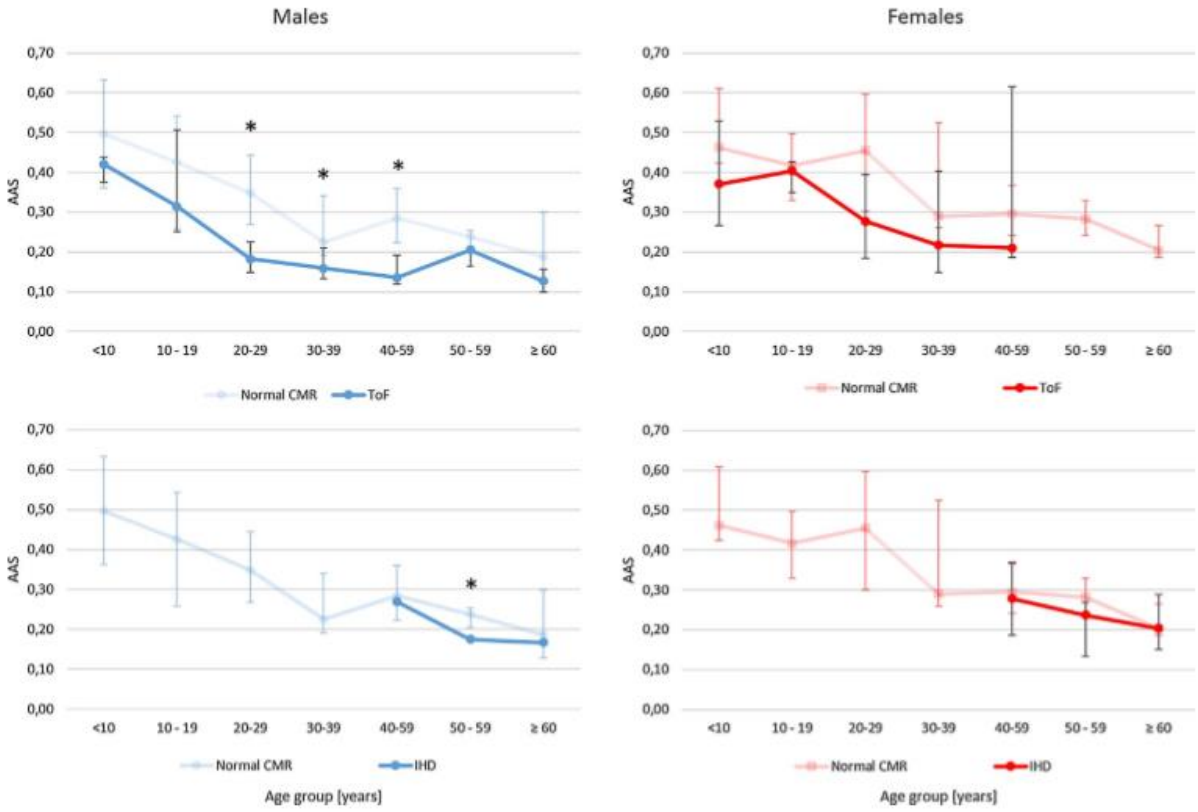

Ascending aortic strain (AAS) values over decades of age in subjects with normal cardiac magnetic resonance (CMR), patients with tetralogy of Fallot (ToF) and ischemic heart disease (IHD), divided by gender. Statistically significant comparisons are marked with a star (*).

Discussion

In this study, AAS values were analyzed in a large consecutive series of patients with different types of CVD and in subjects with normal (unremarkable) CMR. This study proved that difference in age, gender, and CVD independently affect the AAS.

Age distribution of the analyzed sample was characterized by two peaks, the first at age 15 and the second at age 60, as visible in Fig. 11, reflecting the high number of patients with congenital and age-related heart diseases in our series. This was confirmed by the fact that, among the analyzed

CVDs, the most frequent were IHD and ToF, which represent two different pathophysiological processes both affecting AAS: age-related factors and congenital/developmental factors, respectively.

Gender difference in AAS in the whole patient dataset was likely due to a different proportion between males and females in some CVD subgroups, since subjects with normal (unremarkable) CMR showed no significant gender difference in term of AAS. Gender-related differences appeared not to be influenced by age or CVD, although in patients with ToF there was a gender-related difference in AAS, in line with a previous study where differences in functional cardiovascular parameters between male and female patients with ToF was found [82]. Furthermore, other studies demonstrated a gender-related difference in arterial aging and stiffening process, suggesting that hormonal and other gender-specific factors can modulate the aging process [83].

Vascular changes with age are well-known. The progressive decrease in AAS during life reflects physiological and pathological modifications of mechanical, histological, and functional properties of the aortic wall. Moreover, differences in cardiac function and pulse wave reflection by medium and small arteries contribute to AAS. Animal studies indicated that age-related changes in aortic stiffness and strain may not entirely due to pathologic causes such as atherosclerosis and diabetes but also to physiological aging [9]. However, we found that patients with IHD have a significantly lower AAS compared to normal (unremarkable) CMR subjects between 50 and 59 years of age, highlighting the association between coronary artery disease and reduction in aortic elasticity.

Multivariate analysis showed the presence of significant differences in AAS among patient with different age, genders, and cardiovascular conditions. Moreover, these results show that the interaction among these parameters does not impact on AAS. In patients with certain diseases such as IHD, a decrease or increase in AAS is more easily explainable on the basis of different age, morpho-functional or pathophysiologic characteristics. On the other hand, in patients with other diseases such as ToF, the results are less obvious.

Patients with IHD showed a reduced AAS compared to normal CMR subjects between 50 and 59 years of age; this difference is reduced for subjects over 60 years of age, being not significant. This result may be due to a combination of factors: increased aortic stiffness determined by atherosclerosis

(more pronounced in patients with IHD) and reduced cardiac output, implying a decreased stretching of the ascending aorta. This value may however underestimate the real difference because subjects with normal CMR were not really healthy controls but patients with unremarkable CMR who may have had one or more CVD risk factors that could have contributed to a decrease in AAS.

AAS was significantly lower in patients with ToF than in patients with normal CMR, especially in males in the 3rd and 4th decade of life. This result is probably due at least in part to an intrinsic morpho-functional defect in ToF, described by other authors as a fragmentation of elastic fibres in aortic medial wall [84–89]. A similar study by Christensen et al. [89] highlighted the relationship between age at repair of ToF and AAS. One of the most though-provoking results was the poor correlation between AAS and PWV, highlighting the need for a local assessment of the aortic elastic properties. Our results were slightly different, the AAS being higher in the present study, probably due to the age difference in the study population or the timing of the ToF repair, with comparable correlations between AAS and ascending aortic cross-sectional area. The gender difference could reflect differences in biventricular volumes and function, as well as differences in timing and type of ToF treatment. Nonetheless, we could hypothesize that there is also a gender-related factor that affects AAS in ToF patients. AAS was also lower in patients affected by TGA and in those patients that underwent Fontan and Ross procedures, in accordance with previously reported findings [88, 90–92]. These results reaffirm the importance of including aortic morphological and functional evaluation in the follow-up of patients with congenital heart diseases.

Aortic strain reflects vascular compliance in large vessels and is lower in older patients. We did not find a significant difference in subjects over 60 regardless of the pre-existing diseases, probably because of the prevailing aging process [93]. Another possible explanation is that older subjects with a normal (unremarkable) CMR could have been exposed to the same risk factors and have ongoing pathophysiological processes similar to those affecting patients with IHD, making them less suitable for a direct comparison. On the other hand, differences in AAS in young patients with congenital heart disease could reflect a precocious arterial stiffening [10].

This study also showed that aortic strain can be easily and rapidly obtained using phase-contrast sequences usually performed for flow analysis; its evaluation and monitoring could be beneficial in detecting aortic stiffening. Moreover, it may be used for non-invasive follow-up evaluations of aortic condition in CVD patients.

This study is affected by several limitations mainly due to its retrospective design. Firstly, we should consider that prospective studies included blood pressure data measured after the sequence [88] since it is somewhat difficult to measure blood pressure during the acquisition of a CMR sequence. We could not include this parameter in our analysis. However, brachial blood pressure measurements could lead to an overestimation of central blood pressure and biased aortic distensibility. Secondly, we did not use a standardized plane placement on the ascending aorta. The sequences were not purposely acquired to measure aortic cross-sectional area but they were placed by the same operator above the aortic root to evaluate ascending aortic flow. For this reason the systolic motion of the ascending aorta due to myocardial contraction was not accounted for, similarly to another study [89]. Our technique, being simple and not relying on peak flow to choose the timing for plane placement in order to assess minimum and maximum area, is surely less accurate than the one used by Grotenhuis et al. [94]. Finally, we lack really healthy control subjects. Since the differences in terms of AAS were significant when comparing age matched subgroups of patients with normal (unremarkable) CMR and with CVD, we are confident that there was a significant reduction in AAS in at least two of the major subgroups of patients compared to what we expect in normal subjects of similar age.

In conclusion, we found that AAS is independently affected by differences in age, gender, and cardiovascular condition. In particular, this tendency was evident in patients with ToF and IHD, where the aging process seems to prevail on pre-existent differences in terms of AAS in subjects over 60. Our results highlight the possibility to use AAS for a non-invasive assessment of the aortic status in CVD patients. Nevertheless, further investigations on elderly patients and, in particular, in adults with congenital heart disease are advised.

Intra- and inter-reader reproducibility of blood flow measurements on the ascending aorta and pulmonary artery using cardiac magnetic resonance

Introduction

In the past years, cardiovascular magnetic resonance CMR has emerged as an alternative non-invasive imaging technique for the evaluation of patients with cardiovascular disease, providing an accurate anatomic and functional characterization of the heart and great vessels as well as the possibility to investigate nearly the whole spectrum of cardiac disease [95]. Especially for patients affected with congenital heart disease, CMR plays an important role in the quantification of blood flow and evaluation of valve stenosis/insufficiency using PC through-plane sequences [19, 96–103]. The PC sequences were validated in phantom and in vivo studies and have proven to be a reliable tool for the quantitative and qualitative analysis of blood flow and tissue motion.

Despite its importance for the assessment of disease progression, few data are available about the reproducibility of CMR in the measurement of blood flow in patients with valve stenosis and/or insufficiency [96, 104–106]. Moreover, segmentation methods were validated indirectly, through the ability to provide accurate flow measurement [104, 107] or pulse wave velocity [107, 108] or directly in terms of operator variability [104, 105] or agreement with manual tracing [108].

Blood flow measurements are based on the segmentation of a vessel contour that may be performed manually or, more typically, semi-automatically, with the use of computer software likely impacting on measurement reproducibility. Reader experience may play a role as well.

Thus, the aim of our study was to estimate the intra- and inter-reader reproducibility of blood flow CMR measurements through the ascending aorta and main pulmonary artery in patients affected with congenital heart disease or with aortic and/or pulmonary valve disease. The impact on reproducibility of the reader's experience with CMR was also investigated.

Materials and methods

Study design and population

The ethics committee approval was obtained for this retrospective study. A total of 50 consecutive patients affected with a congenital heart disease or with aortic and/or pulmonary valve disease were reviewed. They all underwent CMR at our institution between November 2012 and May 2013. Of 50 patients, 35 were males and 15 females, with a mean age of 27 ± 13 years (mean ± standard deviation). The disease spectrum is shown in Table 12. The majority of patients (n = 28, 56%) had a Tetralogy of Fallot.

Table 12: disease spectrum in 50 studied patients

Category	Detail	*n*	%
Aortic disease	Aortic insufficiency	1	2%
Pulmonary artery disease	Pulmonary insufficiency in ToF	28	56%
	Pulmonary insufficiency	7	14%
	Stenosis of pulmonary artery conduit	6	12%
	Pulmonary stenosis	3	6%
	Pulmonary steno-insuffi-ciency	2	4%
Other	VSD	2	4%
	Truncus arteriosus	1	2%
Total		50	100%

ToF: tetralogy of Fallot; VSD: ventricular septal defect.

Images acquisition

All CMR examinations were performed with a 1.5-T unit with 40-mT/m gradient power (Magnetom Sonata Maestro Class, Siemens Medical Solution, Erlangen, Germany), using a four-channel surface phased-array coil placed over the thorax and with the patient in supine position.

A CMR study included a complete set of short-axis (from base to apex) and long-axis (2-, 3- and 4-chamber views) cine images, using an ECG-triggered breath-hold steady-state free precession sequence acquired with the following technical parameters: TR/TE 4.0/1.5 ms; flip angle 80°; slice thickness 7 mm; time resolution 45 ms; mean acquisition time 14 ± 4 s.

The PC through-plane sequences were used for blood flow quantification. Images perpendicular to the vessel of interest were obtained. A breath-hold turbo spoiled gradient echo sequence (fast low-angle shot) was performed for phase-velocity mapping with the following technical parameters: TR/TE 4.0/3.2 ms; slice thickness 5 mm; VENC from 150 cm/s to 350 cm/s; time resolution 41 ms; mean acquisition time 15 ± 4 s. For each patient, we initially acquired the PC sequence with a VENC of 150 cm/s: in the presence of aliasing, we increased the VENC adding 50 cm/s for each new sequence, step-by-step up to the complete disappearance of the aliasing artifact.

Images analysis

Flow measurements were performed right above the aortic or pulmonary valve in patients with surgical or percutaneous valve replacement. In patients without valve replacement, measurements were performed below, at the level and above the native valve. The PC sequences produced two sets of images: the gradient echo image and the phase velocity map (Fig. 15). The magnitude image depicts the anatomy and allows to identify the vessel boundaries, while the phase velocity map corresponds to blood velocity [96].

Figure 15: example of pulmonary artery segmentation

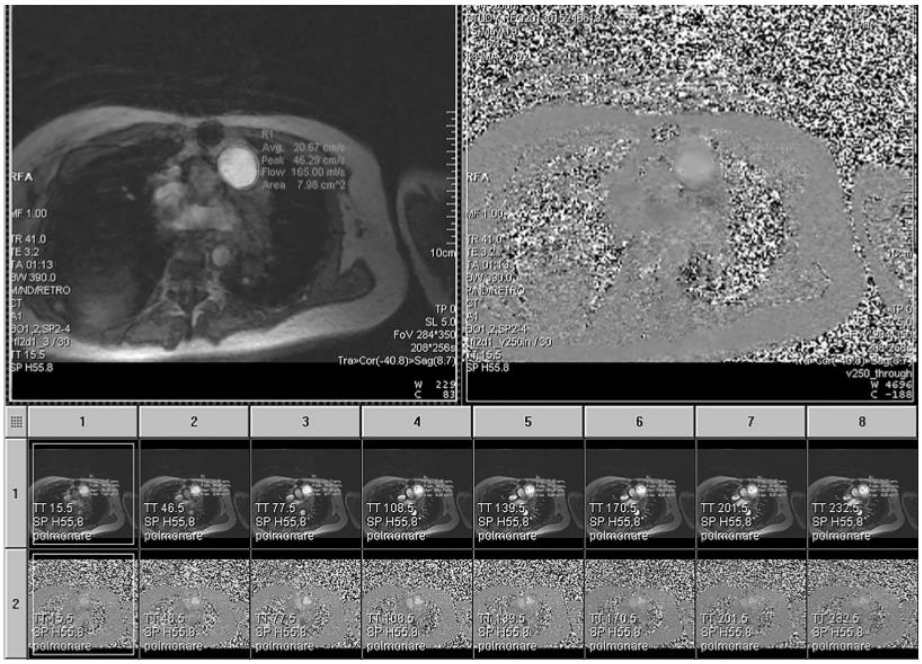

The image represents the pulmonary artery segmentation showing the gradient echo image, with a region of interest right after the valve, and the phase velocity map with the same ROI

Two independent readers (R1 and R2) performed measurements twice, with at least a 10-day interval between the two sessions, for a total of four sessions. These readers had different educational background and different level of training in CMR segmentation. While R1 was a radiology resident with 4 months of full-immersion training (under the supervision of a radiologist with a 5-year experience in CMR), R2 was a technician student with 2 weeks of training (under the supervision of the same experienced radiologist).

Both readers used the Argus software on a remote workstation (Leonardo, Siemens Medical Solution, Erlangen, Germany). For each patient, the reader positioned a region of interest on the vessel boundary of a selected slice and propagated the segmentation through the remaining slices. Then, the software proposed an automated adjustment and the reader was allowed to manually correct the adjusted contours (hence semi-automated method). Blood peak velocity, forward and backward flows were obtained. An example of flow analysis is shown in Fig. 15.

Intra- and inter-reader reproducibility was estimated using the Bland–Altman method; for the inter-reader reproducibility the first measurement of both readers was used. The CoR was calculated as 1.96 × standard deviation of differences of the two compared datasets. Reproducibility was reported as complement to 100% of the ratio between the CoR and the mean. Bland–Altman graphs were plotted as well, showing bias (mean of the differences of the two compared datasets), and 95% limits of agreement (bias ± CoR).

Results

Of 50 analyzed patients, 46 (92%) had a pulmonary disease, two (4%) ventricular septal defect, one (2%) aortic insufficiency, and one (2%) truncus arteriosus. Further details are reported in Table 13.

Image analysis was feasible in all patients and no malformations or artifacts prevented from a correct segmentation. The PC sequence showed no artifacts in patients with a surgical or percutaneous valve replacement. The time needed for measurement was about 5 min per patient, without substantial difference between the two readers.

The mean blood peak velocity of the aortic flow measured by R1 was 103 cm/s, accompanied by a CoR of 1 cm/s, corresponding to an intra-reader reproducibility of 99%; the same data for R2 were 103 cm/s, 9 cm/s, and 92%. The mean blood peak velocity of the pulmonary flow measured by R1 was 180 cm/s, accompanied by a CoR of 1 cm/s, corresponding to an intra-reader reproducibility of 99%; the same data for R2 were 181 cm/s, 3 cm/s, and 98%. Further details are reported in Table 2 for R1 and in Table 3 for R2, while Bland–Altman plots for R1 only are shown in Fig. 16.

Table 13: first reader intra-reader reproducibility

	Aortic flow			Pulmonary flow		
	Peak velocity (cm/s)	Forward (ml/beat)	Backward (ml/beat)	Peak velocity (cm/s)	Forward (ml/beat)	Backward (ml/beat)
Mean	103	69	3	180	91	23
Bias	−0.1	−0.1	−0.1	0.1	0.1	0.3
CoR	1	3	1	1	8	2
Reproducibility	99%	95%	49%	99%	91%	90%

Figure 16: Bland-Altman plot for intra-reader reproducibility

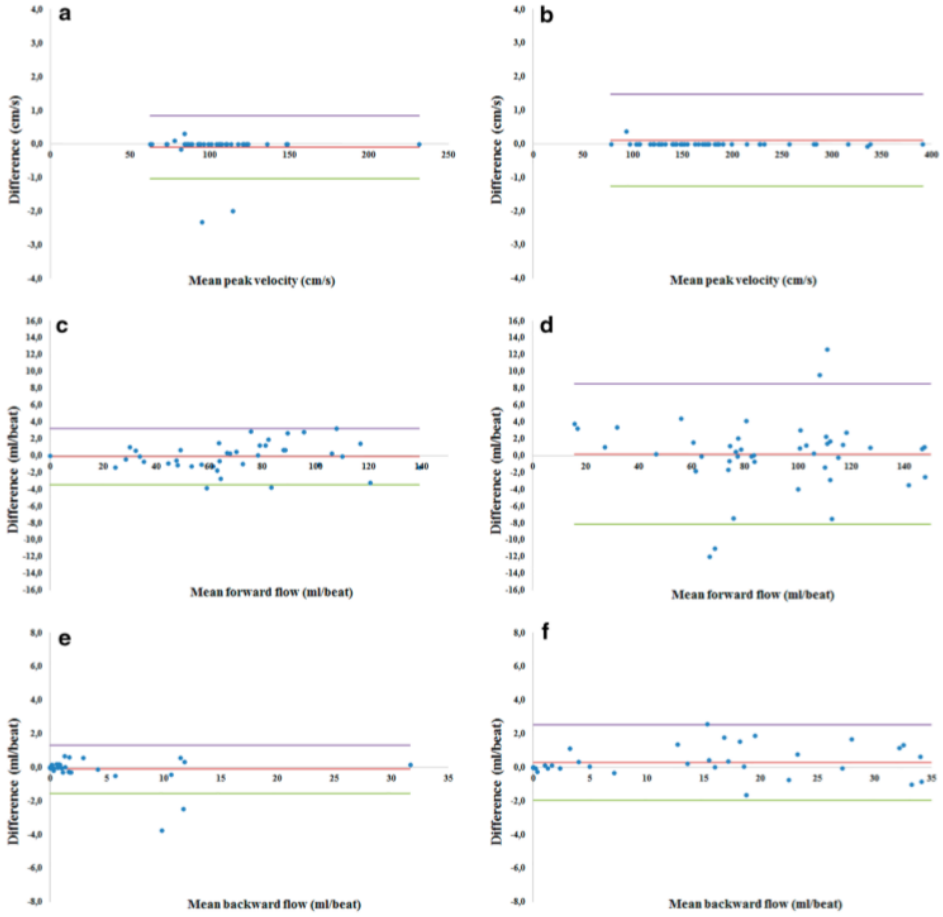

Bland–Altman plots for intra-reader reproducibility analysis of the first reader: a and b peak velocity, c and d forward flow and e and f backward flow of the aorta (left column) and pulmonary artery (right column).

The inter-reader reproducibility analysis of the aortic flow peak velocity showed a CoR of 10 cm/s, over a mean of 103 cm/s, corresponding to an inter-reader reproducibility of 91%; the same data for the pulmonary flow were 7 cm/s, 180 cm/s, and 96%. Further details regarding the inter-reader reproducibility are reported in Table 14, while Bland–Altman plots are shown in Fig. 17.

Table 14: inter-reader reproducibility results

	Aortic flow			Pulmonary flow		
	Peak velocity (cm/s)	Forward (ml/beat)	Backward (ml/beat)	Peak velocity (cm/s)	Forward (ml/beat)	Backward (ml/beat)
Mean	103	69	3	181	89	23
Bias	−0.6	0.7	−0.2	−0.3	1.5	0.1
CoR	9	6	2	3	12	3
Reproducibility	92%	91%	38%	98%	86%	87%

Figure 17: Bland-Altman plot for inter-reader reproducibility

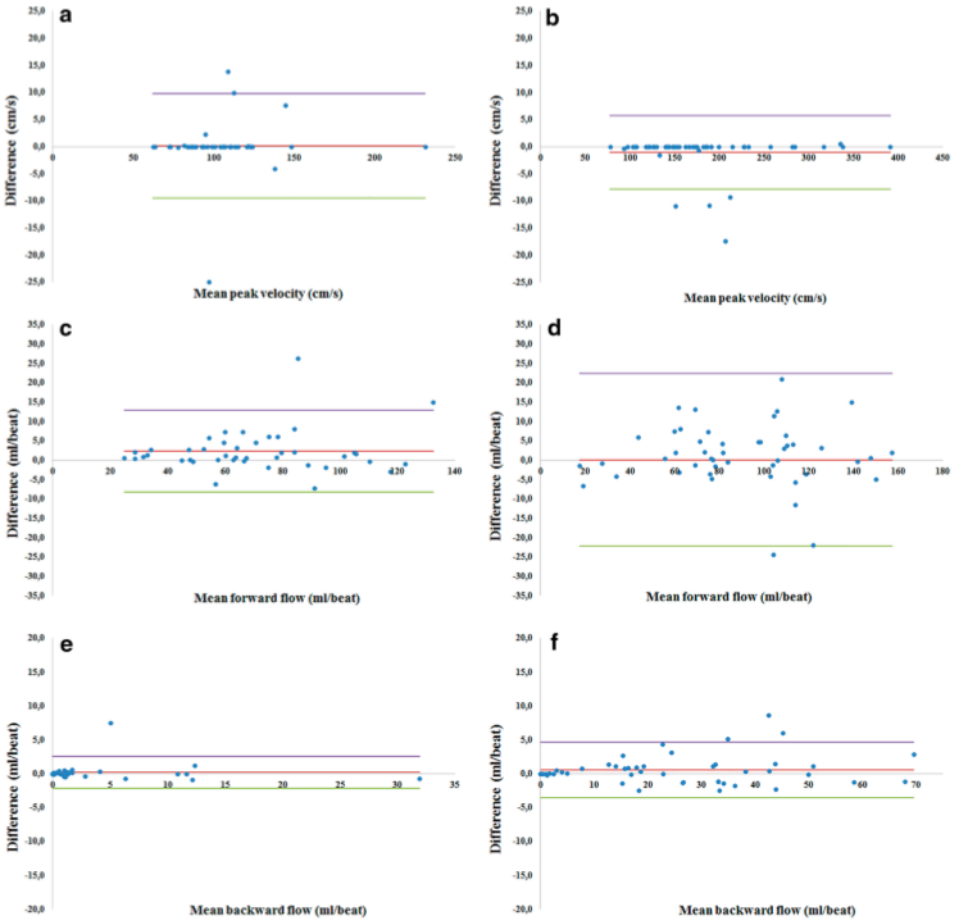

Bland–Altman plots for inter-reader reproducibility analysis: a and b peak velocity, c and d forward flow and e and f backward flow of the aorta (left column) and pulmonary artery (right column).

Discussion

Cardiac magnetic resonance has emerged as a reliable imaging technique for assessing heart valve disease, quantify its severity, and to evaluate its effect on the heart morphology and function [19, 95, 96, 98]. It is used for evaluating cardiomyopathy-related valve dysfunction since more than two decades [109]. Patient management using CMR includes follow-up for treatment effect monitoring or disease progression [110, 111].

Reproducibility means the ability of a reader to provide the same values when repeating the measurement, a number of times. If two or more readers are involved in the patient management, they need to provide as similar as possible results when analyzing a given CMR examination. When a follow-up measurement is performed on a patient, the clinician needs to identify a true change that can be ascribed to treatment effect or worsening of disease, rather than to measurement errors [112]. In this scenario, the readers' experience may play a role and skilled operators may be necessary.

In this study, we obtained a good-to-excellent intrareader reproducibility of CMR in flow measurement for all variables under consideration, except for the backward flow of the ascending aorta. Indeed, intra-reader reproducibility was higher than 90% for the trained reader (R1) and higher than 86% for the lower trained reader (R2). Such a good result may be due thanks to the semi-automated method used for segmentation that is not difficult to be used also by less experienced readers [101]. This means that a reader's learning curve should be short and that the segmentation of vessel boundaries through a semi-automated method may also be performed by not highly specialized personnel. Probably, if we had used a manual method of segmentation we could have found a lower reproducibility for the untrained reader. However, although of a small magnitude, data suggest an additional reproducibility of R1 over R2, likely due to the different educational background and the different level of training [101].

Inter-reader reproducibility, even if reaching a maximum of 96% for the blood peak velocity of the pulmonary artery, decreased to 75 and 82% for the forward and backward flow of the pulmonary artery, respectively, being lower than that observed in previous studies. Van Der Geest et al. compared

an automated contour detection algorithm for analysis of the ascending aorta flow with a fully manual segmentation, showing intra- and inter-reader variability lower than 2% for both manual and automated methods [104]. Conversely, Herment et al. demonstrated a higher inter-reader variability for manual tracing than for automated segmentation using PC CMR images in healthy volunteers and in patients with a dilated aorta [105].

The backward flow of the ascending aorta deserves some considerations. In fact, a low to very low reproducibility for this variable was obtained, being lower than 50% for the intra-reader analysis and equal to 20% for the inter-reader analysis. This is only an apparently negative result being mainly related to the low magnitude of the ascending aorta backward flow, even in patients with aortic insufficiency. Reproducibility being given as percentage of the mean, even subtle measurement variations due to small differences in segmentation may have a strong negative impact on reproducibility.

The major limitation of this study is that results are related to the particular 1.5-T unit used for imaging patients and to the sequences and technical parameters used, also including the use of breath-hold or respiratory gating for avoiding artifacts from respiratory movements. However, 1.5-T magnets are mostly used for cardiac imaging and our imaging protocol is quite generally accepted. Thus, our results should be generalizable. Another limitation may be the study population that included patients affected with different cardiovascular diseases (even if the majority of patients had a Tetralogy of Fallot) who had a pathology of the aortic and/or pulmonary valve. However, we wanted to estimate the intra- and inter-reader reproducibility in a heterogeneous population for a higher generalizability. Probably, limiting to a more homogeneous population could demonstrate an even higher reproducibility.

In conclusion, this study showed a good-to-excellent intra- and inter-reader reproducibility of blood flow measurements in patients with congenital heart disease using CMR and a semi-automated method of segmentation, with a limited impact of the operator's training.

Section III

–

To share or not to share our trial data?

To share or not to share? Expected pros and cons of data sharing in radiological research

Introduction

In clinical research, spontaneous data sharing is not yet as common as it is in other fields such as genetics, astronomy or physics [11]. However, the concept of data sharing has been suggested for many reasons, including the patient-centered nature of medical research and healthcare and the expectation that knowledge from existing data should be maximized to benefit all stakeholders.

Although a transition to data sharing is a process that will take time and planning, those who adopt the principles and practices of open science will likely benefit from it [12, 13]. In addition, the emergence of data sharing as a potential requirement by some agencies and journals warrants attention by the imaging community. Indeed, from July 1st, 2018 the ICMJE will require a data sharing statement as a condition of consideration for publication of clinical trials [14]. In this article, we discuss potential advantages and disadvantages of data sharing.

From open-access to data sharing

A trend towards larger accessibility to scientific medical knowledge is already visible in the progressive tendency of medical journals in ensuring the open-access option, in which the authors or their institutions pay an article-level fee to guarantee the immediate free availability of their papers [113].

In Table 15 we report the policies of all the 18 general imaging journals on access and data sharing [114–125]. This was derived from the current Thomson Reuters list – Radiology, Nuclear Medicine, and Medical Imaging. For comparison, the 17 most-impacted general medicine journals were selected from the current Thomson Reuters list – Medicine, General and Internal [126–143]. Among the 18 imaging journals, four are open access, 12 offer open access as an option (Radiology provides free access 12 months after publication), and two do not offer an open-access option. Among the 17 medical journals, six are open access (The Medical Journal of Australia only for research

articles and case reports), eight offer open access as an option (Journal of the American Medical Association [JAMA] provides free access 6 months after publication), two do not offer an open access option, and one (The New England Journal of Medicine [NEJM]) provides free access to research articles 6 months after publication. Thus, the open access option is currently widely adopted by both general imaging journals (11/18) and general medicine journals (8/17).

Table 15: policies on access and data repository or sharing by major general imaging journals and major general medicine journals

Journal	Access[1]	Data repository or sharing[2]
General imaging journals		
Acad Radiol	Open access option	Not mentioned
Acta Radiol	Open access option	Requested
Am J Roentgenol	No open access option	Not mentioned
BMC Med Imaging	Open access	Encouraged
Br J Radiol	Open access option. Articles freely available more than 12 months after publication	Encouraged
Clin Radiol	Open access option	Not mentioned
Eur J Radiol	Open access option	Not mentioned
Eur Radiol	Open access option	Not mentioned
Invest Radiol	Open access option	Not mentioned
Iran J Radiol	Open access	Not mentioned
J Am Coll Radiol	Open access option	Not mentioned
JBR-BTR	Open access	Not mentioned
Jpn J Radiol	No open access option	Upon request
Korean J Radiol	Open access	Not mentioned
Radiol Med	Open access option	Encouraged
Radiologe	Open access option	Not mentioned
Radiology	Open access option. Articles freely available 12 months after publication	Upon request
Rofo	Open access option	Not mentioned
General medicine journals		
Am J Med	Open access option	Not mentioned
Ann Intern Med	No open access option	Encouraged
BMC Medicine	Open access	Encouraged
Br J Gen Pract	Open access option	Not mentioned
Br Med Bull	Open access option	Not mentioned
BMJ	Open access option	Encouraged
BMJ Open	Open access	Encouraged
CMAJ	Open access option	Requested only for clinical trials of drugs and medical devices
Dtsch Arztebl Int	Open access	Not mentioned
Eur J Clin Invest	Open access option	Encouraged
Int J Med Sci	Open access	Not mentioned
Lancet	Open access option	Encouraged
JAMA	Open access option. Research articles freely available 6 months after publication	Upon request
Med Clin North Am[3]	No open access option	Not mentioned
Med J Aust	Open access for research articles and case reports	Not mentioned
New England J Med	Original articles and special articles freely available 6 months after publication.	Requested for data obtained by microarray
PLoS Med	Open access	Requested

Note: Imaging journals were selected for being general (not subspecialty) journals from the Thomson Reuters list – Radiology, Nuclear Medicine, and Medical Imaging (n=18). For comparison, the general medicine journals from the first quartile were selected from the Thomson Reuterslist – Medicine, General and Internal (n=17).

[1]Most journals offer free accessibility for selected articles.

[2]Despite individual journals do not mention any policy on data sharing, some publishers (e.g. Elsevier) have their own general rules to which refer to. Moreover, when data sharing is encouraged, authors are informed to be prepared to provide original study data if requested by the editors.

[3]Publishes only invited reviews.

The practice of data sharing entails much more than open access. It is the regulated availability of the original participant-by-participant data obtained during a study, which may include data not yet analyzed. Among the 18 general imaging journals, data sharing is not even mentioned by 12 journals, encouraged by three, mandatory only upon request in two, and requested by one. Among the 17 general medicine journals, it is not mentioned by seven journals, encouraged by six, requested by three (NEJM only for data obtained by microarray), and considered mandatory only up on request by one (Table1). In practice, data repository or sharing is currently not mentioned in the instructions for authors of the majority of general imaging journals (14/18) and major general medicine journals (10/17). Despite individual journals do not mention any policy on data sharing, some publishers such as Elsevier have their own general suggestions, which refer to Open Access [118], even though not immediately visible to the authors when they submit a manuscript. When data sharing is encouraged, authors are informed they should be prepared to provide original study data if requested by the editors.

In recent years, several funding bodies declared the necessity for data sharing. In 2015, the U.S. National Institutes of Health (NIH) expressed its intention to request making the digital data from NIH-funded studies publicly available [144]. Regulatory agencies, specifically the European Medicines Agency, have requested greater data sharing by companies manufacturing drugs and clinical devices. Influential organizations such as the World Health Organization and the U.S. National Academy of Medicine published reports asking for responsible sharing of data from clinical trials [145]. Also, several foundations, for instance the Alfred P. Sloan Foundation [146], the Bill and Melinda Gates Foundation [147], the Ford Foundation [148], the Gordon and Betty Moore Foundation [149], and the National Science Foundation [150], require data sharing and data management plans for all research grant proposals.

The pharmaceutical industry also plays a role in promoting data sharing. The Yale University Open Data Access (YODA) project [151] performs independent scientific review of investigators' requests for pharmaceutical and medical data from clinical trials on devices marketed by Johnson & Johnson, including both full clinical study reports and participant level data. Notably, the YODA project has obtained permission to make independent decisions about the release of Johnson &

Johnson's clinical trial data. This project establishes a process in which requests are judged fairly and decisions are made by an independent academic partner, a model that could be applied to other fields of medicine [151].

Another example is the Academic Research Organization Consortium for Continuing Evaluation of Scientific Studies – Cardiovascular (ACCESS CV) [152]. They propose a secure method for sharing patient-sensitive data that combines the protection of patients' identity with the legitimate desire of the scientific community for data access and the viewpoint of the researchers who created the database. This approach consists of the following steps: (1) After publication of the primary results of a trial, researchers interested in the study data may send a request to the trial's publication committee; (2) Twenty-four months after the publication of the primary study, requests should be considered by a review group composed of members of ACCESS CV not involved in the trial, the trial principal investigator, a trial statistician, and a member of the data and safety monitoring board. This committee evaluates all proposals to approve those that are feasible, hypothesis-based, non-duplicative, and guided by investigators with technical capability and a plan for publication. The period of 24 months is chosen to secure the database and to allow the original investigators to perform their own preplanned secondary analyses; (3) All requests and subsequent decisions will be posted on an ACCESS CV Web portal, ideally within 60 days [152].

In the field of radiology, data sharing also means accessibility to medical images. Indeed, "Images are more than pictures, they are data" [153]. This implies access to the images produced in a given study for additional reading, interpretation, and extraction. To this end, several image repositories were created. An example is the XNAT Central [154, 155], a publicly accessible data repository based on the XNAT open-source platform which hosts a wide variety of research imaging datasets, especially from neuroimaging, but also from oncology, orthopedics and cardiology. Other examples are The Cancer Imaging Archive [156] and the Lung Image Database Consortium [157].

Such repositories may be very helpful in several fields, especially for image biomarker development, radionics and machine learning, each field demanding different approaches. Moreover, the integration, standardization and analysis of these data poses a big challenge, the solution to which

may be addressed using cognitive computing. An example of cognitive computing is the system developed by IBM named Watson (IBM Watson Health Imaging, Armonk, NY, USA). It strives to organize available information and present it in a contextually relevant, probability-driven manner to assist healthcare professionals in an objective manner, whether at a reading workstation or at the point-of-care [158]. An important change is underway. To make datasets from medical research publicly available in a timely fashion requires regulations that maximize the benefits and minimize the risks [159, 160]. Indeed, data sharing provides a potential for stimulating new ideas, avoiding duplication of trials, and enhance transparency [144, 161–164] as well as increasing collaboration and interdisciplinary research [11, 165, 166]. However, at the same time, sharing clinical data presents some risks, burdens and challenges such as the need to preserve the privacy of patients, to defend the legitimate economic interests of the sponsors, and to guard against invalid secondary analyses potentially undermining trust in clinical trials or otherwise harming public health [144, 145, 160, 167].

Potential benefits of data sharing

These can be subdivided into: (i) verification and advancement in knowledge; (ii) reduced cost and time for clinical research; and (iii) clinical improvement (Fig. 18).

Figure 18: expected pros and cons of data sharing. IPD individual patient data meta-analyses

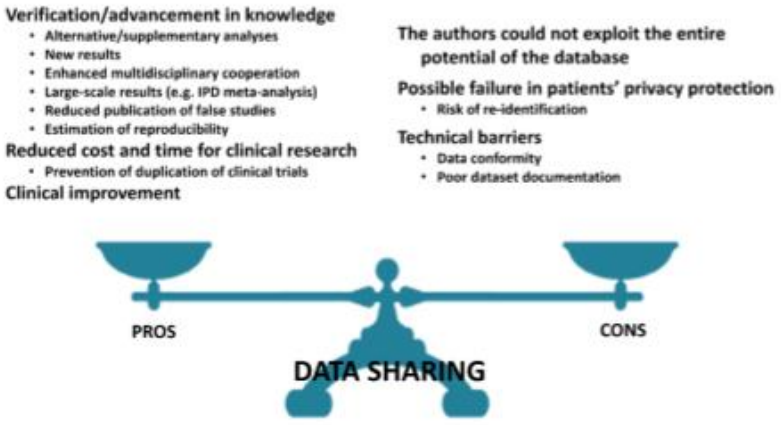

Verification and advancement in knowledge

The first potential implication of data-sharing is the verification by independent authors of the results presented in a given publication. When data are shared, they may be used by other researcher stopper form alternative or supplementary analyses. This ‘second-hand’ analysis may show results in support of the initial findings or could reveal errors or inconsistencies in the original research or could identify issues needing extended analysis.

In other cases, data sharing can allow elucidation of new results. New findings can be disclosed starting from hypotheses not considered by the original study team. New insights can be presented from existing data but not yet analyzed in the original publication(s). Also, investigators may be interested in performing the analysis of datasets coming from various sources to enhance precision, i.e. to perform reproducibility analyses across different databases, regarding established theories or new hypotheses. In fact, reproducibility analysis is crucial for emergent topics in radiology such as standardization of imaging biomarkers, especially from magnetic resonance imaging [168]. The availability of databases from different studies could allow for this gap to be filled and could help in translating new imaging biomarkers into clinical practice [169]. In this regard, reproducibility analysis could become one of the main advantages of data sharing.

The introduction of registries of patients affected with a defined disease could be considered a primitive form of data sharing [170, 171], important not only for widespread diseases, such as cancers, but especially for rare diseases.

Another approach of spontaneous data sharing is that underlying individual patient data meta-analyses [172]. Authors of an individual patient data meta-analysis typically contact the authors of each eligible study asking to share their data, with the aim of creating a new unique individual-patient database. Of note, the power of the individual-patient data approach is higher than that of conventional (study-level) meta-analyses, which rely on complex statistical methods [173]. For instance, in a study published by Marinovich et al. [174] on the agreement between MRI and pathological breast tumor size after treatment, a total of 24 studies (1,228 patients) were eligible for inclusion, but only eight of

these contributed to the individual-patient data analysis for a total of 300 patients. Had regulated data sharing been in place, that individual patient data meta-analysis would have included a much richer dataset. Moreover, data sharing could boost a wider adoption of health technology assessment. Indeed, in the context of a new product evaluation, data sharing may be useful in the validation level, requiring a high number of data/images, rather than at the initial development level.

Another potential advantage of data sharing is to reduce the publication of false studies, especially when the data are intentionally falsified. Recently, 64 articles were retracted from ten Springer journals after editorial checks found fake email addresses, and subsequent internal investigations uncovered fabricated peer-review reports [175]. This retraction came only a few months after BioMed Central had retracted 43 articles for the same reason; however, this phenomenon involved most major publishers such as also SAGE, Elsevier, Informa, and Lippincott Williams & Wilkins [176]. Data sharing might discourage data creation and manipulation, potentially more detectable in a complete database than in reported results.

Reduced cost and time for clinical research

Data sharing could potentially lead to an optimization of time and costs of clinical research by preventing the duplication of trials [177, 178]. For example, costs for the stipulation of insurances for patients' coverage, the purchase of materials or the salaries of the staff responsible for data collection can be avoided. In addition, using an existing shared database, the new results could be obtained many years prior to those derived from a new clinical study.

Clinical improvement

An effect in terms of clearer evidence on the safety and effectiveness of diagnostic procedures and therapies, improving public healthcare [179–181], may be considered the final aim of data sharing. To avoid the loss of findings contained in the original dataset and not used for the primary publication(s) could play a role in this direction [160]. Institutions sharing their data could obtain a more

comprehensive picture about the benefits and risks of a medical decision. However, a real clinical improvement from data sharing is a hypothesis that still needs to be demonstrated.

Potential drawbacks from data sharing

The sharing of clinical databases raises several concerns (see Fig. 18). One of the reasons not to share data is that researchers are evaluated competitively, based on the quality and number of articles published during their career, so they may worry that other people will use their data and efforts to produce new publications. The potential for secondary analyses contradicting initially reported results may be deterrent. Authors may not be willing to share data that had cost them great effort and resources. However, reciprocally, they would also directly benefit from using someone else's data.

Bierer et al. [182] recently suggested formalizing 'data authorship' as an incentive to data sharing: "as a matter of fairness and as a matter of providing an incentive for data sharing, the persons who initially gathered the data should receive appropriate and standardized credit that can be used for academic advancement, for grant applications, and in broader situations".

Another concern is the potential for fault in the patient identity protection caused by the transmission of sensitive information. Data must be de-identified: de-identification, not simply anonymization, consists of transforming a dataset so that the back identification of individuals becomes impossible or extremely difficult. Different regulations may require different degrees of de-identification, particularly in the absence of informed consents specifying the possibility of data sharing. De-identification can be achieved with different types of data transformations that must ensure patient privacy without affecting data quality [183]. However, the de-identified data do not eliminate all risks of re-identification. Moreover, the reduction of this risk to zero may destroy or significantly impair the utility of the data for subsequent analysis or verification. For these reasons, the stipulation of Data Use Agreements (DUAs) is considered a useful strategy and best practice for increasing the benefits and mitigating the risks of clinical data sharing [184]. Specifically, DUAs address important issues such as limitations on date usage, obligations to data safeguard, liability for harm arising from data usage and publication, and privacy rights that are associated with transfer of

confidential or protected data. In contrast, the U.S. Office for Human Research Protections stated that there is no need for separate consent from trial participants for the sharing of de-identified data [14].

A limitation to the adoption of data sharing can originate from technical barriers. The image conformity is influenced by vendor, modality, and acquisition parameters on the one hand; and by image post-processing manufacturer, reconstruction parameters, and software versions, on the other hand. An example is represented by the use in magnetic resonance of arbitrary units that clearly depend on the specific vendor and model, making a between-study comparison impossible. Away to overcome this limitation could be a drastic standardization, with manufacturers defining new shared standards.

Another intrinsic barrier to data sharing could be the poor documentation of datasets, especially if not documented in English. Moreover, important information about methodology might not be contained immediately in the database or immediately retrievable. All these issues should be considered when planning for potential data sharing of research.

To share or not to share?

In conclusion, in a world that moves towards greater transparency and privacy protection, data sharing stands between these two competing interests. Not all concerns on data sharing have already been solved and many questions remain to be addressed: Who is the rightful owner of the data? What is the role of individual patients and advocacy groups in decision making about sharing of data and images? Should Ethics Committees change their approach for study approval? And how? What is the exact role of institutions, especially public ones, that funded the original study? Should patient advocacy groups and funding organizations be involved in decision making about data sharing? These issues must be regulated.

Despite all the above-described issues relating to data sharing, a transition to a more open medical science has begun. If benefits of data sharing will be more and more perceived as prevailing over harms therefrom, this option will win. Researchers and institutions who first seize this opportunity will

be on the wave-front of an innovation likely to be in favor of patients and public health. Radiologists should be kept informed of this emerging issue. It is time to share!

Conclusions

–

Conclusions

Imaging techniques play a main role in heart impairment diagnosis, etiological evaluation and treatment guidance; in particular CCT and CMR could provide additional information, especially in selected populations. This thesis reviewed potential future applications of imaging modalities for the study of CHD to improve the management of these patients.

We contributed to show the possibility to obtain an impressively low ionizing dose reduction in CHD patients using a dedicate acquisition protocol on a standard 64-slice CT scanners. This really open a new windows of opportunities for using CCT in CHD, especially when CMR requires long sedation times and a high spatial resolution is considered useful for treatment planning [3].

On the other hand, CMR holds a pivotal role when functional and flow imaging is required. Firstly, we showed the role of MRS in evaluating the heart dysfunction on patients with HCM demonstrating that 1H-MRS may be used as an additional final phase of CMR protocol in the differential diagnosis between HMC and athlete's heart [4].

Secondly, we successfully validated the use of a BT technique for the segmentation of cine images in patients with FC, also observing a high intra- and inter-reader reproducibility for the assessment of ventricular SV and excellent agreement with aortic flow values used as a benchmark [5].

Third, we highlighted the possibility to use AAS for a non-invasive assessment of the aortic status in CVD patients [6].

Last but not least, we showed a good-to-excellent intra- and inter-reader reproducibility of blood flow measurements in patients with congenital heart disease using CMR and a semi-automated method of segmentation, with a limited impact of the operator’s training [7].

In conclusion CCT and CMR are two fundamental imaging techniques to evaluate patients with complex CHD. In the last years, we are moving from a competition to cooperation between CCT and CMR. Both imaging modalities have limitations and advantages. CCT has a very high spatial resolution and short acquisition time but implies ionizing radiation exposure, while CMR can evaluate

heart function vessel flow but require a long acquisition time and in same patients a long sedation time. On the one side, we confirming the crucial role of CMR when function analysis is required but also showed the relevant possibilities of x-ray dose reduction in CCT, also using standard 64-slice scanners in the study of CHD patients.

To definitively confirm our results, more large and multi-centric studies will be necessary. In this sense, a wide and coordinated cooperation between the different research centers in sharing their data could lead to new and interesting results [15].

References

1. Mitchell SC, Korones SB, Berendes HW (1971) Congenital heart disease in 56,109 births. Incidence and natural history. Circulation 43:323–32.

2. Bernier P-L, Stefanescu A, Samoukovic G, Tchervenkov CI (2010) The Challenge of Congenital Heart Disease Worldwide: Epidemiologic and Demographic Facts. Semin Thorac Cardiovasc Surg Pediatr Card Surg Annu 13:26–34.

3. Secchi F, Di Leo G, Zanardo M, et al (2017) Detection of incidental cardiac findings in noncardiac chest computed tomography. Med (United States). doi: 10.1097/MD.0000000000007531

4. Secchi F, Di Leo G, Petrini M, et al (2017) 1H- and 31P-myocardial magnetic resonance spectroscopy in non-obstructive hypertrophic cardiomyopathy patients and competitive athletes. Radiol Med. doi: 10.1007/s11547-016-0718-2

5. Secchi F, Alì M, Petrini M, et al (2018) Blood-threshold CMR volume analysis of functional univentricular heart. Radiol Med 123:331–337.

6. Scarabello M, Codari M, Secchi F, et al (2018) Strain of ascending aorta on cardiac magnetic resonance in 1027 patients: Relation with age, gender, and cardiovascular disease. Eur J Radiol. doi: 10.1016/j.ejrad.2017.12.002

7. Di Leo G, D'Angelo ID, Alì M, et al (2016) Intra- and inter-reader reproducibility of blood flow measurements on the ascending aorta and pulmonary artery using cardiac magnetic resonance. Radiol Med. doi: 10.1007/s11547-016-0706-6

8. Secchi F, Resta EC, Di Leo G, et al (2014) Segmentation of cardiac magnetic resonance cine images of single ventricle: including or excluding the accessorial ventricle? Int J Cardiovasc Imaging 30:1117–1124.

9. Mattace-Raso FUS, van der Cammen TJM, Hofman A, et al (2006) Arterial stiffness and risk of coronary heart disease and stroke: the Rotterdam Study. Circulation 113:657–63.

10. Redheuil A, Yu W-C, Wu CO, et al (2010) Reduced ascending aortic strain and distensibility: earliest manifestations of vascular aging in humans. Hypertens (Dallas, Tex 1979) 55:319–26.

11. Ross JS, Lehman R, Gross CP (2012) The importance of clinical trial data sharing: toward more open science. Circ Cardiovasc Qual Outcomes 5:238–40.

12. Boulton G, Rawlins M, Vallance P, Walport M (2011) Science as a public enterprise: the case for open data. Lancet (London, England) 377:1633–5.

13. Walport M, Brest P (2011) Sharing research data to improve public health. Lancet 377:537–539.

14. Taichman DB, Sahni P, Pinborg A, et al (2017) Data Sharing Statements for Clinical Trials — A Requirement of the International Committee of Medical Journal Editors. N Engl J Med 376:2277–2279.

15. Sardanelli F, Alì M, Hunink MG, et al (2018) To share or not to share? Expected pros and cons of data sharing in radiological research. Eur Radiol. doi: 10.1007/s00330-017-5165-5

16. Watson TG, Mah E, Joseph Schoepf U, et al (2013) Effective radiation dose in computed tomographic angiography of the chest and diagnostic cardiac catheterization in pediatric patients. Pediatr Cardiol 34:518–524.

17. Jhang WK, Park J-J, Seo D-M, et al (2008) Perioperative evaluation of airways in patients with arch obstruction and intracardiac defects. Ann Thorac Surg 85:1753–8.

18. Taylor AM (2008) Cardiac imaging: MR or CT? Which to use when. PediatrRadiol 38 Suppl 3:S433–S438.

19. Secchi F, Di Leo G, Papini GDE, et al (2011) Cardiac magnetic resonance: impact on diagnosis and management of patients with congenital cardiovascular disease. Clin Radiol 66:720–5.

20. Han BK, Rigsby CK, Hlavacek A, et al (2015) Computed Tomography Imaging in Patients with Congenital Heart Disease Part I: Rationale and Utility. An Expert Consensus Document of the Society of Cardiovascular Computed Tomography (SCCT): Endorsed by the Society of Pediatric Radiology (SPR) and the Nor. J Cardiovasc Comput Tomogr 9:475–492.

21. Meinel FG, Henzler T, Schoepf UJ, et al (2015) ECG-Synchronized CT Angiography in 324 Consecutive Pediatric Patients: Spectrum of Indications and Trends in Radiation Dose. Pediatr Cardiol 36:569–578.

22. Nijhof WH, Van Der Vos CS, Anninga B, et al (2013) Reduction of contrast medium volume in abdominal aorta CTA: Multiphasic injection technique versus a test bolus volume. Eur J Radiol 82:1373–1378.

23. Cademartiri F, Nieman K, van der Lugt A, et al (2004) Intravenous contrast material administration at 16-detector row helical CT coronary angiography: test bolus versus bolus-tracking technique. Radiology 233:817–823.

24. Henzler T, Hanley M, Arnoldi E, et al (2010) Practical strategies for low radiation dose cardiac computed tomography. J Thorac Imaging 25:213–20.

25. Ghoshhajra BB, Lee AM, Engel L-C, et al (2013) Radiation Dose Reduction in Pediatric Cardiac Computed Tomography: Experience from a Tertiary Medical Center. Pediatr Cardiol 171–179.

26. Deak PD, Smal Y, Kalender WA (2010) Multisection CT Protocols: Sex- and Age-specific Conversion Factors Used to Determine Effective Dose from Dose-Length Product 1. Radiology 257:158–166.

27. J. C (1960) A coefficient of agreement for nominal scales. Educ Psychol Meas 20:37–46.

28. Tsai TT, Fattori R, Trimarchi S, et al (2006) Long-term survival in patients presenting with type B acute aortic dissection: insights from the International Registry of Acute Aortic Dissection. Circulation 114:2226–31.

29. Arnold R, Ley S, Ley-Zaporozhan J, et al (2007) Visualization of coronary arteries in patients after childhood Kawasaki syndrome: Value of multidetector CT and MR imaging in comparison to conventional coronary catheterization. Pediatr Radiol 37:998–1006.

30. Lee T, Tsai I-C, Fu Y-C, et al (2006) Using multidetector-row CT in neonates with complex congenital heart disease to replace diagnostic cardiac catheterization for anatomical investigation: initial experiences in technical and clinical feasibility. Pediatr Radiol 36:1273–82.

31. Lukasiewicz A, Bhargavan-Chatfield M, Coombs L, et al (2014) Radiation Dose Index of Renal Colic Protocol CT Studies in the United States: A Report from the American College of Radiology National Radiology Data Registry. Radiology 271:445–451.

32. Cademartiri F, Di Cesare E, Francone M, et al (2015) Italian Registry of Cardiac Computed Tomography. Radiol Medica 120:919–929.

33. Shrimpton PC, Jansen JTM, Harrison JD (2016) Updated estimates of typical effective doses for common CT examinations in the UK following the 2011 national review. Br J Radiol 89:20150346.

34. European Society of Radiology (ESR) (2014) Renewal of radiological equipment. Insights Imaging 5:543–546.

35. Semelka RC, Ramalho M, AlObaidy M, Ramalho J (2016) Gadolinium in Humans: A Family of Disorders. Am J Roentgenol 207:229–233.

36. Charron P, Carrier L, Dubourg O, et al (1997) Penetrance of familial hypertrophic cardiomyopathy. Genet Couns 8:107–14.

37. Maron BJ, Gardin JM, Flack JM, et al (1995) Prevalence of hypertrophic cardiomyopathy in a general population of young adults. Echocardiographic analysis of 4111 subjects in the CARDIA Study. Coronary Artery Risk Development in (Young) Adults. Circulation 92:785–9.

38. Crilley JG, Boehm EA, Blair E, et al (2003) Hypertrophic cardiomyopathy due to sarcomeric gene mutations is characterized by impaired energy metabolism irrespective of the degree of hypertrophy. J Am Coll Cardiol 41:1776–82.

39. Van Driest SL, Ommen SR, Tajik AJ, et al (2005) Sarcomeric genotyping in hypertrophic cardiomyopathy. Mayo Clin Proc 80:463–9.

40. Wigle ED (2001) Cardiomyopathy: The diagnosis of hypertrophic cardiomyopathy. Heart 86:709–14.

41. Lauschke J, Maisch B (2009) Athlete's heart or hypertrophic cardiomyopathy? Clin Res Cardiol 98:80–8.

42. Esposito A, De Cobelli F, Perseghin G, et al (2009) Impaired left ventricular energy metabolism in patients with hypertrophic cardiomyopathy is related to the extension of fibrosis at delayed gadolinium-enhanced magnetic resonance imaging. Heart 95:228–33.

43. Maron MS, Olivotto I, Zenovich AG, et al (2006) Hypertrophic cardiomyopathy is predominantly a disease of left ventricular outflow tract obstruction. Circulation 114:2232–9.

44. Wight JN, Salem D (1995) Sudden cardiac death and the "athlete's heart". Arch Intern Med 155:1473–80.

45. Firoozi S, Sharma S, McKenna WJ (2003) Risk of competitive sport in young athletes with heart disease. Heart 89:710–4.

46. Pelliccia A, Maron BJ, Spataro A, et al (1991) The upper limit of physiologic cardiac hypertrophy in highly trained elite athletes. N Engl J Med 324:295–301.

47. Maron BJ, Pelliccia A, Spirito P (1995) Cardiac disease in young trained athletes. Insights into methods for distinguishing athlete's heart from structural heart disease, with particular emphasis on hypertrophic cardiomyopathy. Circulation 91:1596–601.

48. De Cobelli F, Esposito A, Belloni E, et al (2009) Delayed-enhanced cardiac MRI for differentiation of Fabry's disease from symmetric hypertrophic cardiomyopathy. AJR Am J Roentgenol 192:W97-102.

49. Sardanelli F, Quarenghi M (2006) MR spectroscopy of the heart. Radiol Med 111:1025–34.

50. Holloway CJ, Suttie J, Dass S, Neubauer S (2011) Clinical Cardiac Magnetic Resonance Spectroscopy. Prog Cardiovasc Dis 54:320–327.

51. Beyerbacht HP, Vliegen HW, Lamb HJ, et al (1996) Phosphorus magnetic resonance spectroscopy of the human heart: current status and clinical implications. Eur Heart J 17:1158–66.

52. Lodi R, Rajagopalan B, Blamire AM, et al (2004) Abnormal cardiac energetics in patients carrying the A3243G mtDNA mutation measured in vivo using phosphorus MR spectroscopy. Biochim Biophys Acta 1657:146–50.

53. van Ewijk PA, Schrauwen-Hinderling VB, Bekkers SCAM, et al (2015) MRS: a noninvasive window into cardiac metabolism. NMR Biomed 28:747–66.

54. Bottomley PA, Weiss RG (1998) Non-invasive magnetic-resonance detection of creatine depletion in non-viable infarcted myocardium. Lancet 351:714–8.

55. Faller KME, Lygate CA, Neubauer S, Schneider JE (2013) 1H-MR spectroscopy for analysis of cardiac lipid and creatine metabolism. In: Heart Fail. Rev. pp 657–668

56. Nakae I, Mitsunami K, Omura T, et al (2003) Proton magnetic resonance spectroscopy can detect creatine depletion associated with the progression of heart failure in cardiomyopathy. J Am Coll Cardiol 42:1587–93.

57. Ingwall JS (2009) Energy metabolism in heart failure and remodelling. Cardiovasc Res 81:412–9.

58. Malavazos AE, Di Leo G, Secchi F, et al (2010) Relation of echocardiographic epicardial fat thickness and myocardial fat. Am J Cardiol 105:1831–5.

59. van der Meer RW, Doornbos J, Kozerke S, et al (2007) Metabolic imaging of myocardial triglyceride content: reproducibility of 1H MR spectroscopy with respiratory navigator gating in volunteers. Radiology 245:251–257.

60. Naressi A, Couturier C, Devos JM, et al (2001) Java-based graphical user interface for the MRUI quantitation package. MAGMA 12:141–52.

61. den Hollander JA, Evanochko WT, Pohost GM (1994) Observation of cardiac lipids in humans by localized 1H magnetic resonance spectroscopic imaging. Magn Reson Med 32:175–80.

62. Felblinger J, Jung B, Slotboom J, et al (1999) Methods and reproducibility of cardiac/respiratory double-triggered (1)H-MR spectroscopy of the human heart. Magn Reson Med 42:903–10.

63. Hansch A, Rzanny R, Heyne J-P, et al (2005) Noninvasive measurements of cardiac high-energy phosphate metabolites in dilated cardiomyopathy by using 31P spectroscopic chemical shift imaging. Eur Radiol 15:319–23.

64. Jung WI, Sieverding L, Breuer J, et al (1998) 31P NMR spectroscopy detects metabolic abnormalities in asymptomatic patients with hypertrophic cardiomyopathy. Circulation 97:2536–42.

65. Sardanelli F, Di Leo G (2009) Biostatistics for radiologists: Planning, performing, and writing a radiologic study. Biostat Radiol Planning, Performing, Writ a Radiol Study. doi: 10.1007/978-88-470-1133-5

66. Sai E, Shimada K, Yokoyama T, et al (2015) Evaluation of myocardial triglyceride accumulation assessed on 1H-magnetic resonance spectroscopy in apparently healthy Japanese subjects. Intern Med 54:367–73.

67. Elliott P, McKenna WJ (2004) Hypertrophic cardiomyopathy. Lancet 363:1881–1891.

68. Maron BJ, Maron MS (1997) Hypertrophic cardiomyopathy. Lancet 350:127–133.

69. Nelson MD, Victor RG, Szczepaniak EW, et al (2013) Cardiac steatosis and left ventricular hypertrophy in patients with generalized lipodystrophy as determined by magnetic resonance spectroscopy and imaging. Am J Cardiol 112:1019–24.

70. Utz W, Engeli S, Haufe S, et al (2011) Myocardial steatosis, cardiac remodelling and fitness in insulin-sensitive and insulin-resistant obese women. Heart 97:1585–9.

71. Schrauwen-Hinderling VB, Meex RCR, Hesselink MKC, et al (2011) Cardiac lipid content is unresponsive to a physical activity training intervention in type 2 diabetic patients, despite improved ejection fraction. Cardiovasc Diabetol 10:47.

72. Jonker JT, de Mol P, de Vries ST, et al (2013) Exercise and type 2 diabetes mellitus: changes in tissue-specific fat distribution and cardiac function. Radiology 269:434–42.

73. Pluim BM, Lamb HJ, Kayser HW, et al (1998) Functional and metabolic evaluation of the athlete's heart by magnetic resonance imaging and dobutamine stress magnetic resonance spectroscopy. Circulation 97:666–72.

74. Gutberlet M, Spors B, Grothoff M, et al (2004) Comparison of different cardiac MRI sequences at 1.5 T/3.0 T with respect to signal-to-noise and contrast-to-noise ratios - initial experience. Rofo 176:801–8.

75. Bottomley PA, Weiss RG (2001) Noninvasive localized MR quantification of creatine kinase metabolites in normal and infarcted canine myocardium. Radiology 219:411–8.

76. Sardanelli F, Fausto A, Di Leo G, et al (2009) In vivo proton MR spectroscopy of the breast using the total choline peak integral as a marker of malignancy. Am J Roentgenol 192:1608–1617.

77. Giannattasio C, Achilli F, Failla M, et al (2002) Radial, carotid and aortic distensibility in congestive heart failure: effects of high-dose angiotensin-converting enzyme inhibitor or low-dose association with angiotensin type 1 receptor blockade. J Am Coll Cardiol 39:1275–82.

78. Boutouyrie P, Tropeano AI, Asmar R, et al (2002) Aortic stiffness is an independent predictor of primary coronary events in hypertensive patients: a longitudinal study. Hypertens (Dallas, Tex 1979) 39:10–5.

79. Cavalcante JL, Lima JAC, Redheuil A, Al-Mallah MH (2011) Aortic stiffness: current understanding and future directions. J Am Coll Cardiol 57:1511–22.

80. Durmaz T, Keles T, Bayram NA, et al (2010) Aortic strain, distensibility and elastic modulus are associated with the presence and quantity of coronary calcium. Kardiol Pol 68:1353–9.

81. Dernellis J, Panaretou M (2005) Aortic Stiffness Is an Independent Predictor of Progression to Hypertension in Nonhypertensive Subjects. Hypertension 45:426–431.

82. Sarikouch S, Koerperich H, Dubowy K-O, et al (2011) Impact of Gender and Age on Cardiovascular Function Late After Repair of Tetralogy of Fallot: Percentiles Based on Cardiac Magnetic Resonance. Circ Cardiovasc Imaging 4:703–711.

83. Qiu H, Depre C, Ghosh K, et al (2007) Mechanism of Gender-Specific Differences in Aortic Stiffness With Aging in Nonhuman Primates. Circulation 116:669–676.

84. Niwa K, Perloff JK, Bhuta SM, et al (2001) Structural Abnormalities of Great Arterial Walls in Congenital Heart Disease Light and Electron Microscopic Analyses. Circulation 103:393–400.

85. Niwa K (2005) Aortic root dilatation in tetralogy of Fallot long-term after repair—histology of

the aorta in tetralogy of Fallot: evidence of intrinsic aortopathy. Int J Cardiol 103:117–119.

86. Seki M, Kurishima C, Saiki H, et al (2014) Progressive aortic dilation and aortic stiffness in children with repaired tetralogy of Fallot. Heart Vessels 29:83–87.

87. Niwa K (2002) Progressive Aortic Root Dilatation in Adults Late After Repair of Tetralogy of Fallot. Circulation 106:1374–1378.

88. Rutz T, Max F, Wahl A, et al (2012) Distensibility and diameter of ascending aorta assessed by cardiac magnetic resonance imaging in adults with tetralogy of fallot or complete transposition. Am J Cardiol 110:103–108.

89. Christensen JT, Lu JC, Donohue J, et al (2014) Relation of aortic stiffness and strain by cardiovascular magnetic resonance imaging to age in repaired tetralogy of fallot. Am J Cardiol 113:1031–5.

90. Tomkiewicz-Pajak L, Dziedzic-Oleksy H, Pajak J, et al (2014) Arterial stiffness in adult patients after Fontan procedure. Cardiovasc Ultrasound 12:1–6.

91. Myers KA, Leung MT, Terri Potts M, et al (2013) Noninvasive Assessment of Vascular Function and Hydraulic Power and Efficiency in Pediatric Fontan Patients. J Am Soc Echocardiogr 26:1221–1227.

92. Christensen J, Lu JC, Yu S, et al (2014) Pulse wave velocity does not predict ventricular strain in Ross patients. doi: 10.1186/1532-429X-16-S1-P113

93. Aquaro GD, Cagnolo A, Tiwari KK, et al (2013) Age-dependent changes in elastic properties of thoracic aorta evaluated by magnetic resonance in normal subjects. Interact Cardiovasc Thorac Surg 17:674–679.

94. Grotenhuis HB, Ottenkamp J, Fontein D, et al (2008) Aortic elasticity and left ventricular function after arterial switch operation: MR imaging--initial experience. Radiology 249:801–9.

95. Francone M, Di Cesare E, Cademartiri F, et al (2014) Italian registry of cardiac magnetic resonance. Eur J Radiol 83:e15–e22.

96. Cawley PJ, Maki JH, Otto CM (2009) Cardiovascular Magnetic Resonance Imaging for Valvular Heart Disease: Technique and Validation. Circulation 119:468–478.

97. Di Cesare E, Cademartiri F, Carbone I, et al (2013) Clinical indications for the use of cardiac MRI. By the SIRM Study Group on Cardiac Imaging. Radiol Med 118:752–798.

98. Lopez-Mattei JC, Shah DJ The role of cardiac magnetic resonance in valvular heart disease. Methodist Debakey Cardiovasc J 9:142–8.

99. Donofrio MT, Moon-Grady AJ, Hornberger LK, et al (2014) Diagnosis and treatment of fetal cardiac disease: A scientific statement from the american heart association. Circulation 129:2183–2242.

100. Bonow RO, Carabello BA, Chatterjee K, et al (2006) ACC/AHA 2006 Guidelines for the Management of Patients With Valvular Heart Disease. J Am Coll Cardiol 48:e1–e148.

101. Sardanelli F, Quarenghi M, Di Leo G, et al (2008) Segmentation of cardiac cine MR images of left and right ventricles: Interactive semiautomated methods and manual contouring by two readers with different education and experience. J Magn Reson Imaging 27:785–792.

102. Gatehouse PD, Keegan J, Crowe LA, et al (2005) Applications of phase-contrast flow and velocity imaging in cardiovascular MRI. Eur Radiol 15:2172–2184.

103. Thunberg P, Kähäri A (2011) Visualization of Through-Plane Blood Flow Measurements Obtained from Phase-Contrast MRI. J Digit Imaging 24:470–477.

104. van der Geest RJ, Niezen RA, van der Wall EE, et al Automated measurement of volume flow in the ascending aorta using MR velocity maps: evaluation of inter- and intraobserver variability in healthy volunteers. J Comput Assist Tomogr 22:904–11.

105. Herment A, Kachenoura N, Lefort M, et al (2010) Automated segmentation of the aorta from phase contrast MR images: validation against expert tracing in healthy volunteers and in patients with a dilated aorta. J Magn Reson Imaging 31:881–8.

106. Westenberg JJM, Danilouchkine MG, Doornbos J, et al (2004) Accurate and reproducible mitral valvular blood flow measurement with three-directional velocity-encoded magnetic resonance imaging. J Cardiovasc Magn Reson 6:767–76.

107. Henk CB, Grampp S, Backfrieder W, et al (2003) Automated vessel edge detection in velocity-encoded cine-MR (VEC-MR) flow measurements: a retrospective evaluation in critically ill patients. Eur J Radiol 48:274–81.

108. Groenink M, de Roos A, Mulder BJ, et al (1998) Changes in aortic distensibility and pulse wave velocity assessed with magnetic resonance imaging following beta-blocker therapy in the Marfan syndrome. Am J Cardiol 82:203–8.

109. Sardanelli F, Molinari G, Petillo A, et al MRI in hypertrophic cardiomyopathy: a morphofunctional study. J Comput Assist Tomogr 17:862–72.

110. Secchi F, Resta EC, Piazza L, et al (2014) Cardiac magnetic resonance before and after percutaneous pulmonary valve implantation. Radiol Med 119:400–7.

111. Secchi F, Resta EC, Cannao PM, et al (2015) Four-year cardiac magnetic resonance (CMR) follow-up of patients treated with percutaneous pulmonary valve stent implantation. Eur Radiol 25:3606–3613.

112. Di Leo G (2015) Measurements in radiology: the need for high reproducibility. Pediatr Radiol 45:32–34.

113. Sconfienza LM, Sardanelli F (2013) Radiological journals in the online world: Should we think Open? Eur Radiol 23:1175–1177.

114. RSNA Open Access Policy. Radiological Society of North America Web site. http://pubs.rsna.org/page/openaccess. Accessed 29 Jul 2017

115. Publish open access with Springer. Springer Web site. http://www.springer.com/de/open-access. Accessed 29 Jul 2017

116. Open Access Statement. Iranian Journal of Radiology Web site. http://iranjradiol.com/?page=public_pages&name=Open Access Statement. Accessed 29 Jul 2017

117. About. Journal of the Belgian Society of Radiology Web site. http://www.jbsr.be/about/. Accessed 29 Jul 2017

118. Open Access. Elsevier Web site. https://www.elsevier.com/about/open-science/open-access. Accessed 29 Jul 2017

119. Online Submission and Review System. Investigative Radiology Web site. http://edmgr.ovid.com/ir/accounts/ifauth.htm. Accessed 29 Jul 2017

120. American Journal of Roentgenology Web site. http://www.ajronline.org/. Accessed 29 Jul 2017

121. Acta Radiologica Open submission guidelines. SAGE Publishing Web site. https://us.sagepub.com/en-us/nam/acta-radiologica-open/journal202176#description. Accessed 29 Jul 2017

122. Open access policy. The British Institute of Radiology Web site. http://www.birpublications.org/page/oapolicy. Accessed 29 Jul 2017

123. Guidelines for Authors. Rofo-Fortschr Rontg Web site. http://roefo.thieme.de/documents/10157/18614/RoeFo-Autorenhinweise_Englisch-2017.pdf/ef85bdcc-03d3-41d4-8088-215c16528db9. Accessed 29 Jul 2017

124. Preparing your manuscript. BioMed Central Medical Imaging Web site. https://bmcmedimaging.biomedcentral.com/submission-guidelines/preparing-your-manuscript/technical-advance-article. Accessed 1 Apr 2017

125. Publication Instructions for Authors. Korean Journal of Radiology Web site. https://www.kjronline.org/index.php?body=Instruction. Accessed 29 Jul 2017

126. The New England Journal of Medicine web site.

127. Information for Authors. The Lancet Web site. http://thelancet.com/lancet/information-for-authors/open-access. Accessed 29 Jul 2017

128. MJA Open. Medical Journal of Australia Web site. https://www.mja.com.au/open. Accessed 29 Jul 2017

129. Open Access. Oxford Academic Web site. https://academic.oup.com/journals/pages/open_access. Accessed 29 Jul 2017

130. BJGP editorial process & policies. British Journal of General Practice Web site. http://bjgp.org/authors/bjgp-editorial-process-and-policies. Accessed 29 Jul 2017

131. OnlineOpen. Wiley Author Services Web site. https://authorservices.wiley.com/author-resources/Journal-Authors/licensing-and-open-access/open-access/onlineopen.html. Accessed 29 Jul 2017

132. About BioMed Central. BioMed Central Web site. https://www.biomedcentral.com/about. Accessed 29 Jul 2017

133. About. British Medical Journal Open Web site. http://bmjopen.bmj.com/pages/about/. Accessed 29 Jul 2017

134. Medical Clinics of North America open access option. Elsevier Web site. https://www.elsevier.com/journals/medical-clinics-of-north-america/0025-7125/open-access-options. Accessed 29 Jul 2017

135. Instruction for authors. International Journal of Medical Sciences Web site. http://www.medsci.org/ms/author. Accessed 29 Jul 2017

136. Instruction for Authors. Journal of the American Medical Association Web site. http://jamanetwork.com/journals/jama/pages/instructions-for-authors#SecPublicAccess. Accessed 29 Jul 2017

137. Information for Authors. Annals of Internal Medicine Web site. http://annals.org/aim/pages/authors. Accessed 29 Jul 2017

138. Resources for authors. British Medical Journal Web site. http://www.bmj.com/about-bmj/resources-authors. Accessed 29 Jul 2017

139. Why Publish with PLOS Medicine?. PLoS Medicine Web site. http://journals.plos.org/plosmedicine/s/why-publish-with-plos-medicine. Accessed 29 Jul 2017

140. Fees and funding. BioMed Central Medicine Web site. http://bmcmedicine.biomedcentral.com/submission-guidelines/fees-and-funding. Accessed 29 Jul 2017

141. The American Journal of Medicine open access option. Elsevier Web site. https://www.elsevier.com/journals/the-american-journal-of-medicine/0002-9343/open-access-options. Accessed 29 Jul 2017

142. About CMAJ Open. Canadian Medical Association Jorunal Open Web site. http://cmajopen.ca/site/misc/about.xhtml. Accessed 29 Jul 2017

143. About us. Deutsches Arzteblatt International Web site. https://www.aerzteblatt.de/int/about-us. Accessed 29 Jul 2017

144. Collins FS, Tabak LA (2014) Policy: NIH plans to enhance reproducibility. Nature 505:612–3.

145. Sharing Clinical Trial Data: Maximizing Benefits, Minimizing Risk - PubMed - NCBI. https://www.ncbi.nlm.nih.gov/pubmed/25590113. Accessed 18 Jan 2017

146. Grants. Alfred P. Sloan Foundation Web site. https://sloan.org/grants/apply#tab-grant-proposal-guidelines/. Accessed 1 Apr 2017

147. Open access policy. Bill and Melinda Gates Foundation Web Site. Published January 1, 2017. http://www.gatesfoundation.org/how-we-work/general-information/open-access-policy. Accessed 1 Apr 2017

148. Ford Foundation expands Creative Commons licensing for all grant-funded projects. Ford Foundation Web site. https://www.fordfoundation.org/the-latest/news/ford-foundation-expands-creative-commons-licensing-for-all-grant-funded-projects/. Accessed 1 Apr 2017

149. Data sharing philosophy. Gordon and Betty Moore Foundation Web site. https://www.moore.org/docs/default-source/Grantee-Resources/data-sharing-philosophy.pdf. Accessed 1 Apr 2017

150. Dissemination and Sharing of Research Results. National Science Foundation Web site. https://www.nsf.gov/bfa/dias/policy/dmp.jsp. Accessed 1 Apr 2017

151. Krumholz HM, Ross JS (2011) A model for dissemination and independent analysis of industry data. JAMA 306:1593–4.

152. Guyatt G, Connolly S, Yusuf S, Chalmers I (2016) Sharing Data from Cardiovascular Clinical Trials — A Proposal. 2016–2018.

153. Gillies RJ, Kinahan PE, Hricak H (2016) Radiomics: Images Are More than Pictures, They Are Data. Radiology 278:563–77.

154. Herrick R, Horton W, Olsen T, et al (2016) NeuroImage XNAT Central: Open sourcing imaging research data. Neuroimage 124:1093–1096.

155. About. XNAT Web site. https://www.xnat.org/about/. Accessed 13 Apr 2017

156. Clark K, Vendt B, Smith K, et al (2013) The Cancer Imaging Archive (TCIA): maintaining and operating a public information repository. J Digit Imaging 26:1045–57.

157. Armato SG, McLennan G, Bidaut L, et al (2011) The Lung Image Database Consortium (LIDC) and Image Database Resource Initiative (IDRI): a completed reference database of lung

nodules on CT scans. Med Phys 38:915–31.

158. Chen Y, Elenee Argentinis JD, Weber G (2016) IBM Watson: How Cognitive Computing Can Be Applied to Big Data Challenges in Life Sciences Research. Clin Ther 38:688–701.

159. Loder E (2013) Sharing data from clinical trials: where we are and what lies ahead. BMJ 347:f4794.

160. Mello MM, Francer JK, Wilenzick M, et al (2013) Preparing for responsible sharing of clinical trial data. N Engl J Med 369:1651–8.

161. Anderson BJ, Merry AF (2009) Data sharing for pharmacokinetic studies. Paediatr Anaesth 19:1005–10.

162. Gøtzsche PC (2011) Why we need easy access to all data from all clinical trials and how to accomplish it. Trials 12:249.

163. Berlin JA, Morris S, Rockhold F, et al (2014) Bumps and bridges on the road to responsible sharing of clinical trial data. Clin Trials 11:7–12.

164. Peat G, Riley RD, Croft P, et al (2014) Improving the transparency of prognosis research: the role of reporting, data sharing, registration, and protocols. PLoS Med 11:e1001671.

165. Milia N, Congiu A, Anagnostou P, et al (2012) Mine, yours, ours? Sharing data on human genetic variation. PLoS One 7:e37552.

166. Lee ES, McDonald DW, Anderson N, Tarczy-Hornoch P (2009) Incorporating collaboratory concepts into informatics in support of translational interdisciplinary biomedical research. Int J Med Inform 78:10–21.

167. Antman E (2014) Data sharing in research: benefits and risks for clinicians. BMJ 348:g237–g237.

168. Sardanelli F (2017) Trends in radiology and experimental research. Eur Radiol Exp 1:1.

169. Golay X (2017) The long and winding road to translation for imaging biomarker development: the case for arterial spin labelling (ASL). Eur Radiol Exp 1:3.

170. Grill JD, Holbrook A, Pierce A, et al (2017) Attitudes toward Potential Participant Registries. J Alzheimers Dis 56:939–946.

171. Kasenda B, von Elm E, You J, et al (2014) Prevalence, Characteristics, and Publication of Discontinued Randomized Trials. JAMA 311:1045.

172. Clarke MJ, Stewart LA (1997) Meta-analyses using individual patient data. J Eval Clin Pract 3:207–12.

173. Phi X-A, Houssami N, Obdeijn I-M, et al (2015) Magnetic Resonance Imaging Improves Breast Screening Sensitivity in *BRCA* Mutation Carriers Age ≥ 50 Years: Evidence From an Individual Patient Data Meta-Analysis. J Clin Oncol 33:349–356.

174. Marinovich ML, Macaskill P, Irwig L, et al (2015) Agreement between MRI and pathologic breast tumor size after neoadjuvant chemotherapy, and comparison with alternative tests: individual patient data meta-analysis. BMC Cancer 15:662.

175. Retraction of articles from Springer journals. http://www.springer.com/gp/about-springer/media/statements/retraction-of-articles-from-springer-journals/735218. Accessed 12 Mar 2017

176. Qi X, Deng H, Guo X (2017) Characteristics of retractions related to faked peer reviews: an

overview. Postgrad Med J 93:499–503.

177. Rathi V, Dzara K, Gross CP, et al (2012) Sharing of clinical trial data among trialists: a cross sectional survey. BMJ 345:e7570.

178. Zarin DA (2013) Participant-level data and the new frontier in trial transparency. N Engl J Med 369:468–9.

179. Farrar JT, Troxel AB, Haynes K, et al (2014) Effect of variability in the 7-day baseline pain diary on the assay sensitivity of neuropathic pain randomized clinical trials: an ACTTION study. Pain 155:1622–31.

180. Gabler NB, French B, Strom BL, et al (2012) Validation of 6-Minute Walk Distance as a Surrogate End Point in Pulmonary Arterial Hypertension Trials. Circulation 126:349–356.

181. Gabler NB, French B, Strom BL, et al (2012) Race and sex differences in response to endothelin receptor antagonists for pulmonary arterial hypertension. Chest 141:20–6.

182. Bierer BE, Crosas M, Pierce HH (2017) Data Authorship as an Incentive to Data Sharing. N Engl J Med 376:1684–1687.

183. Prasser F, Bild R, Kuhn KA (2016) A Generic Method for Assessing the Quality of De-Identified Health Data. Stud Health Technol Inform 228:312–6.

184. Barocas S, Nissenbaum H, Lane J, et al Big Data's End Run around Anonymity and Consent. In: Privacy, Big Data, Public Good. Cambridge University Press, New York, pp 44–75

Publications

H-index: 3

Overall citations: 28

1. Scarabello M, Codari M, Secchi F, Cannaò PM, Alì M, Di Leo G, Sardanelli F. Strain of ascending aorta on cardiac magnetic resonance in 1027 patients: Relation with age, gender, and cardiovascular disease (2018) European Journal of Radiology, 99, pp. 34-39. DOI: 10.1016/j.ejrad.2017.12.002

2. Secchi F, Alì M, Petrini M, Pluchinotta FR, Cozzi A, Carminati M, Sardanelli F. Blood-threshold CMR volume analysis of functional univentricular heart (2018) Radiologia Medica, 123 (5), pp. 331-337. DOI: 10.1007/s11547-017-0851-6

3. Sardanelli F, Alì M, Hunink MG, Houssami N, Sconfienza LM, Di Leo G. To share or not to share? Expected pros and cons of data sharing in radiological research (2018) European Radiology, pp. 1-8. Article in Press. DOI: 10.1007/s00330-017-5165-5

4. Cannaò PM, Secchi F, Alì M, D'Angelo ID, Scarabello M, Di Leo G, Sardanelli F. High-quality low-dose cardiovascular computed tomography (CCT) in pediatric patients using a 64-slice scanner (2018) Acta Radiologica. Article in Press. DOI: 10.1177/0284185117752981

5. De Angelis C, Sardanelli F, Perego M, Alì M, Casilli F, Inglese L, Mauri G. Carbon dioxide (CO2) angiography as an option for endovascular abdominal aortic aneurysm repair (EVAR) in patients with chronic kidney disease (CKD) (2017) International Journal of Cardiovascular Imaging, 33 (11), pp. 1655-1662. DOI: 10.1007/s10554-017-1175-2

6. Mauri G, Sconfienza LM, Pescatori LC, Fedeli MP, Alì M, Di Leo G, Sardanelli F. Technical success, technique efficacy and complications of minimally-invasive imaging-guided percutaneous ablation procedures of breast cancer: A systematic review and meta-analysis (2017) European Radiology, 27 (8), pp. 3199-3210. DOI: 10.1007/s00330-016-4668-9

7. Secchi F, Di Leo G, Zanardo M, Alì M, Cannaò PM, Sardanelli F. Detection of incidental cardiac findings in noncardiac chest computed tomography (2017) Medicine (United States), 96 (29), art. no. e7531. DOI: 10.1097/MD.0000000000007531

8. Secchi F, Di Leo G, Petrini M, Spairani R, Alì M, Guazzi M, Sardanelli F. 1H- and31P-myocardial magnetic resonance spectroscopy in non-obstructive hypertrophic cardiomyopathy patients and competitive athletes (2017) Radiologia Medica, 122 (4), pp. 265-272. DOI: 10.1007/s11547-016-0718-2

9. Di Leo G, D'Angelo ID, Alì M, Cannaò PM, Mauri G, Secchi F, Sardanelli F. Intra- and inter-reader reproducibility of blood flow measurements on the ascending aorta and pulmonary artery using cardiac magnetic resonance (2017) Radiologia Medica, 122 (3), pp. 179-185. DOI: 10.1007/s11547-016-0706-6

10. Di Leo G, Fisci E, Secchi F, Alì M, Ambrogi F, Sconfienza LM, Sardanelli F. Diagnostic accuracy of magnetic resonance angiography for detection of coronary artery disease: a systematic review

and meta-analysis (2016) European Radiology, 26 (10), pp. 3706-3718. DOI: 10.1007/s00330-015-4134-0

11. Cannaò PM, Altabella L, Petrini M, Alì M, Secchi F, Sardanelli F. Novel cardiac magnetic resonance biomarkers: Native T1 and extracellular volume myocardial mapping (2016) European Heart Journal, Supplement, 18, pp. E64-E71. DOI: 10.1093/eurheartj/suw022

12. Secchi F, Alì M, Faggiano E, Cannaò PM, Fedele M, Tresoldi S, Di Leo G, Auricchio F, Sardanelli, F. Fractional flow reserve based on computed tomography: An overview (2016) European Heart Journal, Supplement, 18, pp. E49-E56. DOI: 10.1093/eurheartj/suw014

13. Petrini M, Alì M, Cannaò PM, Zambelli D, Cozzi A, Codari M, Malavazos AE, Secchi F, Sardanelli F. Epicardial adipose tissue volume in patients with coronary artery disease or non-ischemic dilated cardiomyopathy: evaluation with cardiac magnetic resonance. (2018) Clin Raidiol, Epub head of print. DOI: 10.1016/j.crad.2018.09.006

Papers under review

1. Secchi F, Monti CB, Alì M, Carbone FS, Cannaò PM, Sardanelli F. Diagnostic value of global cardiac strain in patients with myocarditis. Eur Radiol

2. Alì M, Monti CB, Secchi F, Spairani R, Speciani M, Tritella S, Di Leo G, Sardanelli F. Fast thoracic MRI as an alternative to chest x-ray: a retrospective evaluation of 287 patients. Eur J Radiol

3. Petrini M, Chessa M, Alì M, Cannaò PM, Di Leo G, Secchi F, Sardanelli F. Pulmonary insufficiency: extending the advantage of pulmonary regurgitation volume versus pulmonary regurgitation fraction to a congenital heart disease mixed population. Int J Cardiovasc Imaging

4. Monti CB, Alì M, Melazzini L, Fossati B, Cavalli M, Cardani R, Meola G, Sardanelli F, Secchi F. Cardiac magnetic resonance in myotonic dystrophy type 1: A contribution to risk assessment. International Journal of Cardiology

5. Secchi F, Di Leo G, Delnevo A, Alì M, D'Angelo ID, Nardella VG, Sardanelli F. Peripheral artery disease: how much inter-leg symmetry? A contrast-enhanced magnetic resonance angiography study. British Journal of Radiology

Congress participations

1. **Alì M**, Monti CM, Secchi F, Di Leo G, Sardanelli F, Fast thoracic MRI as an alternative to chest X-ray radiography: a retrospective evaluation of 287 patients. EPOS at ISMRM Italian Chapter, Padova, Italy

2. **Alì M**, Secchi F, Monti CB, Di Leo G, Sardanelli F. Fast thoracic MRI as an alternative to chest X-ray radiography: a retrospective evaluation of 287 patients. EPOS at ESCR/ESTI 2018, Genève, Switzerland

3. **Alì M**, Sardanelli F, Hunink MG, Houssami N, Sconfienza LM., Di Leo G. To share or not to share? Expected pros and cons of data sharing in radiological research. EPOS at Retreat 2018, Baveno, Italy

4. **Alì M**, Monti CB, Carbone F, Secchi F, Cannaà PM, Sardanelli F. Quantitative edema and late gadolinium enhancement thresholds for the diagnosis of myocarditis in suspect cases. Scientific presentation ECR 2018, Wien, Austria

5. **Alì M,** Zanardo M, Cannaò PM, Sardanelli F. Diagnostic Accuracy of Fast Thoracic non-contrast MRI versus Chest Radiography for cardiac and non-cardiac findings. EPOS at ESCR 2017, Milan, Italy

6. **Alì M,** Secchi F, Cannaò PM, Sardanelli F. Chronotropic effect of sedation for cardiac CT in pediatric patients on the image quality: Preliminary results. EPOS at ESCR 2017, Milan, Italy

7. **Alì M**, Zanardo M, Cannaò PM, Secchi F, Di Leo F, Sardanalli F. How many incidental cardiac findings in non-cardiac thorax CT are missed? EPOS at ECR 2017, Wien, Austria

8. **Alì M**, Secchi F, Cannaò P M, Petrini M, Di Leo G, Sardanelli F. Prognostic value of late enhancement in cardiac magnetic resonance in patients with dilated cardiomyopathy. Scientific presentation at 47° Congresso SIRM 2016, Naples, Italy

9. **Alì M**, Secchi F, Cannaò P M, Petrini M, Di Leo G, Sardanelli F. Prognostic value of late enhancement in cardiac magnetic resonance in patients with dilated cardiomyopathy. Scientific presentation at ESCR 2015, Wien, Austria

Teaching activity

1. Jun 19, 2018 – *Metodologia della ricerca: gli organi coinvolti.* Corso elettivo della Laurea Magistrale in Scienze delle Professioni Sanitarie Tecniche Diagnostiche. Università degli Studi di Milano.

Didactic activities

Academic year 2017-2018

1. Jun 20, 2018 – *Costruire un profilo professionale attraverso le competenze trasferibili. Quali possibilità per i dottori di ricerca?* Università degli Studi di Milano.

2. Jun 12-13-14, 2018 – *Poster e presentazioni orali: come presentare i vostri risultati in modo efficace e accattivante.* Università degli Studi di Milano.

3. May 25, 2018 – *Valorizzare creando impresa: fare spin-off in UniMi (seconda parte).* Università degli Studi di Milano.

4. May 23, 2018 – *Valorizzare creando impresa: fare spin-off in UniMi (prima parte).* Università degli Studi di Milano.

5. Mar 8, 2018 – *Tutelare e valorizzare sul mercato i risultati della ricerca in UniMi*. Università degli Studi di Milano.

6. Jan 8-9, 2018 – *Infezioni microbiche emergenti: novità nella diagnosi e nelle strategie vaccinali.* Università degli Studi di Milano.

7. Oct 11, 2017 – *Cardiac MR: introduction in the alphabet of sequences acquisition and analysis*. Gianluca Pontone, Marco Francone, Francesco De Cobelli, Centro Cardiologico Monzino.

8. Sep 30, Oct 1, 27-28-29 – *Corso di Alta Formazione sulla Sperimentazione Clinica dei Farmaci*. Università Pontificia Seraphicum, Roma.

Academic year 2016-2017

1. Sep 29, 2017 – *Research integrity*. Università degli Studi di Milano.

2. Jul 20, 2017 – *Deep learning in imaging: review of basic concepts, current applications and future opportunities*. BJ Erickson, Radiology Department of the Mayo Clinic, Ospedale San Raffaele.

3. Jul 13, 2017 – *Il futuro della Radiologia Milanese: Novità e Ricerche della Scuola di Specializzazione in Radiodiagnostica dell'Università degli Studi di Milano*. Prof. F. Sardanelli, Università degli Studi di Milano.

4. Mar 14 - May 23, 2017 – *Introduction to the methodology of clinical research: theoretical-practical course*. Prof. G. V. Zuccotti and G. Bedogni, Università degli Studi di Milano.

5. Feb 22, 2017 – *Come scrivere un progetto di ricerca – parte 1°. Le 100 cose che avrei voluto sapere quando ero un dottorando*. Università degli Studi di Milano.

6. Feb 14, 2017 – *Scientific papers: from the draft to proof correction.* Università degli Studi di Milano.

7. Jun 28, 2017 – *Radiomica e intelligent imaging: una linea temporale*. Milano.

8. Jun 22, 2017 – *Research Day*, IRCCS Policlinico San Donato.

9. Jun 16, 2017 – *Come scrivere un progetto di ricerca: parte 2. Le 100 cose che avrei voluto sapere quando ero un dottorando*. Università degli Studi di Milano.

10. Dec 13, 2016 – *Ricerca Traslazionale del Beta-Lab. Risultati della Collaborazione tra Medici e Ingegneri*. IRCCS Policlinico San Donato.

11. Nov 24-25, 2016 – *Metodologia della Sperimentazione Clinica. Ospedale San Raffaele.* Dott.ssa M. Gambaro.

12. Oct 25, 2016 – *Corso sulle competenze trasversali - terzo modulo.* Università degli Studi di Milano.

13. Sep 21, 2016 – *Open access – open data e il mondo delle pubblicazioni*. Corso sulle competenze trasversali. Università degli Studi di Milano.

Accademic year 2015-2016

1. Jun 17, 2016 – *Open access – open data e il mondo delle pubblicazioni*. Università degli Studi di Milano.

2. Jun 16, 2016 – *Giornata dei giovani ricercatori.* IRCCS Policlinico San Donato.

3. May 16, 2016 – *Il rischio clinico in Radiologia.* IRCCS Policlinico San Donato.

4. May 26, 2016 – *Il protocollo di ricerca clinica: linee guida per la stesura e criticità.* IRCCS Ospedale San Raffaele.

5. Apr 4, 2016 – *Medicina reale o medicina virtuale?* IRCCS Policlinico San Donato.

6. Mar 7, 2016 – *Accumulo celebrale di Gadolinio. Teorie ed evidenze*. IRCCS Policlinico San Donato.

7. Feb 26, 2016 – *Introduzione alla Diagnostica per Immagini*. Università degli Studi di Milano.

Tutor activities

1. *Carotid ultrasound: reproducibility of manual and automatic calculation of intima-media.* Federico Wiedenmann, Facoltà di Medicina e Chirurgia.

2. *Sign of pulmonary hypertension on Cardiac CT scans*. Chiara Geroli. Facoltà di Medicina e Chirurgia.

3. *Chronotropic effect of sedation for Cardiac CT in paediatric patients: impact on image quality*. Giulia Fior. Facoltà di Medicina e Chirurgia.

4. *Prognostic value of late gadolinium enhancement in non-ischemic dilated cardiomyopathy.* Federica Riva. Facoltà di Medicina e Chirurgia.

5. *Il ruolo dello strain miocardico alla Cardio-RM nelle miocarditi.* Caterina Monti. Facoltà di Medicina e Chirurgia.

6. *Diagnostic accuracy of fast thoracic non-contrast MRI versus chest radiography for cardiac and non-cardiac findings.* Maurizio Speciani. Facoltà di Medicina e Chirurgia.

7. *Studio di Cardio-RM delle miocarditi: edema miocardico e late gadolinium enhancement.* Francesco Saverio Carbone. Facoltà di Medicina e Chirurgia.

8. *Sicurezza e performance diagnostica della RM in pazienti portatori di pacemaker o defibrillatori non RM-compatibili: studio prospettico*. Eyal Elron. Facoltà di Medicina e Chirurgia.

9. *Left ventricular joint points late gadolinium enhancement in patients with congenital heart disease*. Lorenzo Peroncini. Facoltà di Medicina e Chirurgia.

10. *Cardiac Findings in Non-Cardiac Thoracic Computed Tomography*. Khatuna Akhoishvili. Facoltà di Medicina e Chirurgia.

11. *Riduzione di dose radiante in angio TC: valutazione della qualità di immagine e del rapporto segnale-rumore.* Sara Barilatti. Corso di laurea in tecniche di radiologia medica, per immagini e radioterapia.

12. *Valutazione del calibro del tronco e delle arterie polmonari in risonanza magnetica attraverso sequenze con e senza mezzo di contrasto.* Giulia Cirillo. Corso di laurea in tecniche di radiologia medica, per immagini e radioterapia.

Non-academic curriculum vitae

Marco Alì

Curriculum Vitae

76/B, via Sesto, Cremona, 26100, Italy

333-8979379

marco.ali90@gmail.com

DoB: August 6, 1990

Education

Sept 2015 - Sept 2018 — **PhD fellow in Integrated Biomedical Research** of University of Milan at IRCCS Policlinico San Donato.
During my three years of doctoral experience, I published 12 manuscipts focused on the use of imaging techniques for the study of cardiovascular diseases (see the *Publication* section). These works were also presented in several national and international congress (see the *Congress* section) and summarized in my PhD thesis entitled "*Computed tomography and magnetic resonance imaging for the study of congenital heart diseases*".
The participation in these studies allowed me to learn how to manage clinical trials, from the Ethics Committee and Grant Office approval to patient enrollment, and how to perform data analysis and manuscripts drafting.
Thus, in order to deepen the skills acquired in these years in clinical trial management, in September 2017 I attended a theoretical/pratical course in clinical monitoring, where I have dealt with some key topics such as the ICH-GCP (Good Clinical Practice), national and international laws, and clinical trials quality assurance (see *Training* section).

Sept 2012 – Feb 2014 — **Master's degree in Industrial Biotechnology** (103/110) at University of Parma.
Master's thesis intern at AVANTEA Ltd, laboratory of advanced technologies for biotechnology research and animal reproduction, about "*Gene-targeting of "safe-harbour" V2G locus in primary swine fibloblasts using CRISPR/Cas9 techinque*".

Sept 2009 - Sept 2012 — **Bachelor's degree in Biotechnology** (99/110) at University of Parma.
Theisis: "*Genetic and molecular techniques applied to the study of metals up-take in plants*"

Professional experiences

Oct 2015 – present — **Scientific Consultant**, *CDI Centro Diagnostico Italiano S.p.A*

Apr 2015 – Nov 2015 — **Researcher**, *IRCCS Policlinico San Donato*, Unit of Radiodiagnostic, Medical image processing. Main research topic: *cardiovascular imaging*

Jun 2015 – May 2018 — **Board Member**, *Sporting Club Cremona S.Coop a.r.l.*

Training

Clinical Monitor in training — As required by the *italian Ministerial Decree 15.11.2011* in order to act as **Clinical Monitor**, I've done the 40-hour theoretical/Practical course for Clinical Monitor **(**held by Clinical Research Educational Services – CRES in Rome), and from the 1st of April 2015 I've been working in the field of clinical trials at the Radiodiagnostic Unit of IRCCS Policlinico San Donato**.**

Publications

Full papers — Author of **12 full articles published on peer-reviewed international Journals**
ORCID: 0000-0001-8156-7743

H-index — **3**

Overall citations — **28**

Teaching activities

Jun 2018 — *Metodologia della ricerca: gli organi coinvolti.* Corso elettivo della Laurea Magistrale in Scienze delle Professioni Sanitarie Tecniche Diagnostiche. Università degli Studi di Milano.

Journals served as reviewer

- Journal of Cardiology & Clinical Research

Transferable skills

Technical

- Software: Microsoft Office, SPSS, WordPress

Languages

- English: complete professional knowledge
- Italian: mother tongue
- Good public speaking due to theatrical experience

Volunteer experiences and causes

Smile project

2013 - present — Co-Founder at *IlSorrisoQuotidiano.it*

Rotary International

2018 - 2019 — Board member of RC Soresina

2017 - 2018 — Head of focus area "Peace" of the District 2050

From 2016 — Member of Rotary International association

I authorize the processing of my personal data.

Milan, September 28, 2018

Appendix

–

Original Article

Acta Radiologica
2018, Vol. 59(10) 1247–1253

DOI: 10.1177/0284185117752981
journals.sagepub.com/home/acr
SAGE

High-quality low-dose cardiovascular computed tomography (CCT) in pediatric patients using a 64-slice scanner

Paola Maria Cannaò[1], Francesco Secchi[1], Marco Alì[2], Ida Daniela D'Angelo[3], Marco Scarabello[3], Giovanni Di Leo[1] and Francesco Sardanelli[1,4]

Abstract

Background: Cardiovascular computed tomography (CCT) technology is rapidly advancing allowing to perform good quality examinations with a radiation dose as low as 1.2 mSv. However, latest generation scanners are not available in all centers.
Purpose: To estimate radiation dose and image quality in pediatric CCT using a standard 64-slice scanner.
Material and Methods: A total of 100 patients aged 6.9 ± 5.4 years (mean ± standard deviation) who underwent a 64-slice CCT scan using 80, 100, or 120 kVp, were retrospectively evaluated. Radiation effective dose was calculated on the basis of the dose length product. Two independent readers assessed the image quality through signal-to-noise ratio (SNR), contrast-to-noise ratio (CNR), and a qualitative score (3 = very good, 2 = good, 1 = poor). Non-parametric tests were used.
Results: Fifty-five exams were not electrocardiographically (ECG) triggered, 20 had a prospective ECG triggering, and 25 had retrospective ECG triggering. The median effective dose was 1.3 mSv (interquartile range [IQR] = 0.8–2.7 mSv). Median SNR was 30.6 (IQR = 23.4–33.6) at 120 kVp, 29.4 (IQR = 23.7–34.8) at 100 kVp, and 24.7 (IQR = 19.4–34.3) at 80 kVp. Median CNR was 21.0 (IQR = 14.8–24.4), 19.1 (IQR = 15.6–23.9), and 25.3 (IQR = 19.4–33.4), respectively. Image quality was very good, good, and poor in 56, 39, and 5 patients, respectively. No significant differences were found among voltage groups for SNR ($P = 0.486$), CNR ($P = 0.336$), and subjective image quality ($P = 0.296$). The inter-observer reproducibility was almost perfect ($\kappa = 0.880$).
Conclusion: High-quality pediatric CCT can be performed using a 64-slice scanner, with a radiation effective dose close to 2 mSv in about 50% of the cases.

Keywords
Cardiovascular computed tomography, pediatric computed tomography, congenital heart diseases, radiation dose, 64-slice CT, image quality

Date received: 9 August 2017; accepted: 16 December 2017

Introduction

In the setting of congenital heart diseases (CHD), non-invasive imaging techniques such as echocardiography, cardiac magnetic resonance (CMR), and cardiovascular computed tomography (CCT) play a crucial role in the visualization of cardiovascular structures (1).

Echocardiography, being a ubiquitous and radiation-free technique, represents the first approach for patients having or suspected to have CHD, but it has limitations in defining complex anatomy and reliable imaging of coronary arteries, especially in older children who have a poor acoustic window (1,2). CMR is considered the standard of reference for evaluation of ventricular volumes and valve regurgitation but it still usually requires relatively long imaging times and sedation or anesthesia in

[1]Radiology Unit, IRCCS Policlinico San Donato, Donato Milanese, Italy
[2]PhD Course in Integrative Biomedical Research, Università degli Studi di Milano, Milan, Italy
[3]Postgraduation School in Radiodiagnostics, Università degli Studi di Milano, Milan, Italy
[4]Dipartimento di Scienze Biomediche per la Salute, Università degli Studi di Milano, San Donato Milanese, Italy

Corresponding author:
Marco Alì, MSc, Radiology Unit, IRCCS Policlinico San Donato, Via Morandi 30, San Donato Milanese, Italy.
Email: marco.ali90@gmail.com

children aged < 8 years as well as in developmentally delayed patients of all ages (3–5). CCT and invasive angiography expose patients to ionization radiation, with potentially more dangerous effects in younger patients. A previous study demonstrated that the radiation exposure from diagnostic catheterization is substantially higher than that from CCT in a pediatric population (1).

In recent years, CCT technology has advanced rapidly. It now provides improved spatial and temporal resolution. Electrocardiographically (ECG)-gated coronary CCT can now be routinely obtained in pediatric patients with a radiation dose as low as 1.2 mSv using dual-source CCT technology (6). Unfortunately, these scanners are still available in few centers. On the other hand, in order to reduce radiation exposure keeping a good image quality, radiologists can apply tailored protocols for CCT in pediatric patients even using 64-slice scanners which are currently a kind of ''standard'' technology in radiology department.

Thus, our aim was to estimate radiation dose and image quality in pediatric CCT using a 64-slice scanner.

Table 1. Disease distribution in the study population.

Disease	Patients (n)
Known or suspected coronary abnormality	
Anomalous origins	18
Coronary fistula	6
Complex congenital heart disease	
Tetralogy of Fallot	20
Transposition of great arteries	10
Truncus arteriosus	4
Aortic disease	
Stent evaluation in coarctation	18
Interrupted or hypoplastic arch	2
Pulmonary artery disease	
Pulmonary artery stenosis with stent	11
Subvalvar pulmonary stenosis	3
Major aorto-pulmonary collateral arteries in pulmonary atresia	3
Total	100

Material and Methods

Patient population

Ethics Committee approval was obtained for this retrospective study. A total of 100 CCT exams of patients aged < 18 years, performed between January 2010 and December 2016 at our Institution, were retrospectively evaluated. Disease distribution in the study population is summarized in Table 1.

Image acquisition

At our department, all CCT studies, including those performed in pediatric patients, are performed under the direct responsibility of a cardiovascular radiologist. To minimize technical errors, technicians are carefully instructed by the radiologist on a case-by-case basis.

The CCT examinations were performed on a 64-slice CT scanner (Somatom 64, Siemens Healthcare, Erlangen, Germany). Patients aged less than 3 years needed sedation. The administration of sedative drugs happened shortly before the CT exam. The anesthesiologist monitored the patient conditions during the procedure and evaluated the patient status after the exam. Midazolam was administered intravenously (dose of 0.1–1.1 mg/kg), orally (dose of 0.5–0.6 mg/kg), or intramuscularly (only in one patient, dose of 0.2 mg/kg). The administration route of ketamine was intravenous (dose of 0.9–1.9 mg/kg) or intramuscular (dose of 3.3–5.4 mg/kg). Propofol was intravenously administered at a dose of 0.5–2.4 mg/kg. The variability of the administered doses depended on age, comorbidities, and known drug response of the patient.

A tailored CCT protocol was performed according to the clinical question. In the majority of patients (n = 80), the unenhanced scan was waived to reduce the radiation dose. A bolus of contrast material of 5–60 mL (Iopamiro 370, Bracco Imaging S.p.A., Milan, Italy) followed by saline solution in the range of 10–60 mL was intravenously injected by means of a power injector (Empower CTA, EZEM, Westbury, NY, USA) at a flow rate of 1.5–3.0 mL/s according to the patient's characteristics and the clinical question.

When investigating cardiac anatomy or coronary arteries, a test-bolus technique was used. A time-attenuation curve was obtained by measuring the enhancement within a region of interest (ROI) positioned in a ascending aorta or in the pulmonary trunk according to the clinical question. The contrast arrival time was determined from the time to peak enhancement and was used to estimate the scan delay for a full-bolus diagnostic CCT (7).

To acquire an angiogram, we used the bolus tracking technique, based on real-time monitoring of the main bolus during injection to acquire a series of dynamic low-dose monitoring scans at the level of the vessel of interest. The trigger threshold inside the ROI was set at 100 HU above the baseline. The delay between each monitoring scan acquisition was 1.25 s. As soon as the threshold was reached, the table moved to the cranial start position. During this interval the contrast material concentration increased to the desired level of enhancement (8).

The CCT were either performed without ECG synchronization or using a prospective or a retrospective ECG-gating depending on the patient's heart rate and rhythm and on whether an evaluation of myocardial function was indicated (9). Tube voltage was set at 80, 100, or 120 kVp; tube current was set between 36 and 100 mAs, according to body size. The gantry rotation time was 0.33 s; pitch was 0.2–0.5. The reconstruction parameters were set as follows: section thickness = 0.75 mm; reconstruction interval = 0.45mm; matrix size = 512 × 512; and field of view = 250 mm. Two-dimensional images were then transferred to a workstation (Multimodality, Siemens Healthcare, Erlangen, Germany) for obtaining off-line three-dimensional reconstructions.

Radiation exposure

The dose length product (DLP) was retrieved for each patient. The effective dose (ED) in mSv was calculated as DLP*k. The conversion factor for the chest, k (measured in mSv/mGy/cm), varied with age and was estimated from the International Commission on Radiological Protection publication 103 recommendation (10,11). The ED was then evaluated for four patient age groups (newborns < 1 year, 1–5 years, 6–10 years, and 11–17 years), and according the tube voltage used (kVp).

Image quality assessment

Signal-to-noise ratio (SNR) and contrast-to-noise ratio (CNR) were calculated for each scan using the following formulas: $SNR = HU_{\text{left ventricle}}/SD_{\text{air}}$; $CNR = [(HU_{\text{left ventricle}} - HU_{\text{myocardium}})/SD_{\text{air}}]$.

Assessment of subjective image quality was independently performed by two observers with eight and four years of experience in cardiovascular imaging. Image analysis was performed individually and image series were evaluated in a random order. Scans were classified using a three-level scale (3 = very good; 2 = good; and 1 = poor). The two readers agreed on the following criteria:

- images were judged as very good when all structures were well visualized without artifacts;
- images were judged as good when almost all structures were well visualized even though some artifacts were visible;
- images were judged as poor when the vascular structures were not well visualized due to the presence of large artifacts.

Statistical analysis

Statistical analyses were performed using statistical software (SPSS for Windows v.21.0, SPSS Inc., Chicago, IL). Parametric variables were expressed as mean and standard deviation (SD), whereas non-parametric variables were expressed as median and interquartile ranges (IQR). Overall comparisons among groups were performed using the Kruskal–Wallis test; the paired post-hoc analysis of the two groups was performed using the Mann–Whitney U test. A P value < 0.05 was considered as significant.

The inter-observer agreement about the image quality qualitative assessment was evaluated using the Cohen κ, with the following interpretation of the κ values: <0.20 = slight agreement; 0.21−0.40 = fair agreement; 0.41−0.60 = moderate agreement; 0.61−0.80 = substantial agreement; 0.81−1.0 = almost perfect agreement (12).

Results

Study population

The study population included 100 patients (63 boys, 37 girls), aged 6.9 ± 5.4 years (mean ± SD). The most common primary indications for CCT were complex CHD (n = 34), pulmonary arteries abnormalities (n = 22), and coronary arteries abnormalities (n = 24). A detailed list of indications is provided in Table 1.

Radiation exposure

The overall median ED was 1.3 mSv (IQR = 0.8–2.7 mSv). Concerning the subgroup analysis, the median ED was 1.0 mSv (IQR = 0.6–1.4 mSv) for exams performed at 80 kVp, 1.9 mSv (1.1–3.5 mSv) for exams performed at 100 kVp, and 5.1 mSv (3.6–6.0) for exams performed at 120 kVp ($P < 0.001$). Post-hoc analysis is reported in Table 2. Examples of CCT images obtained at 80, 100, and 120 kVp are shown in Figs. 1–4.

Comparing not ECG-triggered, prospectively ECG-triggered, and retrospectively ECG-gated examinations, median ED were 1.1 (0.6–3.1) mSv, 1.3 (1.0–1.8) mSv and 1.7 (1.3–3.5) mSv, respectively ($P < 0.036$). Post-hoc analysis is reported in Table 3.

Finally, a significantly different ED was also found among the age groups ($P < 0.001$). Post-hoc analysis is reported in Table 4.

Image quality

Overall, the image quality was judged by the first reader (most expert) to be very good in 56 examinations (56%), good in 39 (39%), and poor in five (5%). The agreement between the two readers was almost perfect (κ = 0.880). A non-significant difference in terms of subjective image quality was found, both overall and among the three

Table 2. Effective dose by tube voltage.

	Effective dose (mSv)	*P* value
80 kVp (n = 49)	1.0 (0.6–1.4)	<0.001
100 kVp (n = 35)	1.9 (1.1–3.5)	
120 kVp (n = 16)	5.1 (3.6–6.0)	
80 kVp vs. 100 kVp		<0.001
80 kVp vs. 120 kVp		<0.001
100 kVp vs. 120 kVp		0.003

Data of effective dose are medians and interquartile ranges in parentheses. The Kruskal–Wallis test was used for the overall comparison while the Mann–Whitney *U* test was used for the post-hoc analysis.

groups of kilovoltage used ($p \geq 0.296$). In terms of objective image quality, the SNR was 30.6 (IQR = 23.4–33.6), 29.4 (IQR = 23.7–34.8), and 24.7 (IQR = 19.4–34.3), at 120, 100, and 80 kVp, respectively ($P = 0.486$). The median CNR was 21.0 (IQR = 14.8–24.4), 19.1 (IQR = 15.6–23.9), and 25.3 (IQR = 19.4–33.4), at 120, 100 and 80 kVp, respectively ($P = 0.336$).

There were not significant differences according to SNR and CNR in the different age-group patients. In particular, the median of SNR was 30.5 (IQR = 22.5–36.6), 25.2 (IQR = 15.1–30.9), 24.9 (IQR = 20.6–41.1), and 24.4 (IQR = 20.7–30.9) in newborn, 1–5, 6–10, and 11–17 age groups, respectively ($P = 0.227$). The

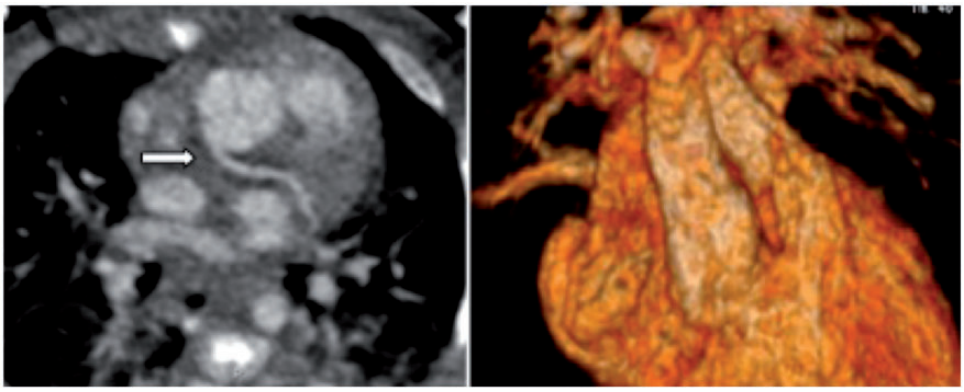

Fig. 1. Cardiac CT of a one-month-old newborn with a double outlet right ventricle. Prospectively ECG-triggered scan for the definition of coronary and intra-cardiac anatomy was performed. Effective dose was 0.3 mSv using 80 kVp. On the left panel, the abnormal origin of left main coronary artery is shown. On the right panel, a 3D reconstruction of great vessels anatomy is shown (double outlet right ventricle).

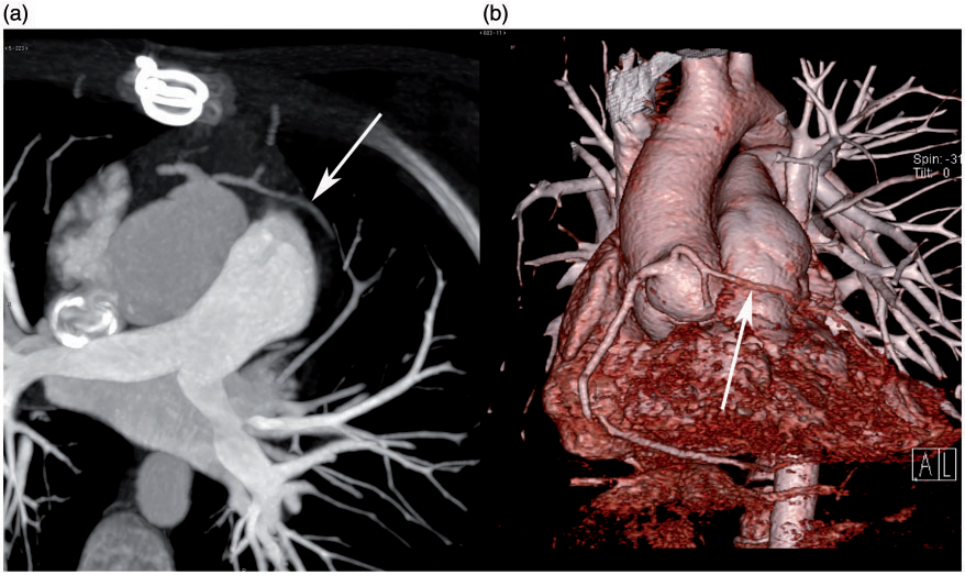

Fig. 2. Cardiac CT of a two-year-old with tetralogy of Fallot with sub-pulmonary stenosis surgically treated. Retrospectively ECG-triggered scan for the definition of coronary and intra-cardiac anatomy was performed before a new surgical procedure. Effective dose was 1.1 mSv using 80 kVp. Anomalous left coronary origin from right sinus passed anterior of right ventricle outflow tract is shown (arrows).

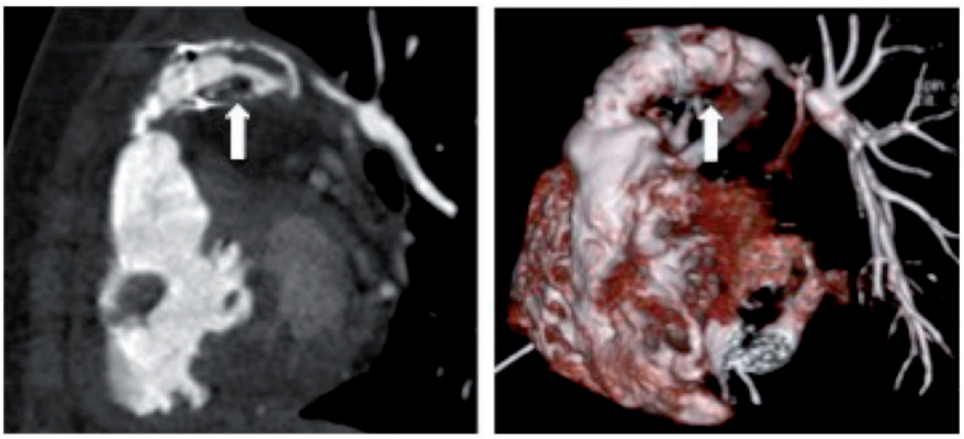

Fig. 3. Cardiac CT of an eight-year-old girl with tetralogy of Fallot treated with a pulmonary conduit. An angiographic not ECG-triggered scan was performed for evaluating pulmonary stents. Effective dose was 1.1 mSv using 100 kVp. On the left panel, a thrombosis of the pulmonary conduit due to endocarditis is shown. On the right panel, a 3D reconstruction of pulmonary conduit and pulmonary arteries is shown.

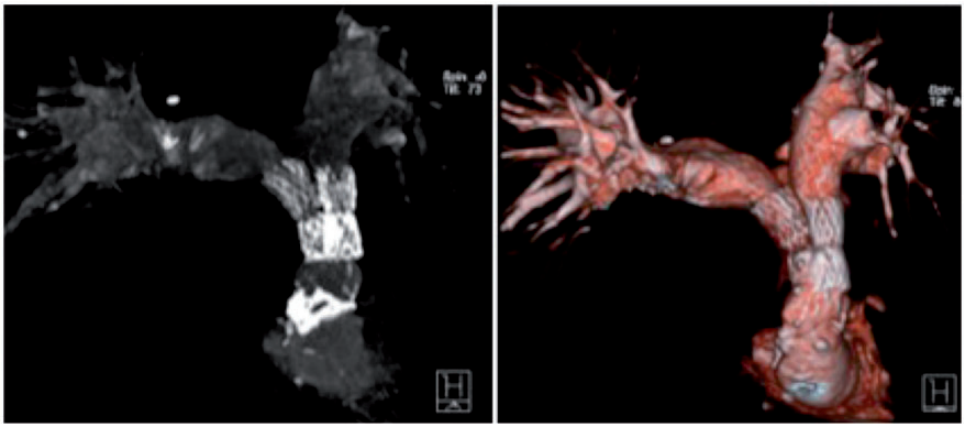

Fig. 4. Cardiac CT of a 14-year-old girl with tetralogy of Fallot and pulmonary stenosis. An angiographic not ECG-triggered scan was performed to evaluate pulmonary stents. The effective dose was 2 mSv using 120 kVp. On the left panel, a maximum intensity projection of both stents is shown. On the right panel, a 3D reconstruction of pulmonary arteries is shown.

mean CNR was 19.4 (IQR = 24.8–23.5), 20.1 (IQR = 10.8–20.9), 23.3 (IQR = 13.7–41.1), and 18.4 (IQR = 10.7–20.8) in newborn, 1–5, 6–10, and 11–17 age groups, respectively ($P = 0.101$).

Discussion

In this study, we assessed radiation exposure and image quality of 64-slice CCT in a consecutive series of 100 pediatric patients. Using a tailored dose-saving protocol with careful radiologist's supervision of technical performance, the overall median ED was limited to 1.3 mSv, including both prospective and retrospective ECG-triggering. Image quality was very good or good in 95/100 patients. Of note, the inter-observer reproducibility for the qualitative evaluation of image quality was almost perfect.

Our results can be favorably compared with those obtained by other authors. Tsai et al. (13) described an average ED for pediatric CCT of 2.6, 2.1, and 2.0 mSv for 16-, 64-, and 128-slice CCT, respectively, using a prospectively triggered acquisition. Conversely, the dose estimated in other studies was 6.8 mSv (10) or 12 mSv (14) using a 64-slice scan with retrospective ECG-gating.

In recent years, the advent of new generation scanners implied a drastic decrease in radiation exposure, also in the pediatric setting. The study published by Han et al. (3) analyzed a cohort of 70 pediatric patients and found an average ED of 1.7 mSv for retrospectively ECG-gated CCT and 0.9 mSv for prospectively ECG-triggered CCT. These findings highlighted the increasing role of CCT in the pediatric setting, in particular as a tool that allows to avoid diagnostic

Table 3. Effective dose for not ECG-synchronized examinations, prospectively ECG-triggered examinations, and retrospectively ECG-gated examinations.

	Effective dose (mSv)	*P* value
A		
Not ECG-synchronized (n = 55)	1.1 (0.6–3.1)	0.036
B		
Prospective ECG-triggering (n = 25)	1.3 (1.0–1.8)	
C		
Retrospective ECG-gating (n = 20)	1.7 (1.3–3.5)	
A vs. B		0.347
A vs. C		0.022
B vs. C		0.027

Data of effective dose are medians and interquartile ranges in parentheses. The Kruskal–Wallis test was used for the overall comparison while the Mann–Whitney *U* test was used for the post-hoc analysis.

Table 4. Effective dose by patient age.

	Effective dose (mSv)	*P* value
A		
Newborn (n = 15)	1.0 (0.5–1.3)	<0.001
B		
1–5 years (n = 25)	0.8 (0.6–1.2)	
C		
6–10 years (n = 27)	1.6 (1.1–2.4)	
D		
11–17 years (n = 33)	3.4 (1.5–5.1)	
A vs. B		0.639
A vs. C		0.038
A vs. D		0.020
B vs. C		0.003
B vs. D		<0.001
C vs. D		0.081

Data of effective dose are medians and interquartile ranges in parentheses. The Kruskal–Wallis test was used for the overall comparison while the Mann–Whitney *U* test was used for the post-hoc analysis.

angiography or to limit or overcoming the diagnostic phase of interventional angiography. In fact, Lee et al. (15) demonstrated that in a population of 14 neonates with complex CHD referred for diagnostic cardiac catheterization after initial assessment with echocardiography and CCT, none of them required additional diagnostic imaging. This is a goal in terms of reduction of radiation dose considering the 13.4 mSv that are required on average for a diagnostic catheterization (1).

Our study showed that using a "standard" 64-slice scanner high-quality images can be obtained with a relatively low radiation exposure, fulfilling the diagnostic aim of the examination. This is an important clinical finding considering that 64-slice CT units remain the most available type of CT scanner in the majority of radiology departments (16–18).

Rapid technological development resulted in accelerated technical and functional obsolescence of imaging equipments, creating a need for renewal (19). A dramatic change in this scenario, in the current era of "spending review" by public health systems, is not expected.

Thus, implementing CCT dose-saving protocols on 64-slice scanners should be considered as mandatory, especially in the pediatric population.

Importantly, since no differences were found in terms of SNR and CNR among the different tube voltages used (120, 100, or 80 kVp), our experience suggests that an 80-kVp protocol could be adequate to image most pediatric patients.

The results in terms of CNR deserve a particular comment. Although the difference among the groups was not statistically significant, probably due to the small sample size combined with data distribution, a higher CNR at the lowest tube voltage (80 kVp) was observed (median 25.3 vs. 21.0 for 120 kVp and 19.1 for 100 kVp). This possible increase in CNR could be explained with the higher contrast effect of the iodinated contrast material at lower voltages (20). Notably, the agreement in image quality evaluation between the two observers was not conditioned by the voltage used.

The approach here presented (tailored protocols under strict control by the cardiovascular radiologist) could be generally applied also to late-generation CT scanners, allowing for a lower and lower dose exposure, in particular in the pediatric population. All these results are inverting the traditional way of thinking about the comparison between CCT and CMR in pediatric patients. Most probably, CMR will no longer be an easy winner because of being radiation-free. As radiation doses go lower and lower, towards 0.1–0.2 mSv, examination time and need for sedation, spatial resolution as well as image quality related to movement artifacts can play in favor of CCT. In addition, when considering the probability of multiple CMR examinations, the potential gadolinium accumulation in the brain should be taken into account (21).

The results of this study should be interpreted in view of its limitations. First, we should consider the retrospective study design. However, we included the whole consecutive series of pediatric patients who underwent CCT at our institution in the study period (starting from the installation of the 64-slice unit). Thus, the study reports what happened in real clinical life. Second, the number of patients is rather small

as CMR is still preferred in the evaluation of CHD patients.

In conclusion, CCT is a valuable imaging modality when evaluating pediatric patients with a large spectrum of known or suspected cardiovascular abnormalities. Using dose-saving techniques, CCT protocols tailored to the pediatric population allowed for performing high-quality CCT in children with a relatively low radiation exposure also using a ''standard'' 64-slices scanner.

Declaration of Conflicting Interests

The author(s) declared the following potential conflicts of interest with respect to the research, authorship, and/or publication of this article: F Secchi and G Di Leo have been sponsored to congresses by Bracco Imaging SpA (Milan, Italy). F Sardanelli received research grants from Bayer Healthcare (Berlin, Germany) and Bracco Imaging SpA (Milan, Italy); moreover is member of advisory board for Bracco Imaging SpA (Milan, Italy) and General Electric Healthcare (Buc, France).

Funding

The author(s) disclosed receipt of the following financial support for the research, authorship, and/or publication of this article: This study was supported by local research funds of the IRCCS Policlinico San Donato, a Clinical Research Hospital partially funded by the Italian Ministry of Health.

References

1. Watson TG, Mah E, Joseph Schoepf U, et al. Effective radiation dose in computed tomographic angiography of the chest and diagnostic cardiac catheterization in pediatric patients. Pediatr Cardiol 2013;34:518–524.
2. Jhang WK, Park J-J, Seo D-M, et al. Perioperative evaluation of airways in patients with arch obstruction and intracardiac defects. Ann Thorac Surg 2008;85:1753–1758.
3. Han BK, Rigsby CK, Hlavacek A, et al. Computed tomography imaging in patients with congenital heart disease Part I: rationale and utility. an expert consensus document of the society of cardiovascular computed tomography (SCCT): endorsed by the Society of Pediatric Radiology (SPR) and the North American Society of Cardiac Imaging (NASCI). Cardiovasc Comput Tomogr 2015;9: 475–492.
4. Taylor AM. Cardiac imaging: MR or CT? Which to use when. Pediatr Radiol 2008;3:S433–S438.
5. Secchi F, Di Leo G, Papini GDE, et al. Cardiac magnetic resonance: Impact on diagnosis and management of patients with congenital cardiovascular disease. Clin Radiol 2011;66:720–725.
6. Meinel FG, Henzler T, Schoepf UJ, et al. ECG-Synchronized CT angiography in 324 consecutive pediatric patients: spectrum of indications and trends in radiation dose. Pediatr Cardiol 2015;36:569–578.
7. Nijhof WH, Van Der Vos CS, Anninga B, et al. Reduction of contrast medium volume in abdominal aorta CTA: multiphasic injection technique versus a test bolus volume. Eur J Radiol 2013;82:1373–1378.
8. Cademartiri F, Nieman K, van der Lugt A, et al. Intravenous contrast material administration at 16-detector row helical CT coronary angiography: test bolus versus bolus-tracking technique. Radiology 2004; 233:817–823.
9. Henzler T, Hanley M, Arnoldi E, et al. Practical strategies for low radiation dose cardiac computed tomography. J Thorac Imaging 2010;25:213–220.
10. Ghoshhajra BB, Lee AM, Engel L-C, et al. Radiation dose reduction in pediatric cardiac computed tomography: experience from a tertiary medical center. Pediatr Cardiol 2013;35:171–179.
11. Deak PD, Smal Y, Kalender WA. Multisection CT Protocols: sex- and age-specific conversion factors used to determine effective dose from dose-length product. Radiology 2010;257:158–166.
12. Cohen J. A coefficient of agreement for nominal scales. Educ Psychol Meas 1960;20:37–46.
13. Tsai TT, Fattori R, Trimarchi S, et al. Long-term survival in patients presenting with type B acute aortic dissection: insights from the International Registry of Acute Aortic Dissection. Circulation 2006;114: 2226–2231.
14. Arnold R, Ley S, Ley-Zaporozhan J, et al. Visualization of coronary arteries in patients after childhood Kawasaki syndrome: Value of multidetector CT and MR imaging in comparison to conventional coronary catheterization. Pediatr Radiol 2007;37:998–1006.
15. Lee T, Tsai I -C, Fu Y-C, et al. Using multidetector-row CT in neonates with complex congenital heart disease to replace diagnostic cardiac catheterization for anatomical investigation: initial experiences in technical and clinical feasibility. Pediatr Radiol 2006;36:1273–1282.
16. Lukasiewicz A, Bhargavan-Chatfield M, Coombs L, et al. Radiation dose index of renal colic protocol CT studies in the united states: a report from the American College of Radiology National Radiology Data Registry. Radiology 2014;271:445–451.
17. Cademartiri F, Di Cesare E, Francone M, et al. Italian Registry of Cardiac Computed Tomography. Radiol Med 2015;120:919–929.
18. Shrimpton PC, Jansen JTM, Harrison JD. Updated estimates of typical effective doses for common CT examinations in the UK following the 2011 national review. Br J Radiol 2016;89:20150346.
19. European Society of Radiology (ESR). Renewal of radiological equipment. Insights Imaging 2014;5:543–546.
20. Sakane M, Kim T, Hori M, et al. Effects of high-concentration contrast material and low-voltage CT on contrast for multiphasic CT of the upper abdomen: comparison using the simulation with virtual monochromatic imaging obtained by fast-switch kVp dual-energy CT. Springerplus 2014;3:234.
21. Semelka RC, Ramalho M, Al Obaidy M, et al. Gadolinium in humans: a family of disorders. Am J Roentgenol 2016;207:229–233.

^{1}H- and ^{31}P-myocardial magnetic resonance spectroscopy in non-obstructive hypertrophic cardiomyopathy patients and competitive athletes

Francesco Secchi, Giovanni Di Leo, Marcello Petrini, Riccardo Spairani, Marco Alì, Marco Guazzi & Francesco Sardanelli

La radiologia medica
Official Journal of the Italian Society of Medical Radiology

ISSN 0033-8362

Radiol med
DOI 10.1007/s11547-016-0718-2

Springer

Radiol med
DOI 10.1007/s11547-016-0718-2

CARDIAC RADIOLOGY

^{1}H- and ^{31}P-myocardial magnetic resonance spectroscopy in non-obstructive hypertrophic cardiomyopathy patients and competitive athletes

Francesco Secchi[1] · Giovanni Di Leo[1] · Marcello Petrini[2] · Riccardo Spairani[2] · Marco Alì[3] · Marco Guazzi[4] · Francesco Sardanelli[1,5]

Received: 1 August 2016 / Accepted: 19 December 2016

Abstract
Purpose The clinical differentiation between athlete's heart and mild forms of non-obstructive hypertrophic cardiomyopathy (HCM) is crucial. We hypothesized that differences do exist between the myocardial metabolism of patients with non-obstructive HCM and competitive athletes (CAs). Our aim was to evaluate myocardial metabolism with ^{31}P-MRS and ^{1}H-MRS in HCM patients and CAs.
Materials and methods After Ethics Committee approval, 15 CAs and 7 HCM patients were prospectively enrolled. They underwent a 1.5-T cardiac MR including electrocardiographically triggered cine images, single-voxel ^{1}H-MRS and multivoxel ^{31}P-MRS. ^{1}H-MRS was performed after imaging using standard coil with the patient in the supine position; thereafter, ^{31}P-MRS was performed using a dedicated coil, in the prone position. Data were reported as median and interquartile range. Mann–Whitney *U* test was used.
Results In CAs, left ventricular mass index was 72 (66–83) g/m^2, septal thickness 10 (10–11) mm, end diastolic volume index 95 (85–102) ml/m^2, end systolic volume index 30 (28–32) ml/m^2 and ejection fraction 68% (65–69%); in HCM patients, 81 (76–111) g/m^2 ($P = 0.052$), 18 (15–21) mm ($P = 0.003$), 73 (58–76) ml/m^2 ($P = 0.029$), 20 (16–34) ml/m^2 ($P = 0.274$) and 68% (55–73%) ($P = 1.000$), respectively. At ^{1}H-MRS, total lipids were 35 (0–183) arbitrary units (au) for CA and 763 (155–1994) au for HCM patients ($P = 0.046$). At ^{31}P-MRS, PCr/γATP was 5 (4–6) au for CA and 4 (2–5) au for HCM patients ($P = 0.230$). Examination time was 20 min for imaging only, 5 min for ^{1}H-MRS and 15 min for ^{31}P-MRS.
Conclusions We observed a significant increase of myocardial lipids, but a preserved PCr/γATP ratio in the metabolism of HCM patients compared with competitive CAs.

Keywords Myocardial metabolism · Athlete's heart · Hypertrophic cardiomyopathy · Magnetic resonance spectroscopy

✉ Marco Alì
marco.ali90@gmail.com

Francesco Secchi
francesco.secchi@grupposandonato.it

Giovanni Di Leo
gianni.dileo77@gmail.com

Marcello Petrini
petrini.marcello@gmail.com

Riccardo Spairani
riki12@gmail.com

Marco Guazzi
marco.guazzi@unimi.it

Francesco Sardanelli
francesco.sardanelli@unimi.it

[1] Unit of Radiology, IRCCS Policlinico San Donato, Via Morandi 30, San Donato Milanese, 20097 Milan, Italy

[2] Postgraduation School in Radiodiagnostics, Università degli Studi di Milano, Via Festa del Perdono 7, 20100 Milan, Italy

[3] Ph.D. Course in Integrated Biomedical Research, Università degli Studi di Milano, Via Mangiagalli 31, 20133 Milan, Italy

[4] Cardiology University Department, IRCCS Policlinico San Donato, Università degli Studi di Milano, Via Morandi 30, San Donato Milanese, 20097 Milan, Italy

[5] Dipartimento di Scienze Biomediche per la Salute, Università degli Studi di Milano, Via Morandi 30, 20133 Milan, Italy

Published online: 09 January 2017

Introduction

Hypertrophic cardiomyopathy (HCM) is the most common genetic cardiac disease with a prevalence of 0.2% [1]. In half the cases, the transmission is autosomal dominant with incomplete penetration [2, 3]. The most common mutations involve sarcomere proteins, particularly C-binding myosin protein, the heavy beta-myosin chain and troponin T [4]. This disease is characterized by hypertrophy of the left ventricle, mostly asymmetric, and is usually located at the basal portion of the septum [5]. Diastolic dysfunction and outflow tract obstruction of the left ventricle may be present, causing major clinical manifestations such as angina, dyspnea, dizziness and syncope [6, 7]. In approximately 30% of HCM patients, ventricular hypertrophy is moderate without obstruction of the outflow tract of the left ventricle, both at rest and under stress and, therefore, the disease is silent [8]. In this form, the clinical onset can be the sudden death induced by rhythm disorders. Indeed, HCM was reported to be responsible for 35% of sudden deaths in young athletes [9, 10].

Competitive athletes with intense and regular training exercise usually develop cardiovascular changes leading to a reversible paraphysiological myocardial hypertrophy known as athlete's heart. This condition shows symmetrical and homogeneous hypertrophy, with variations in the wall thickness smaller than 2 mm [11]. In 2% of such athletes, the left ventricle wall thickness reaches 13–15 mm [12], with a distribution partially overlapped with those measured in mild forms of HCM, especially mutations of troponin T [13]. Thus, it is clinically relevant to differentiate between athlete's heart and mild forms of non-obstructive HCM.

Magnetic resonance spectroscopy (MRS) is a non-invasive diagnostic technique allowing for the in vivo evaluation of myocardial metabolism [14, 15] by measuring the signal intensity of ^{31}P or ^{1}H. In particular, with ^{31}P-MRS, the ratio between phosphocreatine (PCr) and γ-adenosine triphosphate (γATP) may be measured, representing an index of the myocardial energy reserve [3, 16–18]. On the other side, ^{1}H-MRS allows for estimating the total creatine (Cr) (sum of PCr and Cr) [19, 20], which is associated with myocardial contractility [21, 22]; moreover, myocardial lipids may be measured using ^{1}H-MRS [23, 24].

The aim of this study was to evaluate the left ventricle function in patients affected by HCM compared with that of competitive athletes and to assess the myocardial metabolism using ^{31}P-MRS and ^{1}H-MRS in the two populations.

Materials and methods

Study design and inclusion criteria

This prospective cross-sectional study was approved by the local ethics committee and each subject signed a written informed consent. Inclusion criteria were as follows: patients aged 18 years or more with a known diagnosis of non-obstructive HCM, defined as asymmetric hypertrophy of the left ventricle, with the typical patchy pattern with local distribution of late gadolinium enhancement [12, 13]; competitive athletes aged 18 years or more, in good health, without any reported cardiovascular symptoms and with intense exercise training in the month prior to the enrollment, quantified in at least 10 h per week. Exclusion criteria were contraindications to magnetic resonance such as pacemakers/defibrillators, intracranial ferromagnetic vascular clips, intraocular metal fragments, or severe claustrophobia.

Magnetic resonance imaging

Each enrolled subject underwent a 1.5-T magnetic resonance (Magnetom Sonata Maestro Class, Siemens Medical Solutions, Erlangen, Germany), including a morphologic and functional imaging study, with the patient in the supine position.

The imaging protocol included balanced steady-state free precession sequences (true fast imaging with steady-state free precession, true-FISP) using a four-channel surface phased-array coil in the short axis plane covering the entire heart. Technical parameters were as follows: electrocardiographic (ECG)-gating; TR/TE 4.0/1.5 ms; flip angle 80°; slice thickness 8 mm; temporal resolution 45 ms; field of view 300 × 400 mm^2; matrix 119 × 256; 30 phases in breath-hold at end expiration. The kinetic study was processed by manual segmentation using Syngo Argus software (version VE32B, Siemens Medical Solutions, Erlangen, Germany) by a radiologist with a 7-year experience in cardiac MR imaging.

For each subject, the following imaging-derived variables were measured for the left ventricle: end diastolic thickness of the septum; end diastolic thickness of the posterior wall; mass index (i.e., normalized to the body surface area); end diastolic volume index (EDVI); end systolic volume index (ESVI); ejection fraction (EF); stroke volume; and ventricular end diastolic diameter. We have also calculated an asymmetry index, defined as the left ventricle septal-to-posterior wall thickness ratio.

^{1}H-MRS

After morphologic and functional imaging, hydrogen-containing metabolites were measured in a single voxel of 10 × 20 × 40 mm^3 within the interventricular septum. A point-resolved spectroscopy sequence (ECG synchronization; diaphragm navigator; acquisition in the end systolic phase; TR/TE 2000/90 ms; flip angle 90°; number of excitations 150; suppression of the water signal; supine position) was performed using the same four-channel surface phased-array coil used for imaging.

A physicist with 8-year experience in MRS processed all spectra using the jMRUI software that implements the AMARES (Advanced Method for Accurate, Robust, and Efficient Spectral) algorithm quantitation [25]. Pre-processing steps were: apodization (3 Hz), manual or automatic phase correction and subtraction of the baseline with the polynomial method. The area of the two peaks attributable to Cr (3.0 and 3.9 ppm) and the that of the two peaks attributable to lipids (0.9 and 1.3 ppm) were measured and corrected for decay using T2 values published in the literature [26, 27]. The total Cr as well as the total fat was obtained summing up the two relevant components. Data were presented as arbitrary units (au).

^{31}P-MRS

Myocardial phosphates were measured through ^{31}P-MRS using a dedicated surface coil tuned for ^{31}P and with the patient in the prone position. On the basis of repeated low-resolution scout images, we placed a grid of volumes of interest so as to guarantee at least one voxel within the anterior ventricular junction, trying to minimize contamination by ventricular blood. Then, we acquired a multivoxel chemical shift imaging sequence for a single slice (nuclear Overhauser enhancement technique; ECG synchronization for acquisition in the end diastolic phase; TR/TE = 800/2.3 ms; flip angle 90°; grid size 8 × 8×60 mm^3; field of view 300 × 300 mm^2; free breathing).

Pre-processing included: exponential filter, zero-filling from 1024 to 2048 points, Fourier transform, frequency and phase correction and subtraction of the baseline with the polynomial method. All spectra were processed by the same physicist using Spectroscopy-Argus software (version VE32B, Siemens Medical Solutions, Erlangen, Germany). The area under the peak of the following metabolites was measured: PCr at 0 ppm; phosphomonoester (PME) at 5.4 and 6.3 ppm; inorganic phosphate (Pi) at 3.7 and 5.2 ppm; phosphodiester (PDE) at 2–3 ppm; γATP at 16.3 ppm. Moreover, we identified the 2,3-diphosphoglycerate (DPG), contained in red blood cells, at about 5.5 ppm, used to correct data for the blood contamination. To this end, we subtracted 11% and 19% of 2,3-DPG from γATP and PDE, respectively, as already described [28]. The signals of γATP, PCr, PDE and Pi were corrected for decay using T2 values published in the literature [29]. Finally, we calculated the following ratios: PCr/γATP; PDE/γATP; 2,3-DPG/γATP; PME/PCr; and Pi/PCr [29]. Data were reported in au.

Table 1 Distribution of demographics of the study population

	Competitive athletes	HCM patients	*P*
N (male/female)	15 (11/4)	7 (6/1)	0.297*
Age (years)[a]	41 (35–42)	56 (45–62)	0.009[$]
Body mass index (kg/m^2)[a]	22 (20–23)	25 (24–29)	0.041[$]
Weekly training (h)[a]	10 (10–14)	–	–

HCM hypertrophic cardiomyopathy

* χ^2 test. [$] Mann–Whitney *U* test

[a] Data are presented as median and interquartile range in brackets

Statistical analysis

Statistical analysis was performed using non-parametric methods, more appropriate for small samples [30]. Differences between the two groups of subjects were evaluated with the Mann–Whitney *U* test or the χ^2 test, while bivariate correlations were estimated using the Spearman correlation coefficient.

Statistical analysis was performed using SPSS v.17.0 (IBM SPSS Inc., Chicago, IL, USA). Continuous variables were reported as median and interquartile range (IQR) and *P* values <0.050 were considered statistically significant.

Results

Population characteristics

A total of 22 subjects were enrolled, whose characteristics are reported in Table 1. There were 7 HCM patients and 15 competitive athletes. In particular, athletes were nine bikers and six professional volleyball players with a median weekly training of 10 h (IQR 10–14 h). The median body mass index (BMI) in HCM patients (25 kg/m^2; IQR 24–29 kg/m^2) was higher ($P = 0.041$) than that of athletes (22 kg/m^2; IQR 20–23 kg/m^2). Moreover, HCM patients were older than athletes [56 years (IQR 45–62 years) versus 41 years (IQR 35–42 years), $P = 0.009$].

The mean total duration of MR examinations was approximately 40 min: 20 min for imaging, 5 min for ^{1}H-MRS, and 15 min for ^{31}P-MRS. Processing required 5 min.

Table 2 Functional and morphologic variables of the left ventricle in the two groups

	Competitive athletes	HCM patients	*P**
End diastolic volume index (ml/m^2)	95 (85–102)	73 (58–76)	0.029
End systolic volume index (ml/m^2)	30 (28–32)	20 (16–34)	0.274
Stroke volume (ml)	111 (102–142)	74 (72–86)	0.008
Ejection fraction (%)	68 (65–69)	68 (55–73)	1.000
Left ventricle mass index (g/m^2)	72 (66–83)	81 (76–111)	0.052
Interventricular septal thickness (mm)	10 (10–11)	18 (15–21)	0.003
Posterior wall thickness (mm)	8 (7–10)	9 (7–11)	0.520
Asymmetry index	1.1 (1.0–1.3)	2.0 (1.6–2.3)	0.022
Left ventricle diameter (mm)	55 (52–56)	50 (48–52)	0.258

Data are presented as medians and interquartile range in brackets

HCM hypertrophic cardiomyopathy

* Mann–Whitney *U* test

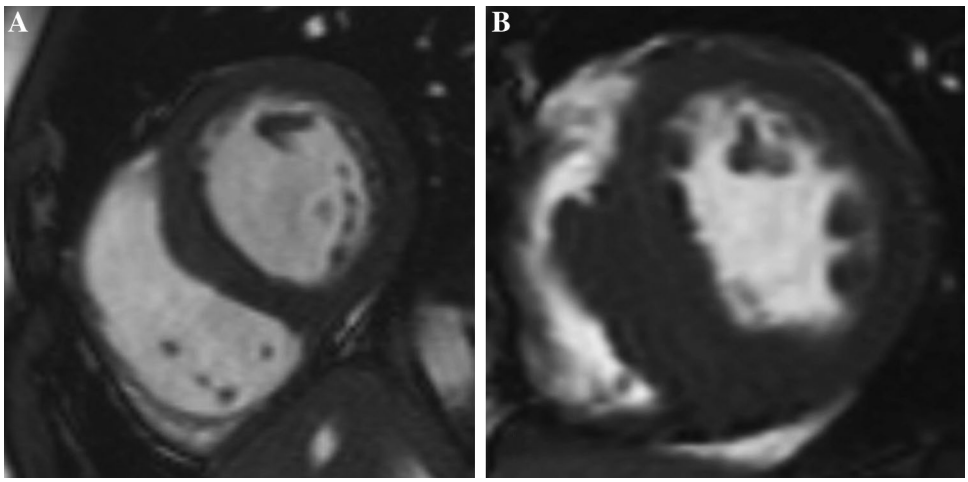

Fig. 1 Cardiac magnetic resonance images in diastolic phase of a mid-ventricular short axis section of an athlete (**a**) and a hypertrophic cardiomyopathy patient (**b**). Note that the septal thickness of the patient is greater than that of the athlete

Morphology and function

The distribution and comparison of morphologic and functional characteristics of the left ventricle in the two groups are shown in Table 2. Of note, HCM patients showed a lower stroke volume than athletes [74 ml (IQR 72–86 ml) versus 111 ml (IQR 102–142 ml), $P = 0.008$], but an equivalent ejection fraction [68% (IQR 55–73%) versus 68% (IQR 65–69%), $P = 1.000$]. Moreover, HCM patients showed a much larger asymmetry index than athletes [2.0 (IQR 1.6–2.3) versus 1.1 (IQR 1.0–1.3), $P = 0.022$]. Figure 1 shows examples of an athlete and a HCM patient.

^{1}H-MRS

The ^{1}H-MRS spectrum of one athlete had too low signal-to-noise ratio that prevented its analysis. The distribution of the variables measured using ^{1}H-MRS in the two groups and their comparison are shown in Table 3. Importantly, the lipid resonance at 1.3 ppm greatly differed between patients and athletes with a much higher content in HCM patients [554 au (IQR 121–2377 au)] than in competitive athletes [0 au (IQR 0–67 au)] ($P = 0.020$); similarly for the total lipid content [763 au (IQR 155–1994 au) versus 35 au (IQR 0–183 au), $P = 0.046$]. Figure 2 shows an example of a hydrogen spectrum of a competitive athlete and a HCM patient.

Table 3 Distribution and comparison of metabolites measured by ^{1}H-MRS in the two groups of subjects

	Competitive athletes[a]	HCM patients[a]	*P**
Creatine at 3.0 ppm	19 (6–33)	0 (0–32)	0.799
Creatine at 3.9 ppm	55 (26–71)	43 (12–93)	0.799
Total creatine	58 (42–110)	95 (24–185)	0.447
Lipids at 0.9 ppm	0 (0–60)	125 (0–275)	0.397
Lipids at 1.3 ppm	0 (0–67)	554 (121–2377)	0.020
Total lipids	35 (0–183)	763 (155–1994)	0.046

HCM hypertrophic cardiomyopathy

* Mann–Whitney *U* test

[a] Data are presented as median and interquartile range in brackets and measured in arbitrary units

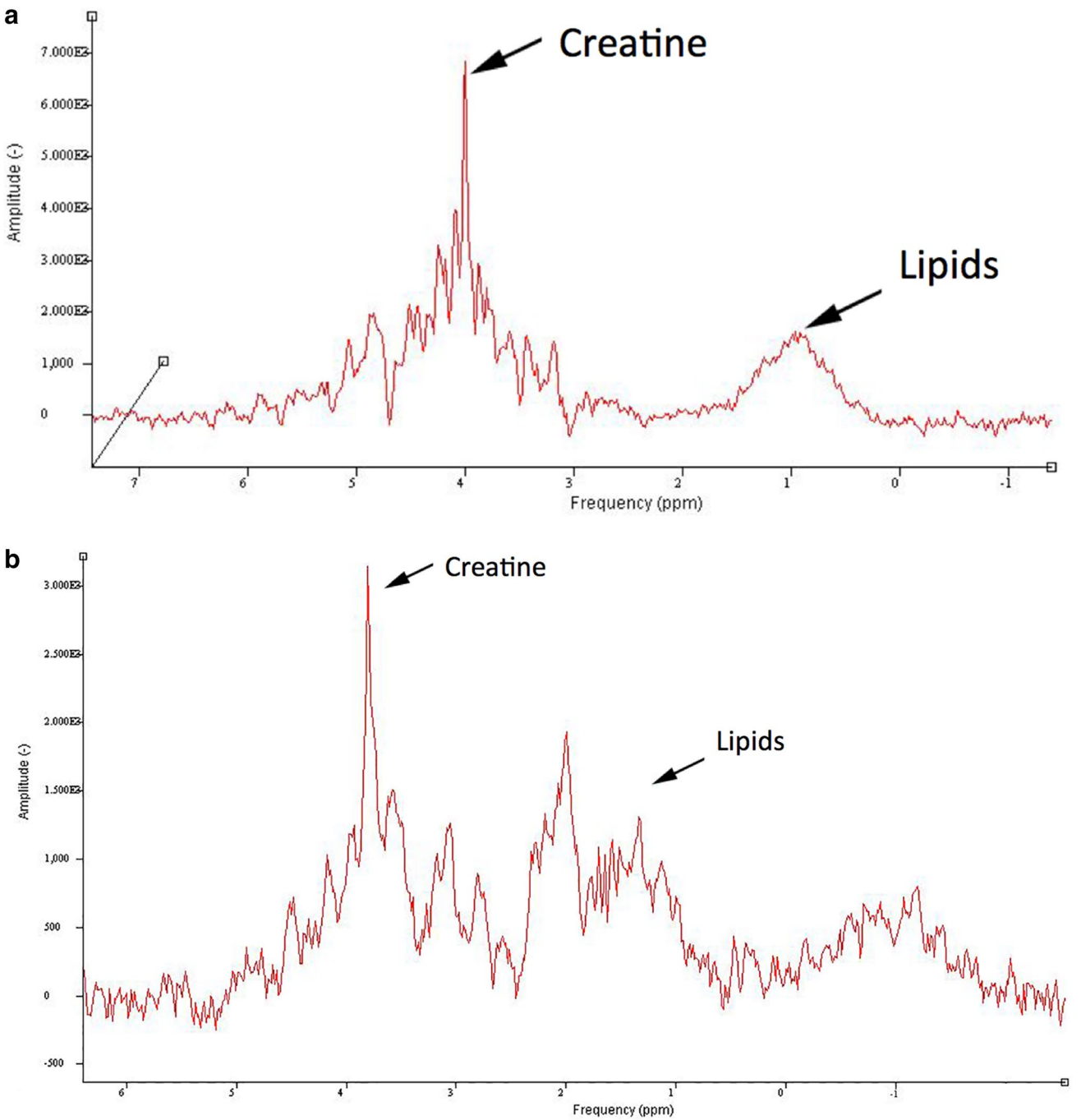

Fig. 2 Example of a hydrogen spectrum obtained in an athlete (**a**) and a hypertrophic cardiomyopathy patient (**b**). Note that the lipid peak is higher in the patient than in the athlete

^{31}P-MRS

Data from ^{31}P-MRS were not available for two HCM patients due to examination interruption for claustrophobia (in one case) or to low signal-to-noise ratio probably related to patient movement (in the other case). The distribution of the phosphate content in the two groups and their comparison are shown in Table 4. No differences between patients and athletes were noted in terms of PCr [22 au (IQR 9–25 au) versus 29 au (IQR 20–36 au), $P = 0.168$] and PCr/γATP [4 (IQR 2–5) versus 5 (IQR 4–6), $P = 0.230$]. Vice versa, a significant difference between patients and athletes was noted in terms of 2,3-DPG/γATP [0.2 (IQR 0.0–0.2) versus 0.5 (IQR 0.3–0.7), $P = 0.008$].

Table 4 Distribution and comparison of phosphate content between the two groups of subjects

	Competitive athletes[a]	HCM patients[a]	*P**
PCr	29 (20–36)	22 (9–25)	0.168
γATP	6 (4–6)	5 (5–6)	0.735
PCr/γATP	5 (4–6)	4 (2–5)	0.230
PDE	7 (4–9)	5 (5–10)	0.612
PME	0.2 (0.0–0.3)	0.4 (0.4–1.8)	0.081
Pi	0.4 (0.0–1.3)	0.4 (0.4–1.7)	0.395
Pi/PCr	0.03 (0.00–004)	0.02 (0.01–0.22)	0.445
PME/PCr	0.01 (0.00–0.01)	0.02 (0.01–0.20)	0.142
PDE/γATP	1.1 (0.6–1.8)	1.1 (0.8–1.7)	0.866
2,3-DPG/γATP	0.5 (0.3–0.7)	0.2 (0.0–0.2)	0.008

HCM hypertrophic cardiomyopathy, *PCr* phopshocreatine, *γATP* γ-adenosine triphosphate, *PDE* phosphodiester, *PME* phosphomonoester, *Pi* inorganic phosphate, *2,3-DPG* 2,3-diphosphoglycerate

* Mann–Whitney *U* test

[a] Data are presented as median and interquartile range in brackets. The content of metabolites is presented in arbitrary units

Figure 3 shows examples of ^{31}P-MRS spectra of an athlete and a HCM patient.

Bivariate correlation analysis

As reported in Tables 2, 3, and 4, the variables found to be significantly different in the two groups at bivariate analysis were: age, BMI, stroke volume, EDVI, left ventricular mass index, interventricular septal thickness, asymmetry index, 2,3-DPG/γATP, lipids at 1.3 ppm and total lipids. Body mass index did not correlate with either lipid resonances at 1.3 ppm ($r = 0.318$, $P = 0.184$) or total lipids ($r = 0.421$, $P = 0.065$).

Discussion

The main finding of this study is that ^{1}H-MRS, performed in only 5 min after a standard cardiac MR examination, enabled detecting increased intramyocardial lipids in HCM patients in comparison with competitive athletes. These results are somewhat new and may open a perspective for future studies aimed at using ^{1}H-MRS in the differential diagnosis between HCM and athlete's heart. This study adds a new potential biomarker to the well-known differences in the left ventricle remodeling and function.

Causes for the accumulation of intramyocardial lipids in early stages of HCM need to be clarified and a thorough explanation is currently not available. Nonetheless, we can hypothesize that the combined effect of lipid deposition superimposed on fibrosis might help to identify individuals at higher risk of arrhythmias. One study showed that increased myocardial triglycerides in healthy subject are positively correlated to the cardiac volumes [31]. However, to our knowledge, pathologic studies demonstrated only fibrosis infiltration and not fat infiltration in HCM patients [32, 33]. Only patients affected with generalized lipodystrophy were proven to present with left ventricle hypertrophy associated with myocardial steatosis [34]. Other authors showed that overweight and obese women show increase of myocardial triglyceride associated with reduction in cardiopulmonary fitness [35]. Similar results were obtained in patients affected by type-2 diabetes [36, 37].

In our study, the phosphate metabolism of athlete's heart was preserved and the PCr/γATP ratio was in the range of normal values [14], as expected [38]. In advanced HCM, this ratio is known to be reduced resulting in heart failure [7]. The ^{31}P-MRS analysis also showed a significant difference between the two groups in terms of 2,3-DPG/γATP, with a lower value in HCM patients than in athletes.

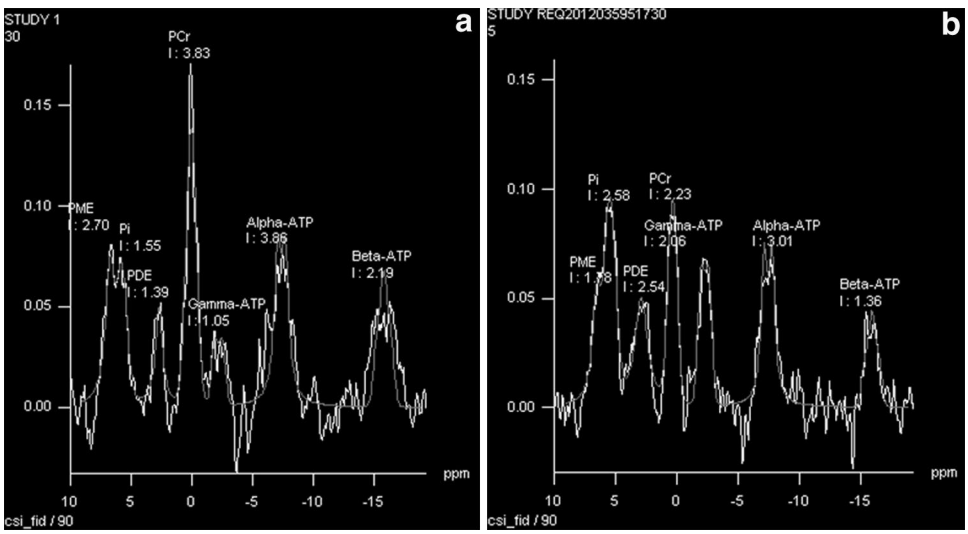

Fig. 3 Examples of ^{31}P-MRS spectra in an athlete (**a**) and a hypertrophic cardiomyopathy patient (**b**). *PCr* phosphocreatine, *ATP* adenosine triphosphate, *PDE* phosphodiester, *Pi* inorganic phosphate, *PME* phosphomonoester. Note that PCr/gamma-ATP ratio is reduced in the HCM patient

Considering that γATP alone was not significantly different in the two groups, an increase of 2,3-DPG may explain the difference in 2,3-DPG/γATP. The reason for this phenomenon could lay in the contamination of the blood pool in the voxel in subjects with a small septum. The variation of PME/PCr and Pi/PCr between the two groups was not significant, in line with the literature [29]. Notably, a not significant difference was observed in terms of PCr/γATP, as an indicator of energy metabolism. This may be due to the normal value of septal thickness in our athlete's population, without any overt athlete's heart condition.

As a potential clinical application of our study, we highlight that while ^{1}H-MRS required only five additional minutes, the ^{31}P-MRS protocol required the extraction of the patient from the magnet, the change of the coil and a new patient positioning in an uncomfortable prone position. This means that the clinical feasibility of cardiac ^{1}H-MRS is much higher than that of cardiac ^{31}P-MRS. Moreover, ^{31}P-MRS is no longer available commercially for 1.5-T MR units. It is offered only for 3-T units, whose results for cardiac imaging were reported to be not clearly better than those obtained with 1.5-T units in terms of image quality [39].

Morphologic and functional imaging data, EDVI and stroke volume, were significantly lower in HCM patients than in athletes, confirming the typical geometric pattern of the disease on one side and the heart adaptation to the intense sport activity on the other, as already reported [6]. A significant increase in left ventricle mass and septal thickness was found in HCM patients compared to athletes, as expected [6]. Interestingly, indexes of systolic function were not significantly different in the two groups, a finding that appears consistent with a relatively early stage of non-obstructive HCM patients.

This study has limitations. First, the number of subjects studied was small and bikers and volley players are different in terms of exercise (low static moderate dynamic for volley; high static and dynamic for cycling), leading to potential differences in cardiac metabolic activity. However, subgroup analysis was not possible due to the lack of statistical power. Second, the higher BMI and age in HCM patients may represent a source of bias, so that we cannot exclude that they can explain the difference in lipid content; however, bivariate correlation analysis between lipids and BMI did not show any significant correlation. Third, we did not calculate the concentrations of metabolites using internal or external references. However, the area under the peak as we used in this work can be considered a valid quantitative approach, utilized in cardiac [28, 40] and non-cardiac studies [41]. Fourth, due to the enrollment criteria, we were not able to test for differences among various underlying etiologies of HCM or specific HCM gene mutations. Fifth, ethical issues prevented from performing late gadolinium enhancement in athletes.

Conclusion

In conclusion, we found a significant increase in myocardial lipids in HCM patients compared to competitive athletes at ^{1}H-MRS. Myocardial ^{1}H-MRS may be an additional final phase of a cardiac MR protocol including standard morphologic and functional imaging in the differential diagnosis between HCM and athlete's heart. Prospective larger studies are needed to confirm this preliminary unexplained, but intriguing observation.

Acknowledgements This research received no specific grants from any funding agency in the public, commercial or not-for-profit sectors.

Compliance with ethical standards

Conflict of interest F Secchi and G. Di Leo have been sponsored to congresses by Bracco Imaging SpA (Milan, Italy). F. Sardanelli is on the speaker's bureau for Bracco Imaging SpA (Milan, Italy) and received research grants from Bayer Healthcare (Berlin, Germany).

Ethical standards This article does not contain any studies with human participants or animals performed by any of the authors.

References

1. Charron P, Carrier L, Dubourg O et al (1997) Penetrance of familial hypertrophic cardiomyopathy. Genet Couns 8:107–114
2. Maron BJ, Gardin JM, Flack JM et al (1995) Prevalence of hypertrophic cardiomyopathy in a general population of young adults. Echocardiographic analysis of 4111 subjects in the CARDIA Study. Coronary Artery Risk Development in (Young) Adults. Circulation 92:785–789
3. Crilley JG, Boehm EA, Blair E et al (2003) Hypertrophic cardiomyopathy due to sarcomeric gene mutations is characterized by impaired energy metabolism irrespective of the degree of hypertrophy. J Am Coll Cardiol 41:1776–1782
4. Van Driest SL, Ommen SR, Tajik AJ et al (2005) Sarcomeric genotyping in hypertrophic cardiomyopathy. Mayo Clin Proc 80:463–469. doi:10.1016/S0025-6196(11)63196-0
5. Wigle ED (2001) Cardiomyopathy: the diagnosis of hypertrophic cardiomyopathy. Heart 86:709–714
6. Lauschke J, Maisch B (2009) Athlete's heart or hypertrophic cardiomyopathy? Clin Res Cardiol 98:80–88
7. Esposito A, De Cobelli F, Perseghin G et al (2009) Impaired left ventricular energy metabolism in patients with hypertrophic cardiomyopathy is related to the extension of fibrosis at delayed gadolinium-enhanced magnetic resonance imaging. Heart 95:228–233
8. Maron MS, Olivotto I, Zenovich AG et al (2006) Hypertrophic cardiomyopathy is predominantly a disease of left ventricular outflow tract obstruction. Circulation 114:2232–2239
9. Wight JN, Salem D (1995) Sudden cardiac death and the "athlete's heart". Arch Intern Med 155:1473–1480

10. Firoozi S, Sharma S, McKenna WJ (2003) Risk of competitive sport in young athletes with heart disease. Heart 89:710–714
11. Pelliccia A, Maron BJ, Spataro A et al (1991) The upper limit of physiologic cardiac hypertrophy in highly trained elite athletes. N Engl J Med 324:295–301
12. Maron BJ, Pelliccia A, Spirito P (1995) Cardiac disease in young trained athletes. Insights into methods for distinguishing athlete's heart from structural heart disease, with particular emphasis on hypertrophic cardiomyopathy. Circulation 91:1596–1601
13. De Cobelli F, Esposito A, Belloni E et al (2009) Delayed-enhanced cardiac MRI for differentiation of Fabry's disease from symmetric hypertrophic cardiomyopathy. AJR Am J Roentgenol 192:97–102
14. Sardanelli F, Quarenghi M (2006) MR spectroscopy of the heart. Radiol Med 111:1025–1034
15. Holloway CJ, Suttie J, Dass S, Neubauer S (2011) Clinical cardiac magnetic resonance spectroscopy. Prog Cardiovasc Dis 54:320–327. doi:10.1016/j.pcad.2011.08.002
16. Beyerbacht HP, Vliegen HW, Lamb HJ et al (1996) Phosphorus magnetic resonance spectroscopy of the human heart: current status and clinical implications. Eur Heart J 17:1158–1166
17. Lodi R, Rajagopalan B, Blamire AM et al (2004) Abnormal cardiac energetics in patients carrying the A3243G mtDNA mutation measured in vivo using phosphorus MR spectroscopy. Biochim Biophys Acta 1657:146–150
18. van Ewijk PA, Schrauwen-Hinderling VB, Bekkers SCAM et al (2015) MRS: a noninvasive window into cardiac metabolism. NMR Biomed 28:747–766. doi:10.1002/nbm.3320
19. Bottomley PA, Weiss RG (1998) Non-invasive magnetic-resonance detection of creatine depletion in non-viable infarcted myocardium. Lancet 351:714–718
20. Faller KME, Lygate CA, Neubauer S, Schneider JE (2013) ^{1}H-MR spectroscopy for analysis of cardiac lipid and creatine metabolism. Heart Fail Rev 18:657–668
21. Nakae I, Mitsunami K, Omura T et al (2003) Proton magnetic resonance spectroscopy can detect creatine depletion associated with the progression of heart failure in cardiomyopathy. J Am Coll Cardiol 42:1587–1593
22. Ingwall JS (2009) Energy metabolism in heart failure and remodelling. Cardiovasc Res 81:412–419
23. Malavazos AE, Di Leo G, Secchi F et al (2010) Relation of echocardiographic epicardial fat thickness and myocardial fat. Am J Cardiol 105:1831–1835. doi:10.1016/j.amjcard.2010.01.368
24. van der Meer RW, Doornbos J, Kozerke S et al (2007) Metabolic imaging of myocardial triglyceride content: reproducibility of ^{1}H MR spectroscopy with respiratory navigator gating in volunteers. Radiology 245:251–257. doi:10.1148/radiol.2451061904
25. Naressi A, Couturier C, Devos JM et al (2001) Java-based graphical user interface for the MRUI quantitation package. MAGMA 12:141–152
26. den Hollander JA, Evanochko WT, Pohost GM (1994) Observation of cardiac lipids in humans by localized ^{1}H magnetic resonance spectroscopic imaging. Magn Reson Med 32:175–180
27. Felblinger J, Jung B, Slotboom J et al (1999) Methods and reproducibility of cardiac/respiratory double-triggered (1)H-MR spectroscopy of the human heart. Magn Reson Med 42:903–910
28. Hansch A, Rzanny R, Heyne J-P et al (2005) Noninvasive measurements of cardiac high-energy phosphate metabolites in dilated cardiomyopathy by using ^{31}P spectroscopic chemical shift imaging. Eur Radiol 15:319–323
29. Jung WI, Sieverding L, Breuer J et al (1998) ^{31}P NMR spectroscopy detects metabolic abnormalities in asymptomatic patients with hypertrophic cardiomyopathy. Circulation 97:2536–2542
30. Sardanelli F, Di Leo G (2009) Biostatistics for radiologists: planning, performing, and writing a radiologic study. Biostat Radiol Plan Perform Writ Radiol Study. doi:10.1007/978-88-470-1133-5
31. Sai E, Shimada K, Yokoyama T et al (2015) Evaluation of myocardial triglyceride accumulation assessed on ^{1}H-magnetic resonance spectroscopy in apparently healthy Japanese subjects. Intern Med 54:367–373. doi:10.2169/internalmedicine.54.3024
32. Elliott P, McKenna WJ (2004) Hypertrophic cardiomyopathy. Lancet 363:1881–1891. doi:10.1016/S0140-6736(04)16358-7
33. Maron BJ, Maron MS (1997) Hypertrophic cardiomyopathy. Lancet 350:127–133. doi:10.1016/S0140-6736(12)60397-3
34. Nelson MD, Victor RG, Szczepaniak EW et al (2013) Cardiac steatosis and left ventricular hypertrophy in patients with generalized lipodystrophy as determined by magnetic resonance spectroscopy and imaging. Am J Cardiol 112:1019–1024. doi:10.1016/j.amjcard.2013.05.036
35. Utz W, Engeli S, Haufe S, Kast P, Hermsdorf M, Wiesner S, Pofahl M, Traber J, Luft FC, Boschmann M, Schulz-Menger J, Jordan J (2011) Myocardial steatosis, cardiac remodelling and fitness in insulin-sensitive and insulin-resistant obesewomen. Heart 97(19):1585–1589
36. Schrauwen-Hinderling VB, Meex RCR, Hesselink MKC et al (2011) Cardiac lipid content is unresponsive to a physical activity training intervention in type 2 diabetic patients, despite improved ejection fraction. Cardiovasc Diabetol 10:47. doi:10.1186/1475-2840-10-47
37. Jonker JT, de Mol P, de Vries ST et al (2013) Exercise and type 2 diabetes mellitus: changes in tissue-specific fat distribution and cardiac function. Radiology 269:434–442. doi:10.1148/radiol.13121631
38. Pluim BM, Lamb HJ, Kayser HW et al (1998) Functional and metabolic evaluation of the athlete's heart by magnetic resonance imaging and dobutamine stress magnetic resonance spectroscopy. Circulation 97:666–672
39. Gutberlet M, Spors B, Grothoff M et al (2004) Comparison of different cardiac MRI sequences at 1.5 T/3.0 T with respect to signal-to-noise and contrast-to-noise ratios—initial experience. Rofo 176:801–808. doi:10.1055/s-2004-813220
40. Bottomley PA, Weiss RG (2001) Noninvasive localized MR quantification of creatine kinase metabolites in normal and infarcted canine myocardium. Radiology 219:411–418. doi:10.1148/radiology.219.2.r01ma39411
41. Sardanelli F, Fausto A, Di Leo G et al (2009) In vivo proton MR spectroscopy of the breast using the total choline peak integral as a marker of malignancy. Am J Roentgenol 192:1608–1617. doi:10.2214/AJR.07.3521

La radiologia medica
https://doi.org/10.1007/s11547-017-0851-6

CARDIAC RADIOLOGY

Blood-threshold CMR volume analysis of functional univentricular heart

Francesco Secchi[1] · Marco Alì[2] · Marcello Petrini[3] · Francesca Romana Pluchinotta[4] · Andrea Cozzi[5] · Mario Carminati[4] · Francesco Sardanelli[1,6]

Received: 27 July 2017 / Accepted: 26 December 2017

Abstract

Purpose To validate a blood-threshold (BT) segmentation software for cardiac magnetic resonance (CMR) cine images in patients with functional univentricular heart (FUH).

Materials and methods We evaluated retrospectively 44 FUH patients aged 25 ± 8 years (mean ± standard deviation). For each patient, the epicardial contour of the single ventricle was manually segmented on cine images by two readers and an automated BT algorithm was independently applied to calculate end-diastolic volume (EDV), end-systolic volume (ESV), stroke volume (SV), ejection fraction (EF), and cardiac mass (CM). Aortic flow analysis (AFA) was performed on through-plane images to obtain forward volumes and used as a benchmark. Reproducibility was tested in a subgroup of 24 randomly selected patients. Wilcoxon, Spearman, and Bland–Altman statistics were used.

Results No significant difference was found between SV (median 57.7 ml; interquartile range 47.9–75.6) and aortic forward flow (57.4 ml; 48.9–80.4) ($p = 0.123$), with a high correlation ($r = 0.789$, $p < 0.001$). Intra-reader reproducibility was 86% for SV segmentation, and 96% for AFA. Inter-reader reproducibility was 85 and 96%, respectively.

Conclusion The BT segmentation provided an accurate and reproducible assessment of heart function in FUH patients.

Keywords Congenital heart disease · Univentricular heart · Cardiac magnetic resonance · Ventricular function · Image segmentation

✉ Marco Alì
marco.ali90@gmail.com

Francesco Secchi
francesco.secchi@grupposandonato.it

Marcello Petrini
petrini.marcello@gmail.com

Francesca Romana Pluchinotta
francesca.pluchinotta@grupposandonato.it

Andrea Cozzi
andrea.cozzi@gmail.com

Mario Carminati
mario.carminati@grupposandonato.it

Francesco Sardanelli
francesco.sardanelli@unimi.it

[1] Unit of Radiology, IRCCS Policlinico San Donato, Via Morandi 30, 20097 San Donato Milanese, Italy

[2] Integrative Biomedical Research, Università degli Studi di Milano, Via Mangiagalli 31, 20133 Milan, Italy

[3] School in Radiodiagnostics, Università degli Studi di Milano, Via Festa del Perdono 7, 20122 Milan, Italy

[4] Department of Pediatric Cardiology and Adult Cingenital Heart Disease, IRCCS Policlinico San Donato, Via Morandi 30, 20097 San Donato Milanese, Italy

[5] Corso di Laurea in Medicina e Chirurgia, Università degli Studi di Milano, Via Festa del Perdono 7, 20122 Milan, Italy

[6] Department of Biomedical Sciences for Health, Università degli Studi di Milano, Via Morandi 30, 20133 San Donato Milanese, Italy

Published online: 22 January 2018

Introduction

The definition of univentricular heart has evolved from a narrow anatomical focus to a comprehensive view of heterogeneous conditions that ultimately result in a functional univentricular heart (FUH) [1–3].

A total cavo-pulmonary connection or Fontan circulation (FC) is the surgical approach of FUH [1, 4–6]. Constant advances in cardiac magnetic resonance (CMR) techniques and equipment in the last decade now grant adequate anatomical detail in addition to the accurate and not operator-dependent functional assessment of ventricular chambers (main and accessory), cardiac valves, and intra- or extracardiac shunts and conduits. Furthermore, the functional evaluation of FC performed by CMR does not require the use of intravenous contrast material. The possibility of using non-contrast radiation-free CMR restricts the use of computed tomography in circumstances that require a detailed anatomical assessment [7–10]. In addition, contrast-enhanced CMR could allow the detection of the myocardial fibrotic evolution, an evaluation still not clinically feasible with computed tomography [11].

Non-invasive imaging techniques play a major role in the follow-up of patients with FC. In particular, CMR is emerging as the leading modality for pre-/post-surgical assessment of congenital heart disease (CHD) as well as for early diagnosis of cardiac and systemic complications, clarifying cardiovascular anatomy and physiology [7, 12–15]. Several studies have progressively asserted the correlation between the prognosis of patients with FC and their ventricular size and function calculated with analysis and segmentation of CMR images, showing it to be equally or more accurate than echocardiographic assessment and distinctly more reproducible [8, 16, 17].

In literature, there is limited experience regarding the volume analysis of FC patients. A study [18] showed that the inclusion of the hypoplastic chamber during the segmentation of cine images of FC patients has no effect on the quantification of cardiac volumes, but may result in a less accurate measurement of the ejection fraction.

The aim of our study is to validate the blood-threshold (BT) segmentation algorithm in CMR cine images for the evaluation of cardiac function in patients with FUH.

Materials and methods

Study population

The ethics committee approval was obtained for this retrospective study (Ethics Committee of the University Hospital San Raffaele; protocol code UH_01; approved on July 14th, 2016). A total of 70 CMR examinations of patients with FUC performed at our institution between March 2008 and March 2015 were initially considered. The inclusion criteria for the re-assessment of the images were: (1) complete acquisition of cardiac volume with cine images; (2) acquisition of through-plane images of flow in the ascending aorta; and (3) the absence of atrial–ventricular valve insufficiency. Therefore, 15 examinations were excluded, and a total of 55 examinations, belonging to 44 patients (7 patients were scanned 2 times and 2 patients 3 times), were included. In case of repeated examinations on the same patient, the time interval was at least 12 months.

The 44 patients included 30 males and 14 females, with a mean age and its corresponding standard deviation (SD) at the first examination of 25 ± 8 years (mean ± standard deviation, SD). The youngest patient was 7-year-old at the time of examination, and the oldest patient was 41-year-old.

Image acquisition

All CMR examinations were performed with a 1.5-T unit (Magnetom Sonata Maestro Class or Magnetom Aera, Siemens Medical Solutions) with 40- or 45-mT/m gradient power, respectively, using a 4- or 18-channel surface phased-array coil placed over the thorax and with the patient in a supine position. The image acquisition was gated to the electrocardiographic (ECG) signal to produce a cine sequence throughout the systole and diastole and to avoid cardiac artifacts.

Each CMR study included a complete set of short-axis (from base to apex) cine images, using an ECG-triggered steady-state free precession pulse sequence acquired with the following technical parameters: repetition time (TR)/echo time (TE) = 4.0/1.5 ms; flip angle 80°; slice thickness 8 mm; time resolution 45 ms; mean acquisition time 14 ± 4 s (mean ± SD); number of phases 30.

Phase contrast (PC) through-plane sequences were used for blood flow quantification [19]. Images perpendicular to the ascending aorta were obtained (1 cm distal to the sinotubular junction). A breath-hold turbo spoiled gradient echo sequence (fast low-angle shot) was performed for phase-velocity mapping with the following technical parameters: TR/TE 4.0/3.2 ms; slice thickness 5 mm; velocity encoding (VENC) from 150 ms to 350 ms; time resolution 41 ms; mean acquisition time 15 ± 4 s. Initially, we acquired the PC sequence with a VENC of 150 ms. In the presence of aliasing, we modified the VENC adding 50 ms for each new sequence, step by step up to the complete disappearance of the aliasing artifact. The PC through-plane sequences produced two sets of images: the magnitude image and the phase-velocity map, the former to provide details on the

anatomy and identify the boundaries of the vessel and the latter for blood flow estimation [20].

Image assessment

Two independent radiologists, R1 and R2, with comparable experience (about 4 years) performed the segmentation of cardiac and flow images using MEDIS QMass 7.6 and QFlow 5.6 (Medis Medical Imaging Systems, Leiden, The Netherlands) [21, 22].

For the segmentation of cardiac images, in each session both readers independently manually traced the epicardial contour of the FUH both in the end-diastolic and end-systolic phases. Thus, the blood-threshold technique (Mass-K mode) was applied using a 50% BT and the end-diastolic volume index (EDVI), end-systolic volume index (ESVI), stroke volume (SV), ejection fraction (EF), and cardiac mass values were calculated in a totally automated way.

For the segmentation of flow images of the ascending aorta, in each session each one of the two readers positioned a region of interest on the vessel boundary of a selected slice. Subsequently, each reader propagated the segmentation through the remaining slices, the software proposed an automated adjustment, and the reader was allowed to manually correct the adjusted contours. For each session, forward flow and backward flow measurements were obtained.

Statistical analysis

Data were reported as mean ± SD or median and interquartile range (IQR) according to normal distribution or non-normal distribution, respectively.

The Wilcoxon test and Spearman correlation were used to compare and correlate the median value of SV and aortic forward flow, respectively.

The Bland–Altman method was used to estimate the intra- and inter-reader reproducibility. The intra-reader reproducibility was performed only for R1 with at least a 10-day interval between the two sessions.

The coefficient of repeatability (CoR) was calculated as 1.96 × SD of differences of the two datasets. Reproducibility was reported as complement to 100% of the ratio between the CoR and the mean. Bias (mean of the differences of the two datasets) and 95% limits of agreement (bias ± 2 SD) were plotted as well.

Results

The image analysis was feasible in all patients and no artifacts prevented readers from performing the segmentation. Fifty-five examinations were analyzed. No clinically relevant aortic regurgitation was found. The median value of the SV and aortic forward flow were 57.7 ml (IQR 47.9–75.6 ml) and 57.4 ml (IQR 48.9–80.4 ml), respectively. We found no significant difference ($p = 0.123$), but a significant correlation ($r = 0.789$, $p < 0.001$) between mean SV and aortic forward flow. All ventricle and aortic functional parameters are shown in Table 1.

The bias between the SV values measured by R1 was 0.12 ml, accompanied by a CoR of 8.1 ml, corresponding to an intra-reader reproducibility of 86%. The bias was − 0.1 ml, accompanied by a CoR of 2 ml corresponding to a reproducibility of 96%.

The inter-reader analysis of SV showed a CoR of 8.63 ml over a bias of − 1.9 ml, corresponding to an inter-reader reproducibility of 85%. The same data for the aortic forward flow were 2.12 ml over a mean difference of 0.24 ml, corresponding to an inter-reader reproducibility of 96%. Bland–Altman plots for intra- and inter-reader reproducibility are shown in Figs. 1a, b and 2a, b, respectively.

An example of segmentation of cine CMR images with the BT technique is shown in Fig. 3.

Discussion

In CMR, ventricular volume and function assessment is achieved through the segmentation of cine images. This post-processing technique, initially exclusively manually performed by trained readers, implies the recognition of the difference between the blood pool in the ventricular cavity, of other anatomical structures normally in the ventricular chamber such as trabeculae and papillary muscles (TPM) as well as of the ventricular walls. Manual tracing of contours for the ventricular walls and TPM by an experienced reader still constitutes the most widely validated and employed approach. However, in the last decade, several studies have validated techniques that, while less time-efficient than a fully automated solution, have tried to address the numerous limitations of the fully automated approach and provided a solid method, well-balanced in terms of cost-effectiveness

Table 1 Ventricle and aortic functional parameters

EDVI (ml/m^2)	63.7 (51.9–82.2)
ESVI (ml/m^2)	26.8 (21.3–46.0)
SV (ml)	57.7 (47.9–75.6)
EF (%)	51.3 (43.4–60.0)
Mass index (g/m^2)	89.2 (73.2–131.4)
Aortic forward flow (ml/heart beat)	57.4 (48.9–80.4)
Aortic backward flow (ml/heart beat)	1.9 (0.5–3.9)

Data reported as median (interquartile interval)

EDVI end-diastolic volume index, *ESVI* end-systolic volume index, *SV* stroke volume, *EF* ejection fraction

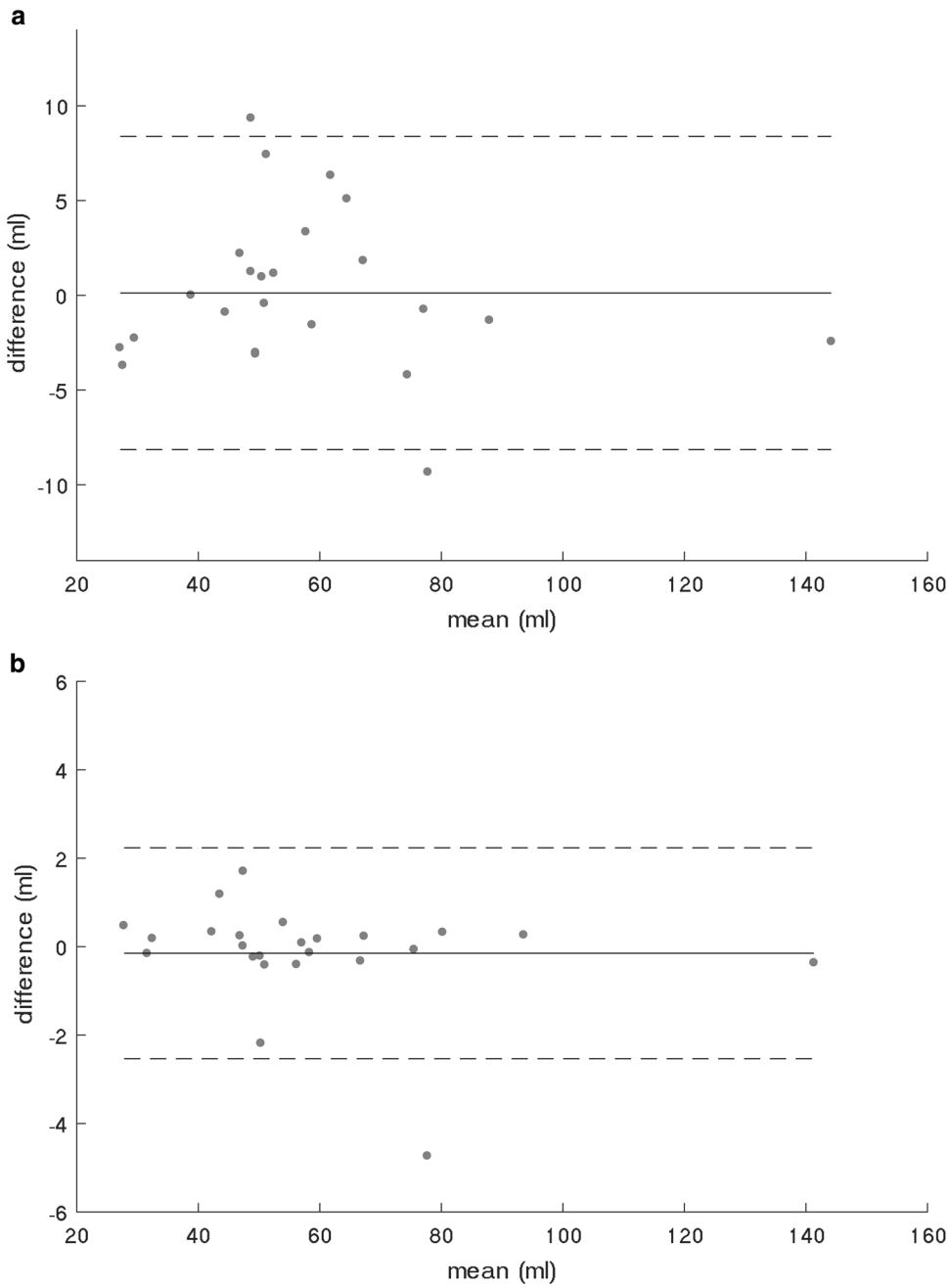

Fig. 1 Bland–Altman plot for intra-reader reproducibility of stroke volume measurement (**a**); Bland–Altman plot for aortic forward flow measurement (**b**)

analysis, to obtain a proper estimate of the ventricular volume and mass with minimal manual input [22–25]. One of these limitations is the unreliable allocation of TPM to the myocardial mass or to the blood pool. TPM allocation was shown to substantially influence the accuracy of ventricular volume and mass assessment. In some recent automatic softwares, there is the possibility to exclude TPM from the blood pool [26–28]. However, in particular conditions such as FUH, the delineation of hypertrabeculations remains difficult.

A BT technique such as the Mass-K Mode algorithm can serve as a time-saving and accurate solution to this clinical issue. In this technique, after the reader has manually traced only the epicardial contours on the end-systolic and end-diastolic phases of the cine images, the software calculates a blood percentage for each pixel inside the contoured area, considering the different signal intensity of the blood and myocardium. After visual inspection, the reader can freely alter, in any slice and phase, the default BT value of signal intensity discrimination. Moreover, semi-automated detection of the epicardial margin can be used, requiring only small manual adjustments on good quality images, further curtailing the time required for the post-processing stage [29].

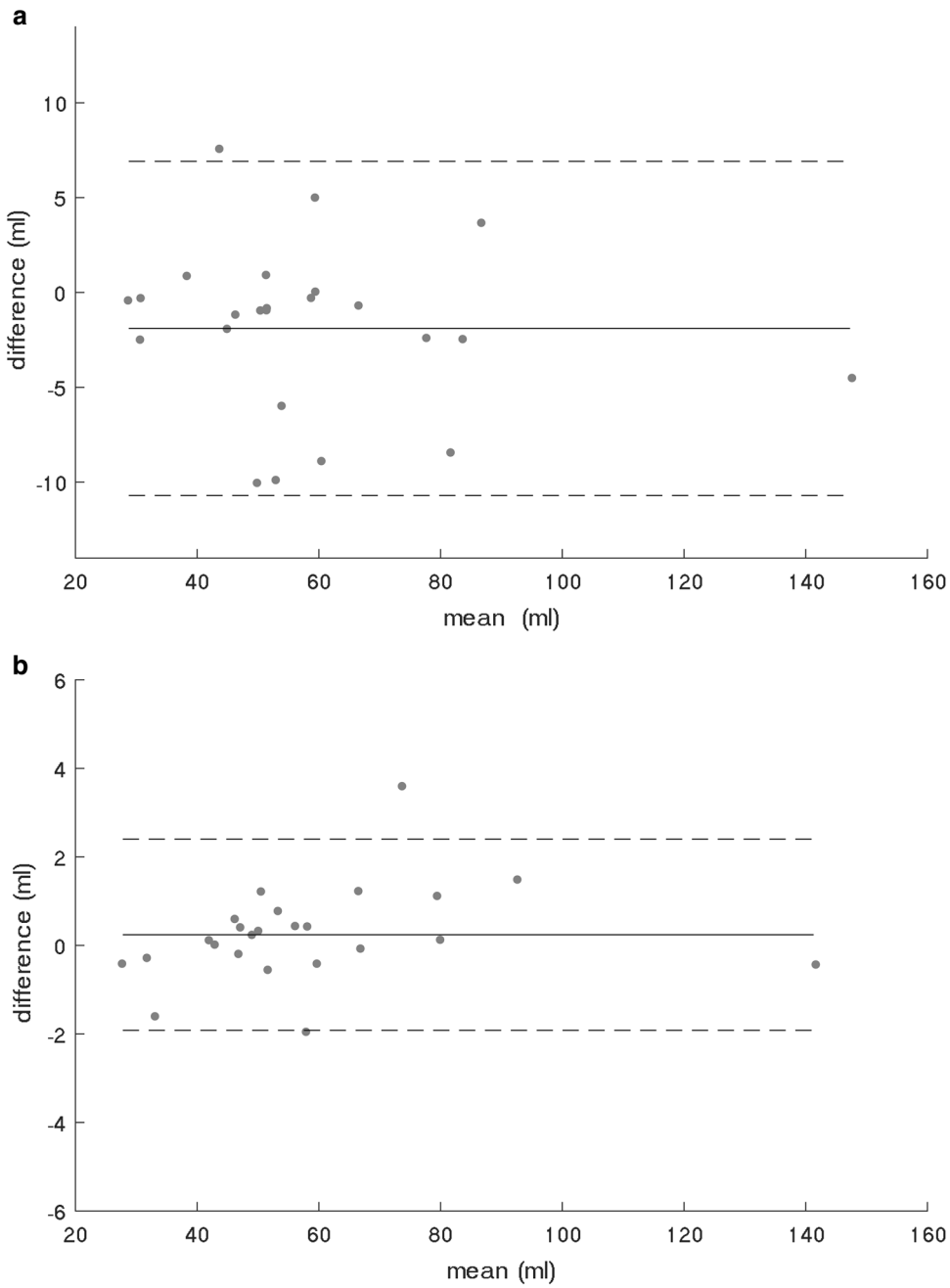

Fig. 2 Bland–Altman plot for inter-reader reproducibility of stroke volume measurement (**a**); Bland–Altman plot for aortic forward flow measurement (**b**)

The Mass-K Mode algorithm has been validated for clinical routine application, showing both accurate and reproducible evaluation of ventricular mass and volume and reduced time of analysis, by Jaspers et al. [29] on phantoms and on 12 patients with normal cardiac anatomy and function and more recently by Varga-Szemes et al. [25] on 137 patients with a broad range of cardiac diseases not including CHD.

The results of our study validate the use of this BT technique in patients with an abnormal cardiac anatomy, such as the one that is found in patients with FC. In the absence of other reference tools to validate ventricular volume assessments, we choose to use aortic flow measurements as an independent benchmark for SV, since previous studies showed it to be a solid and reproducible standard. Of note, we found no significant difference and a significant correlation between the two values [30–32].

In addition, a greater level of automation and a lesser need of manual adjustments granted by the use of the BT technique and the semi-automated recognition of epicardial contours and aortic walls account for the excellent inter- and intra-reader reproducibility of both SV and aortic flow volume (85 and 96%, respectively).

Our study has limitations. First, it is a retrospective study on a relatively small number of subjects and it is

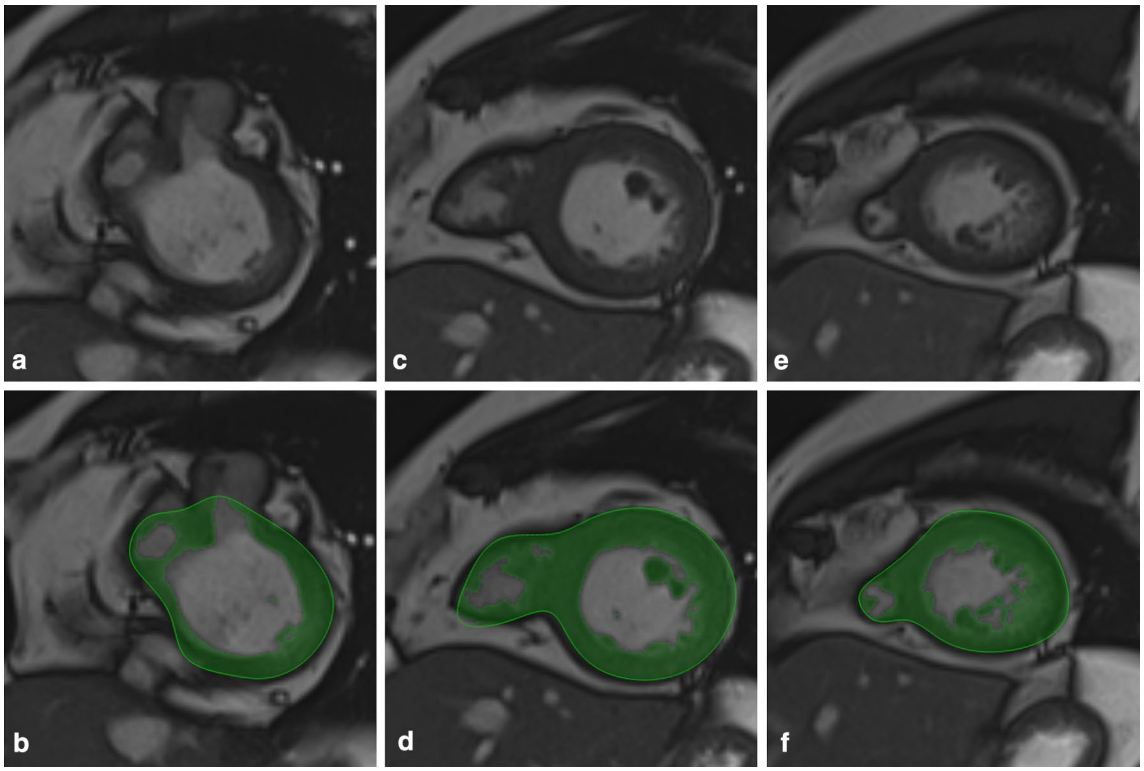

Fig. 3 Example of segmentation of short-axis cine images with blood-threshold technique. **a**, **c**, **e** Short-axis slices of cine images from base to apex without the blood-threshold mode. **b**, **d**, **f** The same images after manual epicardial volume analysis with blood-threshold mode activation

based on a single-center historical series of FC patients; however, FUV patients are a very small population and usually referred to a single center. Second, it is possible that, due to the retrospective design of our study, even small differences in the acquisition parameters, reasonably likely to happen in the absence of a standardized CMR acquisition protocol, may have negatively influenced the quality of cine images and therefore the performance of the BT technique. Third, the study lacks of an independent reference standard, though the aortic flow analysis may be considered substantially independent of the cardiac cine study. Fourth, both readers were equally experienced (about 4 years); further studies are required to investigate reproducibility between readers with different levels of experience. Finally, we should consider the possibility of obtaining the same volume analysis with different softwares; this new function could be integrated in future softwares to be used in FUH patients.

To summarize, we successfully validated the use of a BT technique for the segmentation of cine images in patients with FC. We observed a high intra- and inter-reader reproducibility for the assessment of ventricular SV and excellent agreement with aortic flow values used as a benchmark.

Funding This study was supported by local research funds of the IRCCS Policlinico San Donato, a Clinical Research Hospital partially funded by the Italian Ministry of Health.

Compliance with ethical standards

Ethical standards This article does not contain any studies with human participants or animals performed by any of the authors.

Ethical approval The Ethical Committee of IRCCS Ospedale San Raffaele approved the protocol UH_01 on July 14, 2016. Register 115/INT/2016.

Conflict of interest F Secchi has been sponsored to congresses by Bracco Imaging SpA (Milan, Italy). F. Sardanelli is on the speaker's bureau for Bracco Imaging SpA (Milan, Italy) and received research grants from Bayer Healthcare (Berlin, Germany)

References

1. Khairy P, Poirier N, Mercier L-A (2007) Univentricular heart. Circulation 115:800–812
2. Frescura C, Thiene G (2014) The new concept of univentricular heart. Front Pediatr 2:62
3. Hoffman JI, Kaplan S (2002) The incidence of congenital heart disease. J Am Coll Cardiol 39:1890–1900

4. Frommelt PC, Gerstenberger E, Cnota JF et al (2014) Impact of initial shunt type on cardiac size and function in children with single right ventricle anomalies before the Fontan procedure: the single ventricle reconstruction extension trial. J Am Coll Cardiol 64:2026–2035
5. Rao PS (2015) Fontan operation: indications, short and long term outcomes. Indian J Pediatr 82:1147–1156
6. Yoo SJ, Prsa M, Schantz D et al (2014) MR assessment of abdominal circulation in Fontan physiology. Int J Cardiovasc Imaging 30:1065–1072
7. Kutty S, Rathod RH, Danford DA, Celermajer DS (2015) Role of imaging in the evaluation of single ventricle with the Fontan palliation. Heart 102:174–183
8. Lewis G, Thorne S, Clift P, Holloway B (2015) Cross-sectional imaging of the Fontan circuit in adult congenital heart disease. Clin Radiol 70:667–675
9. Greenberg SB, Bhutta ST (2008) A dual contrast injection technique for multidetector computed tomography angiography of Fontan procedures. Int J Cardiovasc Imaging 24:345–348
10. Walsh M, Noga M, Rutledge J (2015) Cumulative radiation exposure in pediatric patients with congenital heart disease. Pediatr Cardiol 36:289–294
11. Di Cesare E, Cademartiri F, Carbone I et al (2013) Clinical indications for the use of cardiac MRI. By the SIRM Study Group on Cardiac Imaging. Radiol Med 118:752–798
12. Secchi F, Di Leo G, Papini GDE et al (2011) Cardiac magnetic resonance: impact on diagnosis and management of patients with congenital cardiovascular disease. Clin Radiol 66:720–725
13. Lu JC, Dorfman AL, Attili AK et al (2012) Evaluation with cardiovascular MR imaging of baffles and conduits used in palliation or repair of congenital heart disease. Radio Graph 32:E107–E127
14. Secchi F, Resta EC, Piazza L et al (2014) Cardiac magnetic resonance before and after percutaneous pulmonary valve implantation. Radiol Med 119:400–407
15. Secchi F, Resta EC, Cannao PM et al (2015) Four-year cardiac magnetic resonance (CMR) follow-up of patients treated with percutaneous pulmonary valve stent implantation. Eur Radiol 25:3606–3613
16. Rathod RH, Prakash A, Kim YY et al (2014) Cardiac magnetic resonance parameters predict transplantation-free survival in patients with Fontan circulation. Circ Cardiovasc Imaging 7:502–509
17. Ghelani SJ, Harrild DM, Gauvreau K et al (2015) Comparison between echocardiography and cardiac magnetic resonance imaging in predicting transplant-free survival after the Fontan operation. Am J Cardiol 116:1132–1138
18. Secchi F, Resta EC, Di Leo G et al (2014) Segmentation of cardiac magnetic resonance cine images of single ventricle: including or excluding the accessorial ventricle? Int J Cardiovasc Imaging 30:1117–1124
19. Di Leo G, D'Angelo ID, Alì M et al (2017) Intra- and inter-reader reproducibility of blood flow measurements on the ascending aorta and pulmonary artery using cardiac magnetic resonance. Radiol Med 122:179–185
20. Cawley PJ, Maki JH, Otto CM (2009) Cardiovascular magnetic resonance imaging for valvular heart disease: technique and validation. Circulation 119:468–478
21. van der Geest RJ, Niezen RA, van der Wall EE et al (1998) Automated measurement of volume flow in the ascending aorta using MR velocity maps: evaluation of inter- and intraobserver variability in healthy volunteers. J Comput Assist Tomogr 22:904–911
22. Attili AK, Schuster A, Nagel E et al (2010) Quantification in cardiac MRI: advances in image acquisition and processing. Int J Cardiovasc Imaging 26(Suppl 1):27–40
23. Petitjean C, Dacher JN (2011) A review of segmentation methods in short axis cardiac MR images. Med Image Anal 15:169–184
24. Sardanelli F, Quarenghi M, Di Leo G et al (2008) Segmentation of cardiac cine MR images of left and right ventricles: interactive semiautomated methods and manual contouring by two readers with different education and experience. J Magn Reson Imaging 27:785–792
25. Varga-Szemes A, Muscogiuri G, Schoepf UJ et al. (2015) Clinical feasibility of a myocardial signal intensity threshold-based semiautomated cardiac magnetic resonance segmentation method. Eur Radiol 26:1503–1511
26. Chuang ML, Gona P, Hautvast GLTF et al (2012) Correlation of trabeculae and papillary muscles with clinical and cardiac characteristics and impact on CMR measures of LV anatomy and function. JACC Cardiovasc Imaging 5:1115–1123
27. Weinsaft JW, Cham MD, Janik M et al (2008) Left ventricular papillary muscles and trabeculae are significant determinants of cardiac MRI volumetric measurements: effects on clinical standards in patients with advanced systolic dysfunction. Int J Cardiol 126:359–365
28. Papavassiliu T, Kühl HP, Schröder M et al (2005) Effect of endocardial trabeculae on left ventricular measurements and measurement reproducibility at cardiovascular MR imaging. Radiology 236:57–64
29. Jaspers K, Freling HG, Van Wijk K et al (2013) Improving the reproducibility of MR-derived left ventricular volume and function measurements with a semi-automatic threshold-based segmentation algorithm. Int J Cardiovasc Imaging 29:617–623
30. Jeltsch M, Ranft S, Klass O et al (2008) Evaluation of accordance of magnetic resonance volumetric and flow measurements in determining ventricular stroke volume in cardiac patients. Acta Radiol 49:530–539
31. Gatehouse PD, Rolf MP, Graves MJ et al (2010) Flow measurement by cardiovascular magnetic resonance: a multi-centre multi-vendor study of background phase offset errors that can compromise the accuracy of derived regurgitant or shunt flow measurements. J Cardiovasc Magn Reson 12:5
32. Codella NCF, Cham MD, Wong R et al (2010) Rapid and accurate left ventricular chamber quantification using a novel CMR segmentation algorithm: a clinical validation study. J Magn Reson Imaging 31:845–853

European Journal of Radiology 99 (2018) 34–39

Contents lists available at ScienceDirect

European Journal of Radiology

journal homepage: www.elsevier.com/locate/ejrad

Strain of ascending aorta on cardiac magnetic resonance in 1027 patients: Relation with age, gender, and cardiovascular disease

Marco Scarabello[a], Marina Codari[b], Francesco Secchi[b,*], Paola M. Cannaò[b], Marco Alì[c], Giovanni Di Leo[b], Francesco Sardanelli[b,d]

[a] Postgraduate School in Radiodiagnostics, Università degli Studi di Milano, Via Festa del Perdono 7, 20122, Milan, Italy
[b] Unit of Radiology, IRCCS Policlinico San Donato, Via Morandi 30, San Donato Milanese, 20097, Milan, Italy
[c] PhD Course in Integrative Biomedical Research, Department of Biomedical Sciences for Health, Università degli Studi di Milano, Via Mangiagalli, 31, 20133, Milano, Italy
[d] Department of Biomedical Sciences for Health, Università degli Studi di Milano, Via Morandi 30, 20097, San Donato Milanese, Italy

ARTICLE INFO

Keywords:
Magnetic resonance imaging
Ascending aorta
Tetralogy of Fallot
Ischemic heart disease
Aging

ABSTRACT

Objectives: To evaluate ascending aortic strain (AAS) with cardiac magnetic resonance (CMR) in a large consecutive series of patients with different types of cardiovascular disease (CVD).
Methods: Two-dimensional phase-contrast gradient-echo sequences of the ascending aorta were retrospectively reviewed in 1027 patients (726 males, 301 females). Aortic lumen area was segmented using a semi-automatic approach to calculate AAS values. Subgroup analysis was performed for patients with normal CMR, tetralogy of Fallot (ToF), and ischemic heart disease (IHD). Multivariate and post-hoc analyses were performed to evaluate the effect of age, gender, and CVD on AAS values. Shapiro-Wilk, three- and two-way ANOVA, Mann-Whitney *U*, and Spearman correlation statistics were used.
Results: Multivariate analysis showed significant differences in AAS among decades of age ($p < 0.001$), genders ($p = 0.006$) and CVD subgroups ($p < 0.001$) without interaction among these factors. A gender-related difference (higher AAS in females) was significant in ToF ($p = 0.008$), while an AAS reduction during aging was observed in all CVD subgroups. Post-hoc analysis showed a significantly lower AAS in ToF and IHD patients compared to subjects with normal CMR ($p < 0.001$).
Conclusion: Differences in age, gender, and CVD independently affect AAS. The lower AAS observed in ToF fosters its assessment during follow-up in adulthood. Future studies on causes and clinical implications of a higher AAS in females affected by ToF are warranted.

1. Introduction

Arterial stiffness is one of the earliest manifestations of adverse structural and functional changes within the vessel wall. When the aorta is considered, stiffness is a main determinant of age-related systolic and pulse pressure increase, a major predictor of stroke and myocardial infarction, and has been associated with heart failure [1–3]. Pulse wave velocity measured by applanation tonometry is a well-known functional method to non-invasively quantify aortic stiffness providing an average measure of stiffness over a certain vessel length. Conversely, strain, compliance, and distensibility are local markers of arterial elasticity, which can be measured using magnetic resonance (MR) imaging, allowing the detection of more subtle changes in regional stiffness [4].

The use of MR imaging has several advantages over ultrasound imaging including three-dimensional visualization that allows to place the imaging plane perpendicular to the vessel with a high reproducibility. Thus, aortic distensibility can be measured as a change in two-dimensional vessel perimeter or area instead of one-dimensional vessel diameter [4]. Previous authors showed that ascending aortic strain (AAS) measured with cardiac MR (CMR) is markedly decreased before the fifth decade of life and that can be considered as an early manifestation of vascular aging [5]; AAS was also shown to be independently correlated with coronary atherosclerosis and coronary calcium content [6] as well as to be an independent predictor of progression toward hypertension in non-hypertensive subjects [7].

Our aim was to evaluate the AAS in a large consecutive series of patients who underwent CMR, comparing age classes, gender, and different types of cardiovascular diseases (CVD), also including subjects with normal CMR examinations.

Abbreviations: AAS, Ascending aortic strain; CMR, Cardiac magnetic resonance; CVDs, Cardiovascular diseases; ToF, Tetralogy of Fallot; IHD, Ischemic heart disease

* Corresponding author at: Unit of Radiology, IRCCS Policlinico San Donato, Via Morandi 30, San Donato Milanese, 20097, Milan, Italy.
E-mail address: francesco.secchi@grupposandonato.it (F. Secchi).

https://doi.org/10.1016/j.ejrad.2017.12.002
Received 20 July 2017; Received in revised form 16 November 2017; Accepted 5 December 2017

2. Materials and methods

2.1. Study design and population

The local Ethics Committee approved this retrospective study (Ethics Committee of the University Hospital San Raffaele; protocol code AS01; approved on April 7th, 2016) and informed consent was waived. Patients were selected from a database of CMR studies performed between September 2008 and August 2014 at the Radiology unit of the IRCCS Policlinico San Donato, San Donato Milanese, Italy. CMR examinations with an image quality that impairs AAS evaluation were excluded from analysis. Moreover, in the case of multiple CMR examinations in the same patient, only the first one was included.

2.2. Image acquisition

We retrospectively selected images acquired with two different 1.5 T machines. Magnetom Sonata Maestro Class (Siemens, Erlangen, Germany), was used to perform the studies from September 2008 to March 2014 (n = 1294); subsequent studies (n = 69) were performed using Magnetom Aera (Siemens, Erlangen, Germany). Retrospectively electrocardiographically (ECG)-gated breath-hold two-dimensional phase-contrast gradient recalled echo sequences with a through-plane velocity encoding gradient ranging from 150 to 350 cm/s were performed on a transverse plane above the aortic bulb. Sequence parameters were as follows: repetition time 49.75 ms, echo time 3.1 ms, flip angle 30° for Magnetom Sonata; 37.12 ms, 2.47 ms, 20° for Magnetom Aera. Parallel imaging with acceleration factor 2 and retrospective ECG-gating with 30 phases per cycle (with repetition time dependent on the R-R interval) were set on both machines.

2.3. Image analysis

Image post-processing was performed using Argus Flow software (Syngo Argus Flow, version 4.02, Siemens, Erlangen, Germany). Magnitude images were used to semi-automatically segment aortic contours in each cardiac phase. During the segmentation process, an expert cardiac radiologist with 2–7 years of experience in CMR selected the frame with the optimal contrast between aortic lumen and aortic wall. Then, the operator traced in the same frame the aortic contour, which was automatically propagated in all frames of the cardiac cycle and manually corrected when necessary.

The AAS was calculated as defined by Redheuil et al. [5], namely:

$$AAS = \frac{A_{max} - A_{min}}{A_{min}}$$

where A_{max} and A_{min} represent respectively the maximum and minimum aortic cross-sectional area measured during a single cardiac cycle.

2.4. Statistical analysis

The Shapiro-Wilk test was employed to assess normality of data distribution. Due to non-normal data distribution, descriptive statistics are provided as median and corresponding inter quartile range (IQR) values. To evaluate the influence of age, gender, and CVD on the AAS values, we performed a three-way ANOVA test. The log-transformation of the data was obtained to reach the condition of normal distribution needed to perform the tree-way ANOVA. Age was categorized into 7 age bins (0–9, 10–19, 20–29, 30–39, 40–49, 50–59 and ≥60 years). Moreover, post-hoc tests for CVD and age bin factors were performed.

After this global analysis, the statistical differences in AAS values were analysed in the larger subgroups, namely: subjects with normal CMR (i.e. unremarkable examination in subjects examined to exclude cardiac abnormalities), patients with Tetralogy of Fallot (ToF), and patients with ischemic heart disease (IHD). Taking into account only these types of CVD, the evaluation of AAS changes over all the selected age bins was not possible, due to the different age distribution of subjects affected by congenital (ToF) and age-related (IHD) CVD. Therefore, statistical inference on AAS trends over age was evaluated comparing ToF and IHD subjects only with normal CMR subjects. To this aim, the Mann-Whitney *U* tests was used for each age bin. On the other hand, to evaluate the influence of gender and CVD on AAS values, a two-way ANOVA was performed. Also in this case, log-transformation of the data was obtained to perform multivariate analysis. Finally, age was considered as a continuous variable and correlation between age and AAS values was estimated using Spearman correlation coefficient. Statistical significance level was set to $p < 0.050$ and the analysis was performed using SPSS (IBM Corporation, New York, NY, United States).

3. Results

A total of 1363 CMRs were retrieved; among them, 42 examinations were excluded due to an insufficient image quality. Moreover, in order to create homogenous CVD categories, we excluded disease subgroups composed of less than 10 subjects. For this reason, other 294 cases were excluded from the analysed sample.

The final number of analysed patients was 1027. Among them, 726 were men (median age 37 years, IQR18–60) and 301 were women (median age 34 years, IQR 16–54), with borderline significance between genders ($p = 0.051$). Fig. 1 shows age distribution between genders.

Taking into account all the analysed subjects, the median AAS value was 0.25 (IQR 0.17–0.38). Shapiro Wilks test showed that AAS data were not normally distributed ($p < 0.001$) The AAS resulted inversely correlated with age ($\rho = -0.51$, $p < 0.001$). Moreover, women showed a significantly ($p = 0.006$) higher AAS (median 0.28, IQR 0.20–0.41) compared to men (median 0.24, IQR 0.16–0.36). The results of the three-way ANOVA are shown in Table 1. Post-hoc analysis showed significant differences in AAS among all the age bins except for those between 30 and 49 years of age. Fig. 2 shows the AAS trend over decades of age, while results of post-hoc test for different CVD types and their corresponding descriptive statistics are presented in Table 2.

Of the total of 1027 cases, the major subgroups were represented by 192 subjects with normal CMR (128 men, 64 women; median age 36 years, IQR 18–51), 166 patients affected with IHD (132 men, 34 women, median age 64 years, IQR 58–71), and 92 patients affected with ToF (57 men, 35 women; median age 25 years, IQR 14–40). In all the three subgroups, there was no significant difference in terms of age between men and women (normal CMR, $p = 0.997$; IHD, $p = 0.658$, ToF: $p = 0.361$).

Multivariate analysis performed on the subsample composed by these three major subgroups showed significant differences in AAS values between genders ($p = 0.002$) and among CVD subgroups ($p < 0.001$), without interaction between CVD subgroups and genders ($p = 0.119$). In general, median AAS values were higher in women than in men, as can be seen in the boxplot represented in Fig. 3. However, post-hoc analysis showed a significant difference in AAS between men and women only for ToF patients ($p = 0.008$). Moreover, men with ToF showed a significantly lower AAS when compared with men with normal CMR ($p = 0.005$). In the other two subgroups, this difference appeared to be not significant within the analysed sample. No significant difference was found between genders in subjects with normal CMR ($p = 0.728$). In IHD patients, AAS was significantly lower compared to that of normal CMR subjects (men: $p < 0.001$, women: $p = 0.016$), without significant difference between genders ($p = 0.732$).

In subjects with normal CMR, the analysis of AAS trend over age showed an inverse correlation with age both in men ($\rho = -0.53$, $p < 0.001$) and women ($\rho = -0.54$, $p < 0.001$); AAS decreased with age also in IHD patients ($\rho = -0.16$, $p = 0.039$), this correlation remaining significant in women ($\rho = -0.40$, $p = 0.021$) but not in men ($\rho = -0.11$, $p = 0.224$). Evaluating AAS over decades of age, men

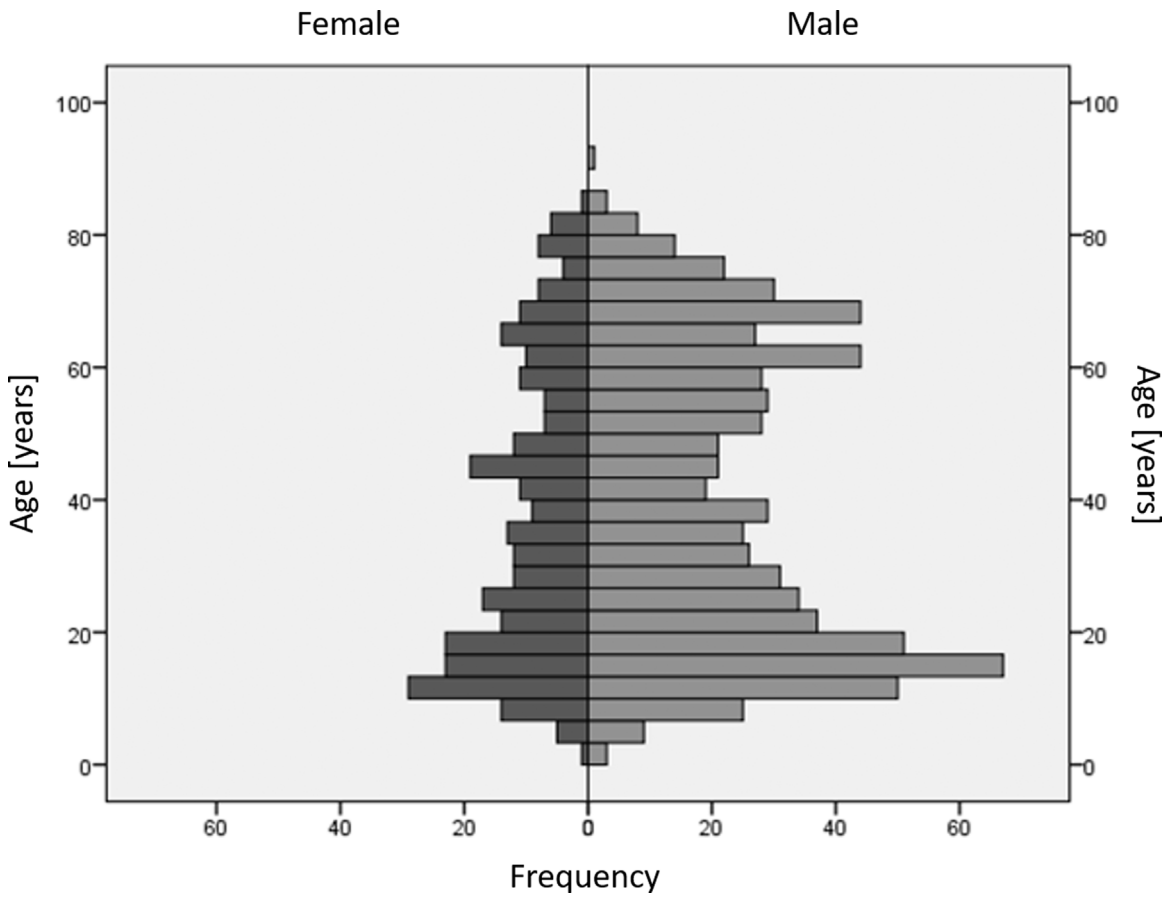

Fig. 1. Age distribution in the analysed sample.
Histograms representing age distribution among different genders in the 1027 analysed patients.

Table 1
Output of the three-way ANOVA analysis that takes into account the effect of age, gender and cardiovascular disease on ascending aortic strain values. Data shows that all the three variables (age, gender and CVD) are independently associated to AAS. Statistically significant p-values are highlighted in bold.

Source	Type III Sum of Squares	df	Mean Square	F	p-value
Age bin	19.170	6	3.195	14.295	**0.000**
Gender	1.670	1	1.670	7.470	**0.006**
CVD	16.400	18	0.911	4.076	**0.000**
CVD * Age bin	20.899	89	0.235	1.051	0.360
CVD * Gender	4.011	18	0.223	0.997	0.460
Gender * Age bin	0.463	6	0.077	0.346	0.913
CVD * Gender * Age bin	10.075	51	0.198	0.884	0.703
Error	187.071	837	0.224		
Total	2272.154	1027			
Corrected Total	348.130	1026			

CVD: cardiovascular disease; df: degrees of freedom.

with IHD had an AAS significantly lower than that of normal CMR subjects only between 50 and 59 years of age ($p = 0.019$). No significant differences were found between women affected with IHD and women with normal CMR for all age bins.

Also in ToF patients the AAS decreased with age, significantly in men ($\rho = -0.66$, $p < 0.001$), not significantly in women ($\rho = -0.28$, $p = 0.106$). Moreover, men affected with ToF belonging to the 20–49 age range had AAS values significantly lower than men with normal CMR (20–29 years, $p = 0.002$; 30–39 years, $p = 0.011$; 40–49 years, $p < 0.001$); after 50 years of age, this difference was not significant. On the other hand, women affected by ToF did not show significantly lower AAS values for all the age bins when compared to normal CMR women. Fig. 4 shows the age-related changes of AAS over decades of age for all the above-mentioned subgroups.

4. Discussion

In this study, AAS values were analysed in a large consecutive series of patients with different types of CVD and in subjects with normal (unremarkable) CMR. This study proved that difference in age, gender, and CVD independently affect the AAS.

Age distribution of the analysed sample was characterized by two peaks, the first at age 15 and the second at age 60, as visible in Fig. 1, reflecting the high number of patients with congenital and age-related heart diseases in our series. This was confirmed by the fact that, among the analysed CVDs, the most frequent were IHD and ToF, which represent two different pathophysiological processes both affecting AAS: age-related factors and congenital/developmental factors, respectively.

Gender difference in AAS in the whole patient dataset was likely due to a different proportion between males and females in some CVD subgroups, since subjects with normal (unremarkable) CMR showed no significant gender difference in term of AAS. Gender-related differences appeared not to be influenced by age or CVD, although in patients with ToF there was a gender-related difference in AAS, in line with a previous study where differences in functional cardiovascular parameters between male and female patients with ToF was found [8]. Furthermore, other studies demonstrated a gender-related difference in arterial aging and stiffening process, suggesting that hormonal and other gender-specific factors can modulate the aging process [9].

Vascular changes with age are well-known. The progressive decrease in AAS during life reflects physiological and pathological

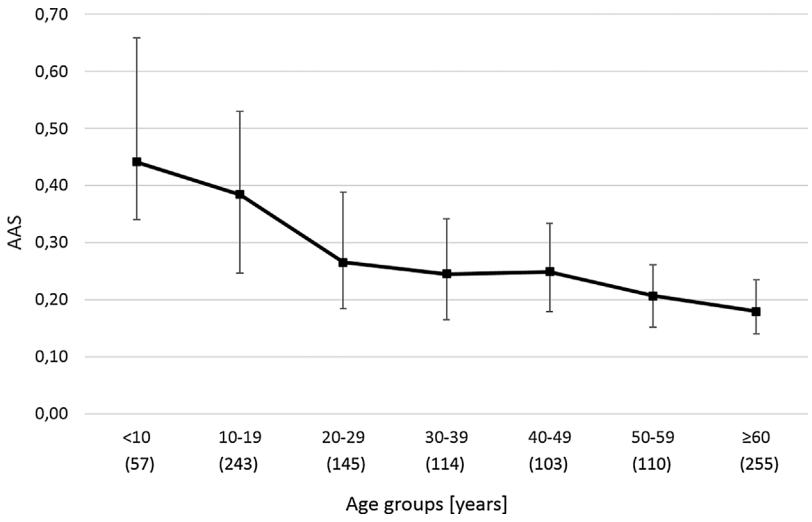

Fig. 2. Ascending Aortic strain over age.
Ascending aortic strain (AAS) values over decades of age in the analysed sample of 1027 consecutive subjects. For each age subgroup the number of included subjects is reported between brackets.

Table 2
Post hoc tests performed on different cardiovascular disease subgroups. In this table are shown only post hoc tests performed between subjects with normal cardiac magnetic resonance and patients with different diseases. Statistically significant p-values are highlighted in bold.

CVD (number of subjects)	Median	Q_1	Q_3	*p-value*
Normal CMR (192)	0.30	0.22	0.41	
Tetralogy of Fallot (92)	0.30	0.16	0.39	< **0.001**
Transposition of the great arteries (61)	0.25	0.18	0.36	**0.006**
Post Melody valve implantation (39)	0.20	0.13	0.31	< **0.001**
Fontan procedure (23)	0.23	0.16	0.34	**0.007**
Bicuspid aortic valve (45)	0.36	0.23	0.61	0.047
Pulmonary insufficiency (70)	0.30	0.18	0.57	0.334
Aortic insufficiency (33)	0.30	0.18	0.42	0.487
Aortic valve stenosis (15)	0.64	0.32	0.90	< **0.001**
Pulmonary valve stenosis (22)	0.26	0.15	0.39	0.088
Ross procedure (10)	0.13	0.09	0.22	< **0.001**
Ascending aortic dilatation (58)	0.18	0.13	0.26	< **0.001**
Ascending aortic aneurysm (19)	0.14	0.10	0.20	< **0.001**
Aortic coarctation (66)	0.41	0.32	0.57	< **0.001**
Ischemic heart disease (166)	0.18	0.14	0.26	< **0.001**
Dilated cardiomyopathy (34)	0.22	0.19	0.30	**0.001**
Hypertrophic cardiomyopathy (31)	0.25	0.19	0.34	0.058
Surgical ventricular restoration (32)	0.22	0.16	0.26	< **0.001**
Left ventricular hypertrophy (19)	0.28	0.18	0.32	0.060

CMR: cardiac magnetic resonance; CVD: cardiovascular disease.

modifications of mechanical, histological, and functional properties of the aortic wall. Moreover, differences in cardiac function and pulse wave reflection by medium and small arteries contribute to AAS. Animal studies indicated that age-related changes in aortic stiffness and strain may not entirely due to pathologic causes such as atherosclerosis and diabetes but also to physiological aging [9]. However, we found that patients with IHD have a significantly lower AAS compared to normal (unremarkable) CMR subjects between 50 and 59 years of age, highlighting the association between coronary artery disease and reduction in aortic elasticity.

Multivariate analysis showed the presence of significant differences in AAS among patient with different age, genders, and cardiovascular conditions. Moreover, these results show that the interaction among these parameters does not impact on AAS. In patients with certain diseases such as IHD, a decrease or increase in AAS is more easily explainable on the basis of different age, morpho-functional or pathophysiologic characteristics. On the other hand, in patients with other diseases such as ToF, the results are less obvious.

Patients with IHD showed a reduced AAS compared to normal CMR subjects between 50 and 59 years of age; this difference is reduced for subjects over 60 years of age, being not significant. This result may be due to a combination of factors: increased aortic stiffness determined by atherosclerosis (more pronounced in patients with IHD) and reduced cardiac output, implying a decreased stretching of the ascending aorta.

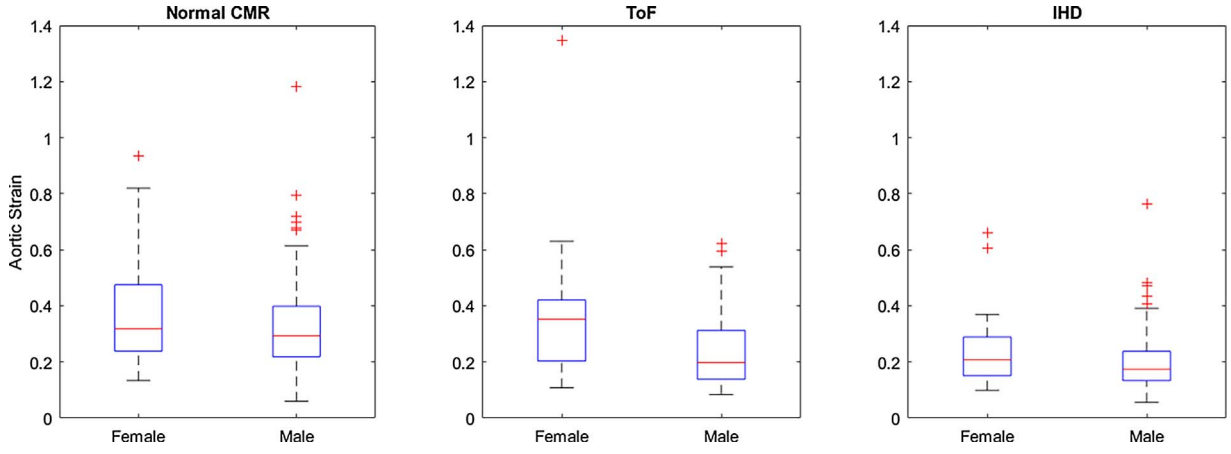

Fig. 3. Subgroup analysis.
Three boxplots that represents ascending aortic strain values in normal cardiac magnetic resonance (CMR) subjects, patients with tetralogy of Fallot (ToF) and ischemic heart disease (IHD), subdivided by gender.

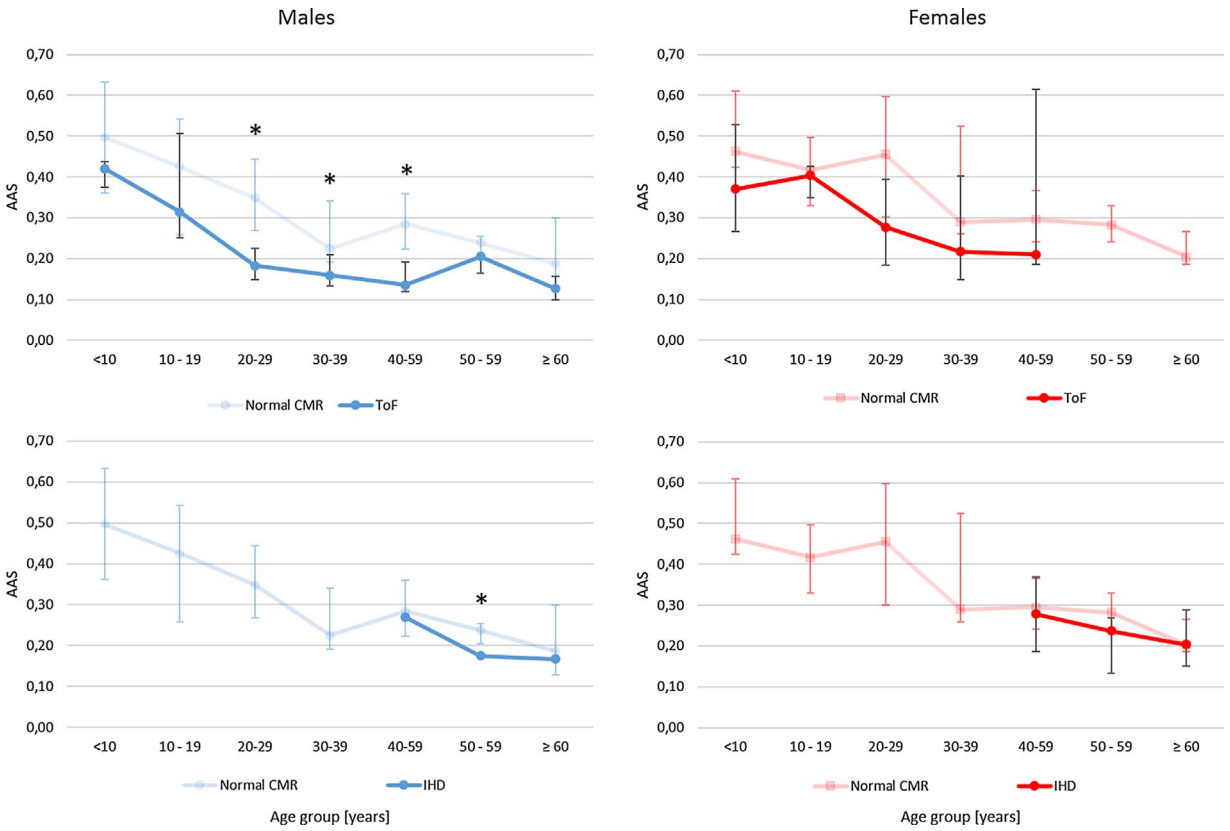

Fig. 4. Ascending aortic strain over age in subgroup analysis.
Ascending aortic strain (AAS) values over decades of age in subjects with normal cardiac magnetic resonance (CMR), patients with tetralogy of Fallot (ToF) and ischemic heart disease (IHD), divided by gender. Statistically significant comparisons are marked with a star (*).

This values may however underestimate the real difference because subjects with normal CMR were not really healthy controls but patients with unremarkable CMR who may have had one or more CVD risk factors that could have contributed to a decrease in AAS.

AAS was significantly lower in patients with ToF than in patients with normal CMR, especially in males in the 3rd and 4th decade of life. This result is probably due at least in part to an intrinsic morpho-functional defect in ToF, described by other authors as a fragmentation of elastic fibres in aortic medial wall [10–15]. A similar study by Christensen et al. [15] highlighted the relationship between age at repair of ToF and AAS. One of the most though-provoking results was the poor correlation between AAS and PWV, highlighting the need for a local assessment of the aortic elastic properties. Our results were slightly different, the AAS being higher in the present study, probably due to the age difference in the study population or the timing of the ToF repair, with comparable correlations between AAS and ascending aortic cross sectional area. The gender difference could reflect differences in biventricular volumes and function, as well as differences in timing and type of ToF treatment. Nonetheless, we could hypothesize that there is also a gender-related factor that affects AAS in ToF patients. AAS was also lower in patients affected by TGA and in those patients that underwent Fontan and Ross procedures, in accordance with previously reported findings [14,16–18]. These results reaffirm the importance of including aortic morphological and functional evaluation in the follow-up of patients with congenital heart diseases.

Aortic strain reflects vascular compliance in large vessels and is lower in older patients. We did not find a significant difference in subjects over 60 regardless of the pre-existing diseases, probably because of the prevailing aging process [19]. Another possible explanation is that older subjects with a normal (unremarkable) CMR could have been exposed to the same risk factors and have ongoing pathophysiological processes similar to those affecting patients with IHD, making them less suitable for a direct comparison. On the other hand, differences in AAS in young patients with congenital heart disease could reflect a precocious arterial stiffening [5].

This study also showed that aortic strain can be easily and rapidly obtained using phase-contrast sequences usually performed for flow analysis; its evaluation and monitoring could be beneficial in detecting aortic stiffening. Moreover, it may be used for non-invasive follow-up evaluations of aortic condition in CVD patients.

This study is affected by several limitations mainly due to its retrospective design. Firstly, we should consider that prospective studies included blood pressure data measured after the sequence [14] since it is somewhat difficult to measure blood pressure during the acquisition of a CMR sequence. We could not include this parameter in our analysis. However, brachial blood pressure measurements could lead to an overestimation of central blood pressure and biased aortic distensibility. Secondly, we did not use a standardized plane placement on the ascending aorta. The sequences were not purposely acquired to measure aortic cross sectional area but they were placed by the same operator above the aortic root to evaluate ascending aortic flow. For this reason the systolic motion of the ascending aorta due to myocardial contraction was not accounted for, similarly to another study [15]. Our technique, being simple and not relying on peak flow to choose the timing for plane placement in order to assess minimum and maximum area, is surely less accurate than the one used by Grotenhuis et al. [20]. Finally, we lack really healthy control subjects. Since the differences in terms of AAS were significant when comparing age matched subgroups of patients with normal (unremarkable) CMR and with CVD, we are confident that there was a significant reduction in AAS in at least two of the major subgroups of patients compared to what we expect in normal subjects of similar age.

In conclusion, we found that AAS is independently affected by differences in age, gender, and cardiovascular condition. In particular, this

tendency was evident in patients with ToF and IHD, where the aging process seems to prevail on pre-existent differences in terms of AAS in subjects over 60. Our results highlight the possibility to use AAS for a non-invasive assessment of the aortic status in CVD patients. Nevertheless, further investigations on elderly patients and, in particular, in adults with congenital heart disease are advised.

Funding

This study was supported by local research funds of the IRCCS Policlinico San Donato, a Clinical Research Hospital partially funded by the Italian Ministry of Health.

Conflict of interest

None.

References

[1] F.U.S. Mattace-Raso, T.J.M. Van Der Cammen, A. Hofman, N.M. Van Popele, M.L. Bos, M.A.D.H. Schalekamp, R. Asmar, R.S. Reneman, A.P.G. Hoeks, M.M.B. Breteler, J.C.M. Witteman, Arterial stiffness and risk of coronary heart disease and stroke: the Rotterdam study, Circulation 113 (2006) 657–663, http://dx.doi.org/10.1161/CIRCULATIONAHA.105.555235.

[2] C. Giannattasio, F. Achilli, M. Failla, A. Capra, A. Vincenzi, F. Valagussa, G. Mancia, Radial, carotid and aortic distensibility in congestive heart failure: effects of high-dose angiotensin-converting enzyme inhibitor or low-dose association with angiotensin type 1 receptor blockade, J. Am. Coll. Cardiol. 39 (2002) 1275–1282, http://dx.doi.org/10.1016/S0735-1097(02)01755-2.

[3] P. Boutouyrie, A.I. Tropeano, R. Asmar, I. Gautier, A. Benetos, P. Lacolley, S. Laurent, Aortic stiffness is an independent predictor of primary coronary events in hypertensive patients: a longitudinal study, Hypertension 39 (2002) 10–15, http://dx.doi.org/10.1161/hy0102.099031.

[4] J.L. Cavalcante, J.A.C. Lima, A. Redheuil, M.H. Al-Mallah, Aortic stiffness: current understanding and future directions, J. Am. Coll. Cardiol. 57 (2011) 1511–1522, http://dx.doi.org/10.1016/j.jacc.2010.12.017.

[5] A. Redheuil, W.C. Yu, C.O. Wu, E. Mousseaux, A. De Cesare, R. Yan, N. Kachenoura, D. Bluemke, J.A.C. Lima, Reduced ascending aortic strain and distensibility: earliest manifestations of vascular aging in humans, Hypertension 55 (2010) 319–326, http://dx.doi.org/10.1161/HYPERTENSIONAHA.109.141275.

[6] T. Durmaz, T. Keles, N.A. Bayram, H. Ayhan, M. Akcay, M.R. Metin, E. Bozkurt, Aortic strain, distensibility and elastic modulus are associated with the presence and quantity of coronary calcium, Kardiol. Pol. 68 (2010) 1353–1359 http://www.ncbi.nlm.nih.gov/pubmed/21174289.

[7] J. Dernellis, M. Panaretou, Aortic stiffness is an independent predictor of progression to hypertension in nonhypertensive subjects, Hypertension 45 (2005) 426–431, http://dx.doi.org/10.1161/01.HYP.0000157818.58878.93.

[8] S. Sarikouch, H. Koerperich, K.O. Dubowy, D. Boethig, P. Boettler, T.S. Mir, B. Peters, T. Kuehne, P. Beerbaum, Impact of gender and age on cardiovascular function late after repair of tetralogy of fallot: percentiles based on cardiac magnetic resonance, Circ. Cardiovasc. Imaging 4 (2011) 703–711, http://dx.doi.org/10.1161/CIRCIMAGING.111.963637.

[9] H. Qiu, C. Depre, K. Ghosh, R.G. Resuello, F.F. Natividad, F. Rossi, A. Peppas, Y.T. Shen, D.E. Vatner, S.F. Vatner, Mechanism of gender-specific differences in aortic stiffness with aging in nonhuman primates, Circulation 116 (2007) 669–676, http://dx.doi.org/10.1161/CIRCULATIONAHA.107.689208.

[10] K. Niwa, J.K. Perloff, S.M. Bhuta, H. Laks, D.C. Drinkwater, J.S. Child, P.D. Miner, Structural abnormalities of great arterial walls in congenital heart disease light and electron microscopic analyses, Circulation 103 (2001) 393–400, http://dx.doi.org/10.1161/01.cir.103.3.393.

[11] K. Niwa, Aortic root dilatation in tetralogy of fallot long-term after repair – histology of the aorta in tetralogy of Fallot: evidence of intrinsic aortopathy, Int. J. Cardiol. 103 (2005) 117–119, http://dx.doi.org/10.1016/j.ijcard.2004.07.002.

[12] M. Seki, C. Kurishima, H. Saiki, S. Masutani, H. Arakawa, M. Tamura, H. Senzaki, Progressive aortic dilation and aortic stiffness in children with repaired tetralogy of Fallot, Heart Vessels 29 (2014) 83–87, http://dx.doi.org/10.1007/s00380-013-0326-1.

[13] K. Niwa, S.C. Siu, G.D. Webb, M.A. Gatzoulis, Progressive aortic root dilatation in adults late after repair of tetralogy of Fallot, Circulation 106 (2002) 1374–1378, http://dx.doi.org/10.1161/01.CIR.0000028462.88597.AD.

[14] T. Rutz, F. Max, A. Wahl, K. Wustmann, K. Khattab, J.P. Pfammatter, A. Kadner, M. Schwerzmann, Distensibility and diameter of ascending aorta assessed by cardiac magnetic resonance imaging in adults with tetralogy of fallot or complete transposition, Am. J. Cardiol. 110 (2012) 103–108, http://dx.doi.org/10.1016/j.amjcard.2012.02.055.

[15] J.T. Christensen, J.C. Lu, J. Donohue, S. Yu, M.G. Mahani, P.P. Agarwal, A.L. Dorfman, Relation of aortic stiffness and strain by cardiovascular magnetic resonance imaging to age in repaired tetralogy of fallot, Am. J. Cardiol. 113 (2014) 1031–1035, http://dx.doi.org/10.1016/j.amjcard.2013.11.067.

[16] L. Tomkiewicz-Pajak, H. Dziedzic-Oleksy, J. Pajak, M. Olszowska, J. Kolcz, M. Komar, P. Podolec, Arterial stiffness in adult patients after Fontan procedure, Cardiovasc. Ultrasound 12 (2014) 15, http://dx.doi.org/10.1186/1476-7120-12-15.

[17] K.A. Myers, M.T. Leung, M. Terri Potts, J.E. Potts, G.G.S. Sandor, Noninvasive assessment of vascular function and hydraulic power and efficiency in pediatric Fontan patients, J. Am. Soc. Echocardiogr. 26 (2013) 1221–1227, http://dx.doi.org/10.1016/j.echo.2013.06.013.

[18] J. Christensen, J.C. Lu, S. Yu, J. Donohue, P.P. Agarwal, M.G. Mahani, A.L. Dorfman, Pulse wave velocity does not predict ventricular strain in Ross patients, J. Cardiovasc. Magn. Reson. 16 (2014) P113, http://dx.doi.org/10.1186/1532-429X-16-S1-P113.

[19] G.D. Aquaro, A. Cagnolo, K.K. Tiwari, G. Todiere, S. Bevilacqua, G. Di Bella, L. Ait-Ali, P. Festa, M. Glauber, M. Lombardi, Age-dependent changes in elastic properties of thoracic aorta evaluated by magnetic resonance in normal subjects, Interact. Cardiovasc. Thorac. Surg. 17 (2013) 674–679, http://dx.doi.org/10.1093/icvts/ivt261.

[20] H.B. Grotenhuis, J. Ottenkamp, D. Fontein, H.W. Vliegen, J.J.M. Westenberg, L.J.M. Kroft, A. de Roos, Aortic elasticity and left ventricular function after arterial switch operation: MR imaging–initial experience, Radiology 249 (2008) 801–809, http://dx.doi.org/10.1148/radiol.2492072013.

Intra- and inter-reader reproducibility of blood flow measurements on the ascending aorta and pulmonary artery using cardiac magnetic resonance

Giovanni Di Leo, Ida Daniela D'Angelo, Marco Alì, Paola Maria Cannaò, Giovanni Mauri, Francesco Secchi & Francesco Sardanelli

La radiologia medica
Official Journal of the Italian Society of Medical Radiology

ISSN 0033-8362

Radiol med
DOI 10.1007/s11547-016-0706-6

Springer

Radiol med
DOI 10.1007/s11547-016-0706-6

CARDIAC RADIOLOGY

Intra- and inter-reader reproducibility of blood flow measurements on the ascending aorta and pulmonary artery using cardiac magnetic resonance

Giovanni Di Leo[1] · Ida Daniela D'Angelo[2] · Marco Alì[3] · Paola Maria Cannaò[1] · Giovanni Mauri[1] · Francesco Secchi[1] · Francesco Sardanelli[1,4]

Received: 28 April 2016 / Accepted: 31 October 2016

Abstract The aim of our study was to estimate the intra- and inter-reader reproducibility of blood flow measurements in the ascending aorta and main pulmonary artery using cardiac magnetic resonance (CMR) and a semi-automated segmentation method. The ethics committee approved this retrospective study. A total of 50 consecutive patients (35 males and 15 females; mean age±standard deviation 27±13 years) affected by congenital heart disease were reviewed. They underwent CMR for flow analysis of the ascending aorta and main pulmonary artery (1.5 T, through-plane phase-contrast sequences). Two independent readers (R1, trained radiology resident; R2, lower-trained technician student) obtained segmented images twice (>10-day interval), using a semi-automated method of segmentation. Peak velocity, forward and backward flows were obtained. Bland–Altman analysis was used and reproducibility was reported as complement to 100% of the ratio between the coefficient of repeatability and the mean. R1 intra-reader reproducibility for the aorta was 99% (peak velocity), 95% (forward flow) and 49% (backward flow); for the pulmonary artery, 99%, 91% and 90%, respectively. R2 intra-reader reproducibility was 92%, 91% and 38%; 98%, 86% and 87%, respectively. Inter-reader reproducibility for the aorta was 91%, 85% and 20%; for the pulmonary artery 96%, 75%, and 82%, respectively. Our results showed a good to excellent reproducibility of blood flow measurements of CMR together with a semiautomated method of segmentation, for all variables except the backward flow of the ascending aorta, with a limited impact of operator's training.

Keywords Cardiac magnetic resonance · Reproducibility · Heart valve · Phase-contrast sequences · Blood flow

✉ Marco Alì
marco.ali90@gmail.com

Giovanni Di Leo
gianni.dileo77@gmail.com

Ida Daniela D'Angelo
idanieladangelo@libero.it

Paola Maria Cannaò
paola.m.cannao@gmail.com

Giovanni Mauri
vanni.mauri@gmail.com

Francesco Secchi
francesco.secchi@grupposandonato.it

Francesco Sardanelli
francesco.sardanelli@unimi.it

[1] Radiology Unit, Research Hospital Policlinico San Donato, Via Morandi 30, 20097 San Donato Milanese, Italy

[2] Postgraduation School in Radiodiagnostic, Università degli Studi di Milano, Via Festa del Perdono 7, 20122 Milan, Italy

[3] PhD Course in Integrative Biomedical Research, Università degli Studi di Milano, Via Mangiagalli 31, 20133 Milan, Italy

[4] Department of Biomedical Science for Health, Università degli Studi di Milano, Via Morandi 30, 20097 San Donato Milanese, Italy

Introduction

In the past years, cardiovascular magnetic resonance (CMR) has emerged as an alternative non-invasive imaging technique for the evaluation of patients with cardiovascular disease, providing an accurate anatomic and functional characterization of the heart and great vessels as well as the possibility to investigate nearly the whole spectrum of cardiac disease [1]. Especially for patients affected with congenital heart disease, CMR plays an important role in

Published online: 22 November 2016

the quantification of blood flow and evaluation of valve stenosis/insufficiency using phase-contrast (PC) through-plane sequences [2–11]. The PC sequences were validated in phantom and in vivo studies and have proven to be a reliable tool for the quantitative and qualitative analysis of blood flow and tissue motion [12].

Despite its importance for the assessment of disease progression, few data are available about the reproducibility of CMR in the measurement of blood flow in patients with valve stenosis and/or insufficiency [2, 13–15]. Moreover, segmentation methods were validated indirectly, through the ability to provide accurate flow measurement [13, 16] or pulse wave velocity [16, 17] or directly in terms of operator variability [13, 14] or agreement with manual tracing [17].

Blood flow measurements are based on the segmentation of a vessel contour that may be performed manually or, more typically, semi-automatically, with the use of computer software likely impacting on measurement reproducibility. Reader experience may play a role as well.

Thus, the aim of our study was to estimate the intra- and inter-reader reproducibility of blood flow CMR measurements through the ascending aorta and main pulmonary artery in patients affected with congenital heart disease or with aortic and/or pulmonary valve disease. The impact on reproducibility of the reader's experience with CMR was also investigated.

Materials and methods

The ethics committee approval was obtained for this retrospective study. A total of 50 consecutive patients affected with a congenital heart disease or with aortic and/or pulmonary valve disease were reviewed. They all underwent CMR at our institution between November 2012 and May 2013. Of 50 patients, 35 were males and 15 females, with a mean age of 27 ± 13 years (mean ± standard deviation). The disease spectrum is shown in Table 1. The majority of patients ($n = 28$, 56%) had a Tetralogy of Fallot.

All CMR examinations were performed with a 1.5-T unit with 40-mT/m gradient power (Magnetom Sonata Maestro Class, Siemens Medical Solution, Erlangen, Germany), using a four-channel surface phased-array coil placed over the thorax and with the patient in supine position.

A CMR study included a complete set of short-axis (from base to apex) and long-axis (2-, 3- and 4-chamber views) cine images, using an ECG-triggered breath-hold steady-state free precession sequence acquired with the following technical parameters: TR/TE 4.0/1.5 ms; flip angle 80°; slice thickness 7 mm; time resolution 45 ms; mean acquisition time 14 ± 4 s.

Table 1 Disease spectrum in 50 studied patients

Category	Detail	*n*	%
Aortic disease	Aortic insufficiency	1	2%
Pulmonary artery disease	Pulmonary insufficiency in ToF	28	56%
	Pulmonary insufficiency	7	14%
	Stenosis of pulmonary artery conduit	6	12%
	Pulmonary stenosis	3	6%
	Pulmonary steno-insufficiency	2	4%
Other	VSD	2	4%
	Truncus arteriosus	1	2%
Total		50	100%

ToF tetralogy of fallot, *VSD* ventricular septal defect

The PC through-plane sequences were used for blood flow quantification. Images perpendicular to the vessel of interest were obtained. A breath-hold turbo spoiled gradient echo sequence (fast low-angle shot) was performed for phase-velocity mapping with the following technical parameters: TR/TE 4.0/3.2 ms; slice thickness 5 mm; velocity encoding (VENC) from 150 cm/s to 350 cm/s; time resolution 41 ms; mean acquisition time 15 ± 4 s. For each patient, we initially acquired the PC sequence with a VENC of 150 cm/s: in the presence of aliasing, we increased the VENC adding 50 cm/s for each new sequence, step-by-step up to the complete disappearance of the aliasing artifact.

Flow measurements were performed right above the aortic or pulmonary valve in patients with surgical or percutaneous valve replacement. In patients without valve replacement, measurements were performed below, at the level and above the native valve. The PC sequences produced two sets of images: the gradient echo image and the phase velocity map (Fig. 1). The magnitude image depicts the anatomy and allows to identify the vessel boundaries, while the phase velocity map corresponds to blood velocity [2].

Two independent readers (R1 and R2) performed measurements twice, with at least a 10-day interval between the two sessions, for a total of four sessions. These readers had different educational background and different level of training in CMR segmentation. While R1 was a radiology resident with 4 months of full-immersion training (under the supervision of a radiologist with a 5-year experience in CMR), R2 was a technician student with 2 weeks of training (under the supervision of the same experienced radiologist).

Both readers used the Argus software on a remote workstation (Leonardo, Siemens Medical Solution, Erlangen,

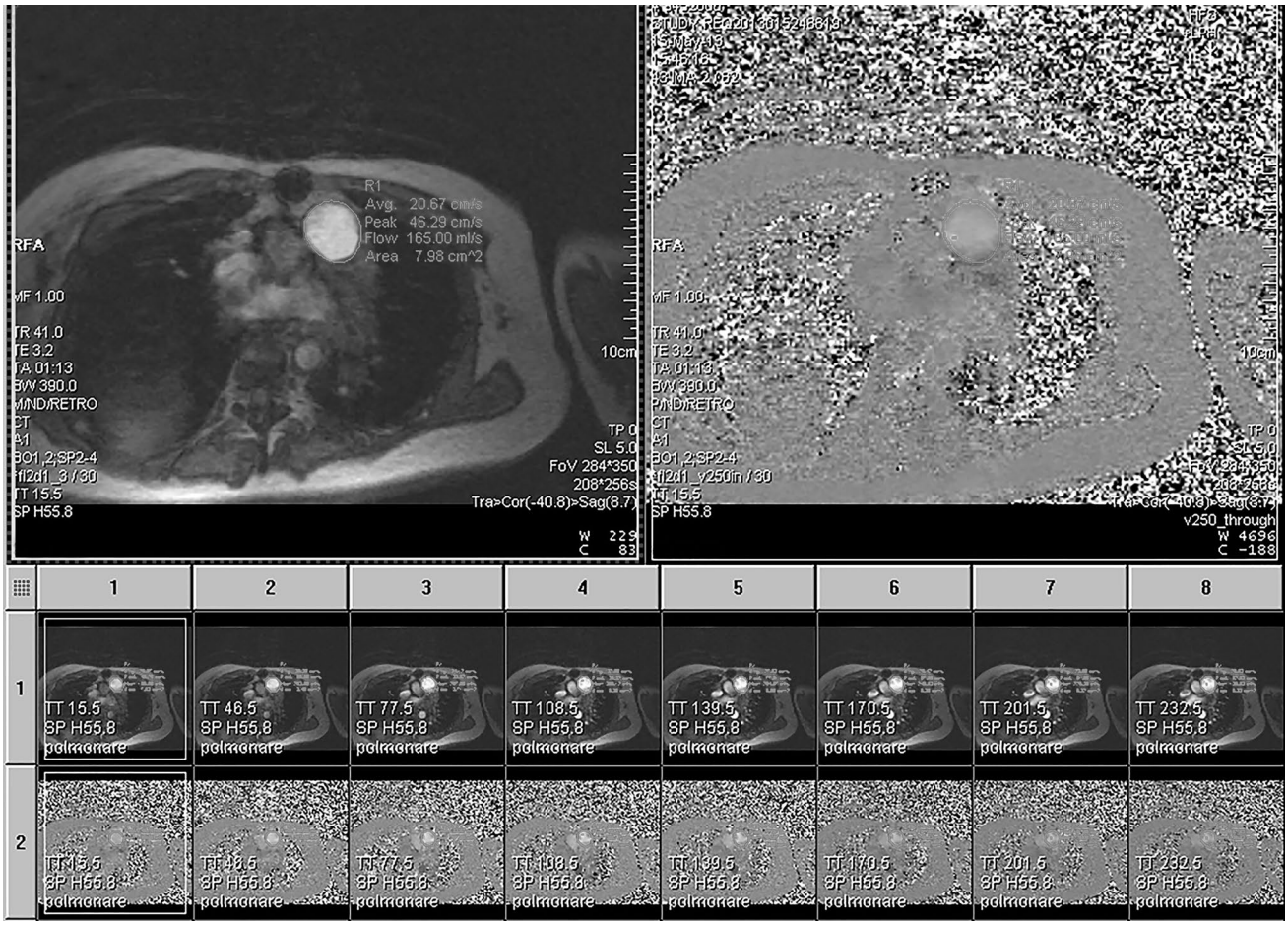

Fig. 1 Example of the segmentation of the pulmonary artery, showing the gradient echo image, with a region of interest *right* after the valve, and the phase velocity map with the same ROI

Germany). For each patient, the reader positioned a region of interest on the vessel boundary of a selected slice and propagated the segmentation through the remaining slices. Then, the software proposed an automated adjustment and the reader was allowed to manually correct the adjusted contours (hence semi-automated method). Blood peak velocity, forward and backward flows were obtained. An example of flow analysis is shown in Fig. 1.

Intra- and inter-reader reproducibility was estimated using the Bland–Altman method; for the inter-reader reproducibility the first measurement of both readers was used. The coefficient of repeatability (CoR) was calculated as 1.96 × standard deviation of differences of the two compared datasets. Reproducibility was reported as complement to 100% of the ratio between the CoR and the mean. Bland–Altman graphs were plotted as well, showing bias (mean of the differences of the two compared datasets), and 95% limits of agreement (bias ± CoR).

Results

Of 50 analyzed patients, 46 (92%) had a pulmonary disease, two (4%) ventricular septal defect, one (2%) aortic insufficiency, and one (2%) truncus arteriosus. Further details are reported in Table 1.

Image analysis was feasible in all patients and no malformations or artifacts prevented from a correct segmentation. The PC sequence showed no artifacts in patients with a surgical or percutaneous valve replacement. The time needed for measurement was about 5 min per patient, without substantial difference between the two readers.

The mean blood peak velocity of the aortic flow measured by R1 was 103 cm/s, accompanied by a CoR of 1 cm/s, corresponding to an intra-reader reproducibility of 99%; the same data for R2 were 103 cm/s, 9 cm/s, and 92%. The mean blood peak velocity of the pulmonary flow measured by R1 was 180 cm/s, accompanied by a CoR of 1 cm/s,

Table 2 Intra-reader reproducibility of the first reader

	Aortic flow			Pulmonary flow		
	Peak velocity (cm/s)	Forward (ml/beat)	Backward (ml/beat)	Peak velocity (cm/s)	Forward (ml/beat)	Backward (ml/beat)
Mean	103	69	3	180	91	23
Bias	−0.1	−0.1	−0.1	0.1	0.1	0.3
CoR	1	3	1	1	8	2
Reproducibility	99%	95%	49%	99%	91%	90%

The first reader was a radiology resident (see text)

CoR coefficient of repeatability

Table 3 Intra-reader reproducibility of the second reader

	Aortic flow			Pulmonary flow		
	Peak velocity (cm/s)	Forward (ml/beat)	Backward (ml/beat)	Peak velocity (cm/s)	Forward (ml/beat)	Backward (ml/beat)
Mean	103	69	3	181	89	23
Bias	−0.6	0.7	−0.2	−0.3	1.5	0.1
CoR	9	6	2	3	12	3
Reproducibility	92%	91%	38%	98%	86%	87%

The second reader was a technician student (see text)

CoR coefficient of repeatability

corresponding to an intra-reader reproducibility of 99%; the same data for R2 were 181 cm/s, 3 cm/s, and 98%. Further details are reported in Table 2 for R1 and in Table 3 for R2, while Bland–Altman plots for R1 only are shown in Fig. 2.

The inter-reader reproducibility analysis of the aortic flow peak velocity showed a CoR of 10 cm/s, over a mean of 103 cm/s, corresponding to an inter-reader reproducibility of 91%; the same data for the pulmonary flow were 7 cm/s, 180 cm/s, and 96%. Further details regarding the inter-reader reproducibility are reported in Table 4, while Bland–Altman plots are shown in Fig. 3.

Discussion

Cardiac magnetic resonance has emerged as a reliable imaging technique for assessing heart valve disease, quantify its severity, and to evaluate its effect on the heart morphology and function [1–3, 7]. It is used for evaluating cardiomyopathy-related valve dysfunction since more than two decades [18]. Patient management using CMR includes follow-up for treatment effect monitoring or disease progression [19, 20].

Reproducibility means the ability of a reader to provide the same values when repeating the measurement a number of times. If two or more readers are involved in the patient management, they need to provide as similar as possible results when analyzing a given CMR examination. When a follow-up measurement is performed on a patient, the clinician needs to identify a true change that can be ascribed to treatment effect or worsening of disease, rather than to measurement errors [21]. In this scenario, the readers' experience may play a role and skilled operators may be necessary.

In this study, we obtained a good-to-excellent intra-reader reproducibility of CMR in flow measurement for all variables under consideration, except for the backward flow of the ascending aorta. Indeed, intra-reader reproducibility was higher than 90% for the trained reader (R1) and higher than 86% for the lower trained reader (R2). Such a good result may be due thanks to the semi-automated method used for segmentation that is not difficult to be used also by less experienced readers [9]. This means that a reader's learning curve should be short and that the segmentation of vessel boundaries through a semi-automated method may also be performed by not highly specialized personnel. Probably, if we had used a manual method of segmentation we could have found a lower reproducibility for the untrained reader. However, although of a small magnitude, data suggest an additional reproducibility of R1 over R2, likely due to the different educational background and the different level of training [9].

Inter-reader reproducibility, even if reaching a maximum of 96% for the blood peak velocity of the pulmonary artery, decreased to 75 and 82% for the forward and backward flow of the pulmonary artery, respectively, being lower than

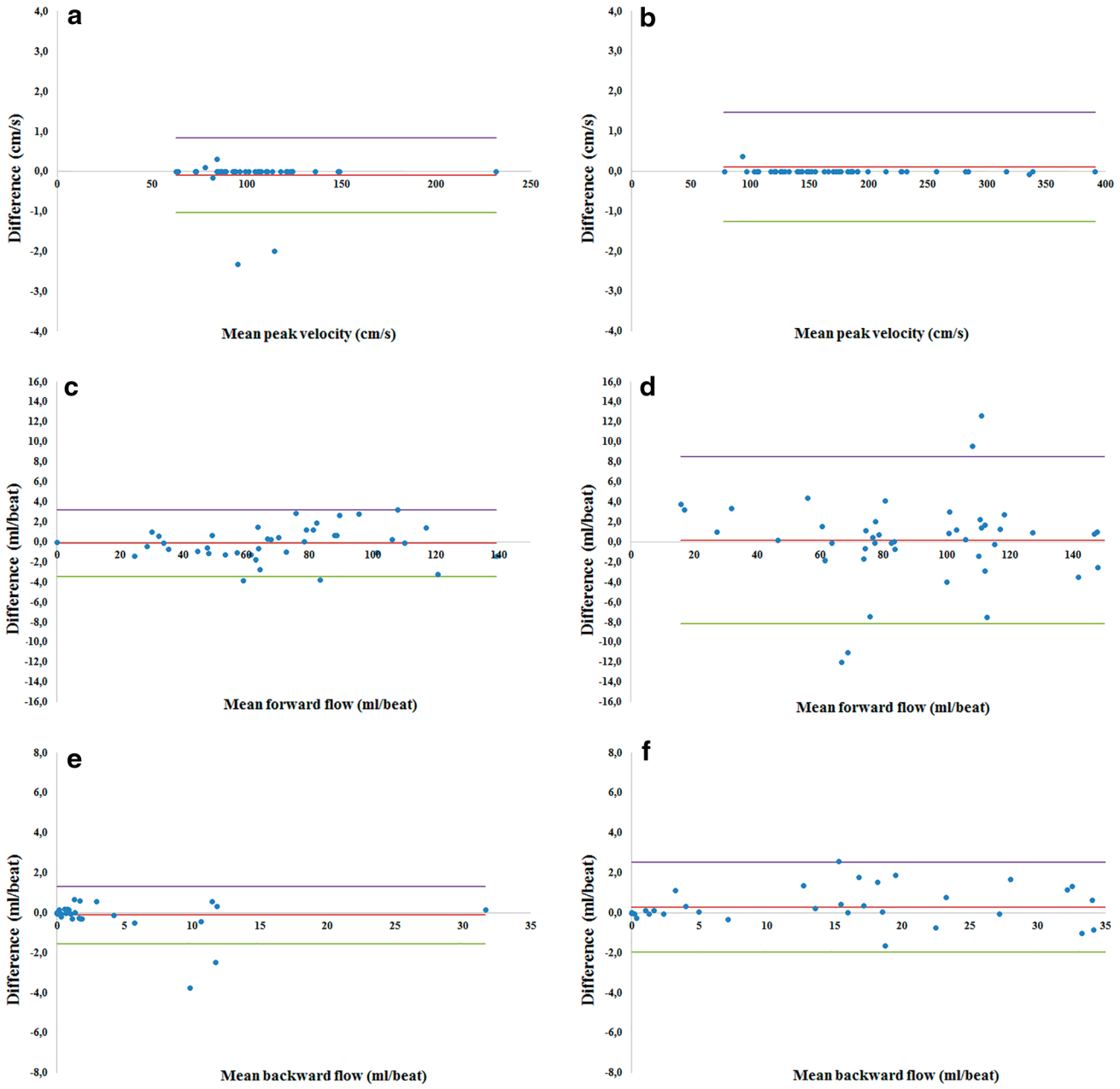

Fig. 2 *Bland–Altman plots* for intra-reader reproducibility analysis of the first reader: **a** and **b** peak velocity, **c** and **d** forward flow and **e** and **f** backward flow of the aorta (left column) and pulmonary artery (right column)

Table 4 Inter-reader reproducibility analysis

	Aortic flow			Pulmonary flow		
	Peak velocity (cm/s)	Forward (ml/beat)	Backward (ml/beat)	Peak velocity (cm/s)	Forward (ml/beat)	Backward (ml/beat)
Mean	103	70	3	180	89	24
Bias	0.1	2.3	0.2	−1.0	0.1	0.6
CoR	10	11	2	7	22	4
Reproducibility	91%	85%	20%	96%	75%	82%

CoR coefficient of repeatability

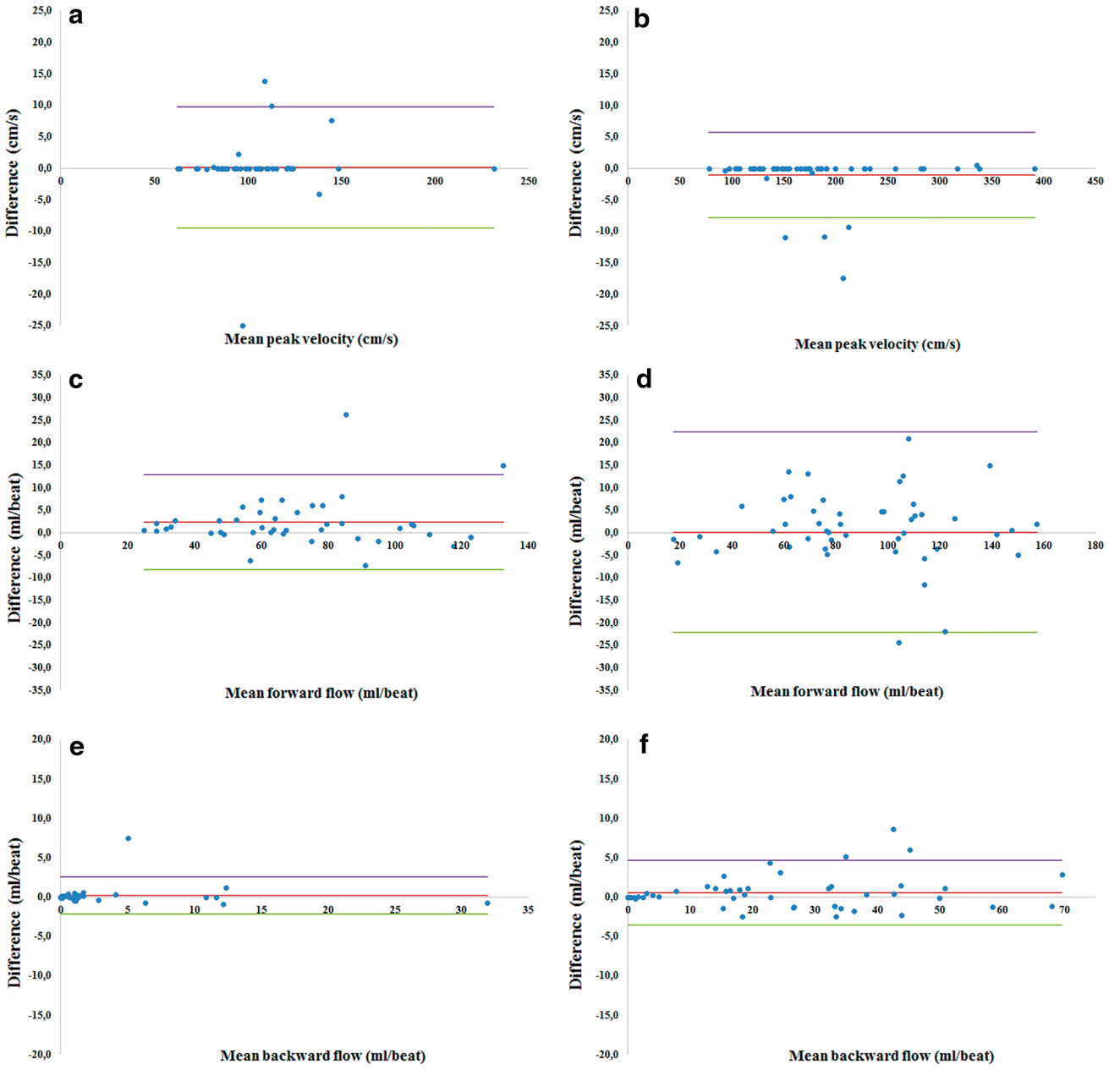

Fig. 3 *Bland–Altman plots* for inter-reader reproducibility analysis: **a** and **b** peak velocity, **c** and **d** forward flow and **e** and **f** backward flow of the aorta (left column) and pulmonary artery (right column)

that observed in previous studies. Van Der Geest et al. compared an automated contour detection algorithm for analysis of the ascending aorta flow with a fully manual segmentation, showing intra- and inter-reader variability lower than 2% for both manual and automated methods [13]. Conversely, Herment et al. demonstrated a higher inter-reader variability for manual tracing than for automated segmentation using PC CMR images in healthy volunteers and in patients with a dilated aorta [14].

The backward flow of the ascending aorta deserves some considerations. In fact, a low to very low reproducibility for this variable was obtained, being lower than 50% for the intra-reader analysis and equal to 20% for the inter-reader analysis. This is only an apparently negative result being mainly related to the low magnitude of the ascending aorta backward flow, even in patients with aortic insufficiency. Reproducibility being given as percentage of the mean, even subtle measurement variations due to small

differences in segmentation may have a strong negative impact on reproducibility.

The major limitation of this study is that results are related to the particular 1.5-T unit used for imaging patients and to the sequences and technical parameters used, also including the use of breath-hold or respiratory gating for avoiding artifacts from respiratory movements. However, 1.5-T magnets are mostly used for cardiac imaging and our imaging protocol is quite generally accepted. Thus, our results should be generalizable. Another limitation may be the study population that included patients affected with different cardiovascular diseases (even if the majority of patients had a Tetralogy of Fallot) who had a pathology of the aortic and/or pulmonary valve. However, we wanted to estimate the intra- and inter-reader reproducibility in a heterogeneous population for a higher generalizability. Probably, limiting to a more homogeneous population could demonstrate an even higher reproducibility.

In conclusion, this study showed a good-to-excellent intra- and inter-reader reproducibility of blood flow measurements in patients with congenital heart disease using CMR and a semi-automated method of segmentation, with a limited impact of the operator's training.

Compliance with ethical standards

Conflict of interest F. Secchi and G. Di Leo have been sponsored to congresses by Bracco Imaging SpA (Milan, Italy). F. Sardanelli is on the speaker's bureau for Bracco Imaging SpA (Milan, Italy) and received research Grants from Bayer Healthcare (Berlin, Germany).

Ethical statement The ethics committee approval was obtained for this retrospective study.

Funding This research received no specific Grant from any funding agency in the public, commercial, or not-for-profit sectors.

References

1. Francone M, Di Cesare E, Cademartiri F et al (2014) Italian registry of cardiac magnetic resonance. Eur J Radiol 83:15–22
2. Cawley PJ, Maki JH, Otto CM (2009) Cardiovascular magnetic resonance imaging for valvular heart disease: technique and validation. Circulation 119:468–478
3. Lopez-Mattei JC, Shah DJ (2013) The role of cardiac magnetic resonance in valvularheart disease. Methodist Debakey Cardiovasc J 9:142–148
4. Di Cesare E, Cademartiri F, Carbone I et al (2012) Clinical indications for the use of cardiac MRI. By the SIRM study group on cardiac imaging. Radiol Med 118:752–798
5. American College of Cardiology, American Heart Association Task Force on Practice Guidelines (Writing Committee to revise the 1998 guidelines for the management of patients with valvular heart disease), Society of Cardiovascular Anesthesiologists, Bonow RO, Carabello BA, Chatterjee K et al (2006) ACC/AHA 2006 guidelines for the management of patients with valvular heart disease: a report of the american college of cardiology/american heart association task force on practice guidelines (writing committee to revise the 1998 guidelines for the management of patients with valvular heart disease) developed in collaboration with the society of cardiovascular anesthesiologists endorsed by the society for cardiovascular angiography and interventions and the society of thoracic surgeons. J Am Coll Cardiol 48:e1 148
6. Gatehouse PD, Keegan J, Crowe LA et al (2005) Applications of phase-contrast flow and velocity imaging in cardiovascular MRI. Eur Radiol 15:2172–2184
7. Secchi F, Di Leo G, Papini GD et al (2011) Cardiac magnetic resonance: impact on diagnosis and management of patients with congenital cardiovascular disease. Clin Radiol 66:720–725
8. Secchi F, Iozzelli A, Papini GD et al (2009) MR imaging of aortic coarctation. Radiol Med 114:524–537
9. Sardanelli F, Quarenghi M, Di Leo G, Boccaccini L, Schiavi A (2008) Segmentation of cardiac cine MR images of left and right ventricles: interactive semiautomated methods and manual contouring by two readers with different education and experience. J Magn Reson Imaging 27:785–792
10. Thunberg P, Kähäri A (2011) Visualization of through-plane blood flow measurements obtained from phase-contrast MRI. J Digit Imaging 24:470–477
11. Saremi Farhood (2014) Cardiac CT and MR for adult and congenital heart disease. Springer, New York
12. Jung Bernd, Markl Michael (2012) Phase-contrast MRI and flow quantification. In: Car JC, Carroll TJ (eds) Magnetic resonance angiography. Springer, New York, pp 51–64
13. van der Geest RJ, Niezen RA, van der Wall EE, de Roos A, Reiber JH (1998) Automated measurement of volume flow in the ascending aorta using MR velocity maps: evaluation of inter- and intraobserver variability in healthy volunteers. J Comput Assist Tomogr 22:904–911
14. Herment A, Kachenoura N, Lefort M et al (2010) Automated segmentation of the aorta from phase contrast MR images: validation against expert tracing in healthy volunteers and in patients with a dilated aorta. J Magn Reson Imaging 31:881–888
15. Westenberg JJ, Danilouchkine MG, Doornbos J et al (2004) Accurate and reproducible mitral valvular blood flow measurement with three-directional velocity-encoded magnetic resonance imaging. J Cardiovasc Magn Reson 6:767–776
16. Henk CB, Grampp S, Backfrieder W, Liskutin J, Czerny C, Mostbeck GH (2003) Automated vessel edge detection in velocity-encoded cine-MR (VEC-MR) flow measurements: a retrospective evaluation in critically ill patients. Eur J Radiol 48:274–281
17. Groenink M, de Roos A, Mulder BJ, Spaan JA, van der Wall EE (1998) Changes in aortic distensibility and pulse wave velocity assessed with magnetic resonance imaging following beta-blocker therapy in the Marfan syndrome. Am J Cardiol 82:203–208
18. Sardanelli F, Molinari G, Petillo A et al (1993) MRI in hypertrophic cardiomyopathy: a morphofunctional study. J Comput Assist Tomogr 17:862–872
19. Secchi F, Resta EC, Piazza L et al (2014) Cardiac magnetic resonance before and after percutaneous pulmonary valve implantation. Radiol Med 119:400–407
20. Secchi F, Resta EC, Cannaò PM et al (2015) Four-year cardiac magnetic resonance (CMR) follow-up of patients treated with percutaneous pulmonary valve stent implantation. Eur Radiol 25:3606–3613
21. Di Leo G (2015) Measurements in radiology: the need for high reproducibility. Pediatr Radiol 45:32–34

Eur Radiol
https://doi.org/10.1007/s00330-017-5165-5

RADIOLOGICAL EDUCATION

To share or not to share? Expected pros and cons of *data sharing* in radiological research

Francesco Sardanelli[1,2] · **Marco Alì**[3] · **Myriam G. Hunink**[4,5] · **Nehmat Houssami**[6] · **Luca M. Sconfienza**[1,7] · **Giovanni Di Leo**[2]

Received: 1 August 2017 / Revised: 6 October 2017 / Accepted: 31 October 2017

Abstract

The aims of this paper are to illustrate the trend towards *data sharing*, i.e. the regulated availability of the original patient-level data obtained during a study, and to discuss the expected advantages (pros) and disadvantages (cons) of data sharing in radiological research. Expected pros include the potential for verification of original results with alternative or supplementary analyses (including estimation of reproducibility), advancement of knowledge by providing new results by testing new hypotheses (not explored by the original authors) on pre-existing databases, larger scale analyses based on individual-patient data, enhanced multidisciplinary cooperation, reduced publication of false studies, improved clinical practice, and reduced cost and time for clinical research. Expected cons are outlined as the risk that the original authors could not exploit the entire potential of the data they obtained, possible failures in patients' privacy protection, technical barriers such as the lack of standard formats, and possible data misinterpretation. Finally, open issues regarding data ownership, the role of individual patients, advocacy groups and funding institutions in decision making about sharing of data and images are discussed.

Key Points

- *Regulated availability of patient-level data of published clinical studies (data-sharing) is expected.*
- *Expected benefits include verification/advancement of knowledge, reduced cost/time of research, clinical improvement.*
- *Potential drawbacks include faults in patients' identity protection and data misinterpretation.*

Keywords Confidentiality · Database · Data sharing · Information dissemination · Radiology

Introduction

In clinical research, spontaneous *data sharing* is not yet as common as it is in other fields such as genetics, astronomy or physics [1]. However, the concept of data sharing has been suggested for many reasons, including the patient-centred nature of medical research and healthcare and the expectation

✉ Francesco Sardanelli
francesco.sardanelli@unimi.it

[1] Department of Biomedical Sciences for Health, Università degli Studi di Milano, Via L. Mangiagalli 31, 20133 Milan, Italy

[2] Radiology Unit, IRCCS Policlinico San Donato, Via Morandi 30, 20097 San Donato Milanese Milan, Italy

[3] PhD Course in Integrative Biomedical Research, Università degli Studi di Milano, Via L. Mangiagalli 31, 20133 Milan, Italy

[4] Departments of Radiology and Epidemiology, Erasmus University Medical Center, PO Box 2040, Rotterdam, The Netherlands

[5] Department of Health Policy and Medicine, Harvard School of Public Health, Harvard University, 677 Huntington Avenue, Boston, MA 02115, USA

[6] Screening and Test Evaluation Program, School of Public Health, Sydney Medical School, University of Sydney, Edward Ford Building, Room A27, Sydney, NSW 2006, Australia

[7] Unit of Diagnostic and Interventional Radiology, IRCCS Istituto Ortopedico Galeazzi, Via Riccardo Galeazzi 4, 20161 Milan, Italy

Published online: 18 January 2018

that knowledge from existing data should be maximized to benefit all stakeholders.

Although a transition to data sharing is a process that will take time and planning, those who adopt the principles and practices of open science will likely benefit from it [2, 3]. In addition, the emergence of data sharing as a potential requirement by some agencies and journals warrants attention by the imaging community. Indeed, from July 1st, 2018 the *International Committee of Medical Journal Editors* (ICMJE) will require a data sharing statement as a condition of consideration for publication of clinical trials [4].

In this article, we discuss potential advantages and disadvantages of data sharing.

From *open-access* to *data sharing*

A trend towards larger accessibility to scientific medical knowledge is already visible in the progressive tendency of medical journals in ensuring the *open-access* option, in which the authors or their institutions pay an article-level fee to guarantee the immediate free availability of their papers [5].

In Table 1 we report the policies of all the 18 general imaging journals on access and data sharing [6–17]. This was derived from the current Thomson Reuters list – Radiology, Nuclear Medicine, and Medical Imaging. For comparison, the 17 most-impacted general medicine journals were selected from the current Thomson Reuters list – Medicine, General and Internal [18–35]. Among the 18 imaging journals, four are open access, 12 offer open access as an option (*Radiology* provides free access 12 months after publication), and two do not offer an open-access option. Among the 17 medical journals, six are open access (*The Medical Journal of Australia* only for research articles and case reports), eight offer open access as an option (*Journal of the American Medical Association* [JAMA] provides free access 6 months after publication), two do not offer an open access option, and one (*The New England Journal of Medicine* [NEJM]) provides free access to research articles 6 months after publication. Thus, the open access option is currently widely adopted by both general imaging journals (11/18) and general medicine journals (8/17).

The practice of data sharing entails much more than open access. It is the *regulated availability of the original participant-by-participant data obtained during a study, which may include data not yet analysed.* Among the 18 general imaging journals, data sharing is not even mentioned by 12 journals, encouraged by three, mandatory only upon request in two, and requested by one. Among the 17 general medicine journals, it is not mentioned by seven journals, encouraged by six, requested by three (NEJM only for data obtained by microarray), and considered mandatory only upon request by one (Table 1). In practice, data repository or sharing is currently not mentioned in the instructions for authors of the majority of general imaging journals (14/18) and major general medicine journals (10/17). Despite individual journals do not mention any policy on data sharing, some publishers such as Elsevier have their own general suggestions, which refer to Open Access [8], even though not immediately visible to the authors when they submit a manuscript. When data sharing is encouraged, authors are informed they should be prepared to provide original study data if requested by the editors.

In recent years, several funding bodies declared the necessity for data sharing. In 2015, the U.S. National Institutes of Health (NIH) expressed its intention to request making the digital data from NIH-funded studies publicly available [36]. Regulatory agencies, specifically the European Medicines Agency, have requested greater data sharing by companies manufacturing drugs and clinical devices. Influential organizations such as the World Health Organization and the U.S. National Academy of Medicine published reports asking for responsible sharing of data from clinical trials [37]. Also, several foundations, for instance the Alfred P. Sloan Foundation [38], the Bill and Melinda Gates Foundation [39], the Ford Foundation [40], the Gordon and Betty Moore Foundation [41], and the National Science Foundation [42], require data sharing and data management plans for all research grant proposals.

The pharmaceutical industry also plays a role in promoting data sharing. The *Yale University Open Data Access* (YODA) project [43] performs independent scientific review of investigators' requests for pharmaceutical and medical data from clinical trials on devices marketed by Johnson & Johnson, including both full clinical study reports and participant-level data. Notably, the YODA project has obtained permission to make independent decisions about the release of Johnson & Johnson's clinical trial data. This project establishes a process in which requests are judged fairly and decisions are made by an independent academic partner, a model that could be applied to other fields of medicine [44].

Another example is the *Academic Research Organization Consortium for Continuing Evaluation of Scientific Studies – Cardiovascular* (ACCESS CV) [45]. They propose a secure method for sharing patient-sensitive data that combines the protection of patients' identity with the legitimate desire of the scientific community for data access and the viewpoint of the researchers who created the database. This approach consists of the following steps: (1) After publication of the primary results of a trial, researchers interested in the study data may send a request to the trial's publication committee; (2) Twenty-four months after the publication of the primary study, requests should be considered by a review group composed of members of ACCESS CV not involved in the trial, the trial principal investigator, a trial statistician, and a member of the data and safety monitoring board. This committee evaluates all proposals to approve those that are feasible,

Table 1 Policies on access and data repository or sharing by major general imaging journals and major general medicine journals

Journal	Access[1]	Data repository or sharing[2]
General imaging journals		
Acad Radiol	Open access option	Not mentioned
Acta Radiol	Open access option	Requested
Am J Roentgenol	No open access option	Not mentioned
BMC Med Imaging	Open access	Encouraged
Br J Radiol	Open access option. Articles freely available more than 12 months after publication	Encouraged
Clin Radiol	Open access option	Not mentioned
Eur J Radiol	Open access option	Not mentioned
Eur Radiol	Open access option	Not mentioned
Invest Radiol	Open access option	Not mentioned
Iran J Radiol	Open access	Not mentioned
J Am Coll Radiol	Open access option	Not mentioned
JBR-BTR	Open access	Not mentioned
Jpn J Radiol	No open access option	Upon request
Korean J Radiol	Open access	Not mentioned
Radiol Med	Open access option	Encouraged
Radiologe	Open access option	Not mentioned
Radiology	Open access option. Articles freely available 12 months after publication	Upon request
Rofo	Open access option	Not mentioned
General medicine journals		
Am J Med	Open access option	Not mentioned
Ann Intern Med	No open access option	Encouraged
BMC Medicine	Open access	Encouraged
Br J Gen Pract	Open access option	Not mentioned
Br Med Bull	Open access option	Not mentioned
BMJ	Open access option	Encouraged
BMJ Open	Open access	Encouraged
CMAJ	Open access option	Requested only for clinical trials of drugs and medical devices
Dtsch Arztebl Int	Open access	Not mentioned
Eur J Clin Invest	Open access option	Encouraged
Int J Med Sci	Open access	Not mentioned
Lancet	Open access option	Encouraged
JAMA	Open access option. Research articles freely available 6 months after publication	Upon request
Med Clin North Am[3]	No open access option	Not mentioned
Med J Aust	Open access for research articles and case reports	Not mentioned
New England J Med	Original articles and special articles freely available 6 months after publication.	Requested for data obtained by microarray
PLoS Med	Open access	Requested

Note: Imaging journals were selected for being general (not subspecialty) journals from the Thomson Reuters list – Radiology, Nuclear Medicine, and Medical Imaging (n=18). For comparison, the general medicine journals from the first quartile were selected from the Thomson Reuters list – Medicine, General and Internal (n=17)

[1] Most journals offer free accessibility for selected articles

[2] Despite individual journals do not mention any policy on data sharing, some publishers (e.g. Elsevier) have their own general rules to which refer to. Moreover, when data sharing is encouraged, authors are informed to be prepared to provide original study data if requested by the editors

[3] Publishes only invited reviews

hypothesis-based, non-duplicative, and guided by investigators with technical capability and a plan for publication. The period of 24 months is chosen to secure the database and to allow the original investigators to perform their own preplanned secondary analyses; (3) All requests and subsequent decisions will be posted on an ACCESS CV Web portal, ideally within 60 days [45].

In the field of radiology, data sharing also means accessibility to medical images. Indeed, "Images are more than pictures, they are data" [46]. This implies access to the images produced in a given study for additional reading, interpretation, and extraction. To this end, several image repositories were created. An example is the XNAT Central [47, 48], a publicly accessible data repository based on the XNAT open-source platform which hosts a wide variety of research imaging datasets, especially from neuroimaging, but also from oncology, orthopaedics and cardiology. Other examples are *The Cancer Imaging Archive* [49] and the *Lung Image Database Consortium* [50].

Such repositories may be very helpful in several fields, especially for image biomarker development, radiomics and machine learning, each field demanding different approaches. Moreover, the integration, standardization and analysis of these data poses a big challenge, the solution to which may be addressed using cognitive computing. An example of cognitive computing is the system developed by IBM named Watson (IBM Watson Health Imaging, Armonk, NY, USA). It strives to organize available information and present it in a contextually relevant, probability-driven manner to assist healthcare professionals in an objective manner, whether at a reading workstation or at the point-of-care [51]. An important change is underway. To make datasets from medical research publicly available in a timely fashion requires regulations that maximize the benefits and minimize the risks [52, 53]. Indeed, data sharing provides a potential for stimulating new ideas, avoiding duplication of trials, and enhance transparency [36, 54–57] as well as increasing collaboration and interdisciplinary research [1, 58, 59]. However, at the same time, sharing clinical data presents some risks, burdens and challenges such as the need to preserve the privacy of patients, to defend the legitimate economic interests of the sponsors, and to guard against invalid secondary analyses potentially undermining trust in clinical trials or otherwise harming public health [36, 37, 53, 60].

Potential benefits of data sharing

These can be subdivided into: (i) *verification and advancement in knowledge*; (ii) *reduced cost and time for clinical research*; and (iii) *clinical improvement* (Fig. 1).

Verification and advancement in knowledge

The first potential implication of data-sharing is the *verification by independent authors* of the results presented in a given publication. When data are shared, they may be used by other researchers to perform *alternative or supplementary analyses*. This 'second-hand' analysis may show results in support of the initial findings or could reveal errors or inconsistencies in the original research, or could identify issues needing extended analysis.

In other cases, data sharing can allow elucidation of *new results*. New findings can be disclosed starting from hypotheses not considered by the original study team. New insights can be presented from existing data but not yet analysed in the original publication(s). Also, investigators may be interested in *performing the analysis of datasets coming from various sources to enhance precision*, i.e. to perform reproducibility analyses across different databases, regarding established theories or new hypotheses. In fact, reproducibility analysis is crucial for emergent topics in radiology such as standardization of imaging biomarkers, especially from magnetic resonance imaging [61]. The availability of databases from different studies could allow for this gap to be filled and could help in translating new imaging biomarkers into clinical practice [62]. In this regard, reproducibility analysis could become one of the main advantages of data sharing.

The introduction of *registries of patients affected with a defined disease* could be considered a primitive form of data sharing [63, 64], important not only for widespread diseases, such as cancers, but especially for rare diseases.

Another approach of spontaneous data sharing is that underlying *individual patient data meta-analyses* [65]. Authors of an individual patient data meta-analysis typically contact the authors of each eligible study asking to share their data, with the aim of creating a new unique individual-patient database. Of note, the power of the individual-patient data approach is higher than that of conventional (study-level) meta-analyses, which rely on complex statistical methods [66]. For instance, in a study published by Marinovich et al. [67] on the agreement between MRI and pathological breast tumour size after treatment, a total of 24 studies (1,228 patients) were eligible for inclusion, but only eight of these contributed to the individual-patient data analysis for a total of 300 patients. Had regulated data sharing been in place, that individual-patient data meta-analysis would have included a much richer dataset. Moreover, data sharing could boost a wider adoption of health technology assessment. Indeed, in the context of a new product evaluation, data sharing may be useful in the validation level, requiring a high number of data/images, rather than at the initial development level.

Another potential advantage of data sharing is *to reduce the publication of false studies*, especially when the data are intentionally falsified. Recently, 64 articles were retracted from

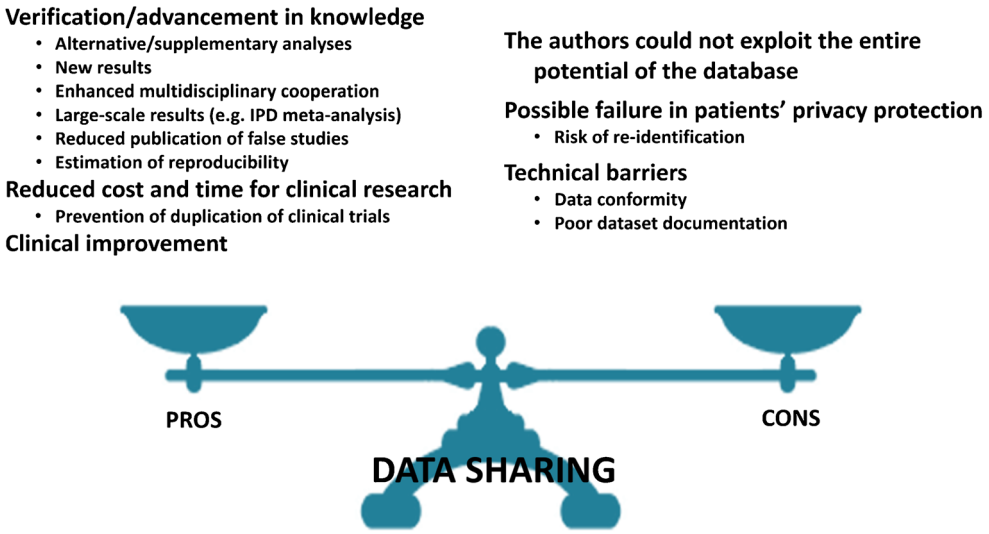

Fig. 1 Expected pros and cons of data sharing. *IPD* individual patient data meta-analyses

ten *Springer* journals after editorial checks found fake email addresses, and subsequent internal investigations uncovered fabricated peer-review reports [68]. This retraction came only a few months after *BioMed Central* had retracted 43 articles for the same reason; however, this phenomenon involved most major publishers such as also SAGE, Elsevier, Informa, and Lippincott Williams & Wilkins [69]. Data sharing might discourage data creation and manipulation, potentially more detectable in a complete database than in reported results.

Reduced cost and time for clinical research

Data sharing could potentially lead to an optimization of time and costs of clinical research by *preventing the duplication of trials* [70, 71]. For example, costs for the stipulation of insurances for patients' coverage, the purchase of materials or the salaries of the staff responsible for data collection can be avoided. In addition, using an existing shared database, the new results could be obtained many years prior to those derived from a new clinical study.

Clinical improvement

An effect in terms of clearer evidence on the safety and effectiveness of diagnostic procedures and therapies, improving public healthcare [72–74], may be considered the final aim of data sharing. To avoid the loss of findings contained in the original dataset and not used for the primary publication(s) could play a role in this direction [53]. Institutions sharing their data could obtain a more comprehensive picture about the benefits and risks of a medical decision. However, a real clinical improvement from data sharing is a hypothesis that still needs to be demonstrated.

Potential drawbacks from data sharing

The sharing of clinical databases raises several concerns (see Fig. 1). One of the reasons not to share data is that researchers are evaluated competitively, based on the quality and number of articles published during their career, so they may worry that other people will use their data and efforts to produce new publications. The potential for secondary analyses contradicting initially reported results may be a deterrent. Authors may not be willing to share data that had cost them great effort and resources. However, reciprocally, they would also directly benefit from using someone else's data.

Bierer et al. [75] recently suggested formalizing 'data authorship' as an incentive to data sharing: "as a matter of fairness and as a matter of providing an incentive for data sharing, the persons who initially gathered the data should receive appropriate and standardized credit that can be used for academic advancement, for grant applications, and in broader situations".

Another concern is the potential for fault in the patient identity protection caused by the transmission of sensitive information. Data must be de-identified: *de-identification*, not simply anonymization, consists of transforming a dataset so that the back identification of individuals becomes impossible or extremely difficult. Different regulations may require different degrees of de-identification, particularly in the absence of informed consents specifying the possibility of data sharing. De-identification can be achieved with different types of data transformations that must ensure patient privacy without affecting data quality [76]. However, the de-identified data do not eliminate all risks of re-identification. Moreover, the reduction of this risk to zero may destroy or significantly impair the utility of the data for subsequent analysis or

verification. For these reasons, the stipulation of Data Use Agreements (DUAs) is considered a useful strategy and best practice for increasing the benefits and mitigating the risks of clinical data sharing [77]. Specifically, DUAs address important issues such as limitations on date usage, obligations to data safeguard, liability for harm arising from data usage and publication, and privacy rights that are associated with transfer of confidential or protected data. In contrast, the U.S. Office for Human Research Protections stated that there is no need for separate consent from trial participants for the sharing of de-identified data [4].

A limitation to the adoption of data sharing can originate from *technical barriers*. The image conformity is influenced by vendor, modality, and acquisition parameters on the one hand; and by image post-processing manufacturer, reconstruction parameters, and software versions, on the other hand. An example is represented by the use in magnetic resonance of arbitrary units that clearly depend on the specific vendor and model, making a between-study comparison impossible. A way to overcome this limitation could be a drastic standardization, with manufacturers defining new shared standards.

Another intrinsic barrier to data sharing could be the *poor documentation of datasets*, especially if not documented in English. Moreover, important information about methodology might not be contained immediately in the database or immediately retrievable. All these issues should be considered when planning for potential data sharing of research.

To share or not to share?

In conclusion, in a world that moves towards greater transparency and privacy protection, data sharing stands between these two competing interests. Not all concerns on data sharing have already been solved and many questions remain to be addressed: Who is the rightful owner of the data? What is the role of individual patients and advocacy groups in decision making about sharing of data and images? Should Ethics Committees change their approach for study approval? And how? What is the exact role of institutions, especially public ones, that funded the original study? Should patient advocacy groups and funding organizations be involved in decision making about data sharing? These issues must be regulated.

Despite all the above-described issues relating to data sharing, a transition to a more open medical science has begun. If benefits of data sharing will be more and more perceived as prevailing over harms therefrom, this option will win. Researchers and institutions who first seize this opportunity will be on the wave-front of an innovation likely to be in favour of patients and public health. Radiologists should be kept informed of this emerging issue. It is time to share!

Acknowledgements This article has been promoted by the European Network for Assessment of Imaging in Medicine, a joint initiative of the European Institute for Biomedical Imaging Research (http://www.eibir.org/scientific-activities/joint-initiatives/euroaim/)

Funding This article was supported by local research funds of the IRCCS Policlinico San Donato, a Clinical Research Hospital partially funded by the Italian Ministry of Health.

Compliance with ethical standards

Guarantor The scientific guarantor of this publication is prof. Francesco Sardanelli.

Conflict of interest The authors of this manuscript declare no relationships with any companies whose products or services may be related to the subject matter of the article.

Statistics and biometry No complex statistical methods were necessary for this paper.

Informed consent This study is not on human subjects

Ethical approval Institutional Review Board approval was not required because this is an editorial article.

Methodology This is an editorial article

References

1. Ross JS, Lehman R, Gross CP (2012) The importance of clinical trial data sharing: toward more open science. Circ Cardiovasc Qual Outcomes 5:238–240
2. Boulton G, Rawlins M, Vallance P, Walport M (2011) Science as a public enterprise: the case for open data. Lancet 377:1633–1635
3. Walport M, Brest P (2011) Sharing research data to improve public health. Lancet (London, England) 377:537–539
4. Taichman DB, Sahni P, Pinborg A et al (2017) Data sharing statements for clinical trials—A requirement of the International Committee of Medical Journal Editors. N Engl J Med 376:2277–2279
5. Sconfienza LM, Sardanelli F (2013) Radiological journals in the online world: should we think open? Eur Radiol 23:1175–1177
6. RSNA open access policy. Radiological Society of North America web site. http://pubs.rsna.org/page/openaccess. Accessed 29 July 2017
7. Publish open access with Springer. Springer web site. http://www.springer.com/de/open-access. Accessed 29 July 2017
8. Open access. Elsevier web site. https://www.elsevier.com/about/open-science/open-access. Accessed 29 July 2017
9. Online submission and review system. Investigative Radiology web site. http://edmgr.ovid.com/ir/accounts/ifauth.htm. Accessed 29 July 2017
10. American Journal of Roentgenology web site. http://www.ajronline.org/. Accessed 29 July 2017
11. Acta Radiologica open submission guidelines. SAGE Publishing web site. https://us.sagepub.com/en-us/nam/acta-radiologica-open/journal202176#description. Accessed 29 July 2017
12. Open access policy. The British Institute of Radiology web site. http://www.birpublications.org/page/oapolicy. Accessed 29 Jul 2017

13. Guidelines for authors. Rofo-Fortschr Rontg web site. http://roefo.thieme.de/documents/10157/18614/RoeFo-Autorenhinweise_Englisch-2017.pdf/ef85bdcc-03d3-41d4-8088-215c16528db9. Accessed 29 July 2017
14. BioMed Central Medical Imaging web site. https://bmcmedimaging.biomedcentral.com/about. Accessed 29 July 2017
15. Publication instructions for authors. Korean Journal of Radiology web site. https://www.kjronline.org/index.php?body=Instruction. Accessed 29 July 2017
16. Open access statement. Iranian Journal of Radiology web site. http://iranjradiol.com/?page=public_pages&name=Open Access Statement. Accessed 29 July 2017
17. Journal of the Belgian Society of Radiology web site. http://www.jbsr.be/about/. Accessed 29 July 2017
18. The New England Journal of Medicine web site. http://www.nejm.org/page/about-nejm/history-and-mission. Accessed 29 July 2017
19. Information for authors. The Lancet web site. http://thelancet.com/lancet/information-for-authors/open-access. Accessed 29 July 2017
20. Instruction for authors. Journal of the American Medical Association web site. http://jamanetwork.com/journals/jama/pages/instructions-for-authors#SecPublicAccess. Accessed 29 July 2017
21. Information for authors. Annals of Internal Medicine web site. http://annals.org/aim/pages/authors. Accessed 29 July 2017
22. Resources for authors. British Medical Journal web site. http://www.bmj.com/about-bmj/resources-authors. Accessed 29 July 2017
23. Why publish with PLOS Medicine? PLoS Medicine web site. http://journals.plos.org/plosmedicine/s/why-publish-with-plos-medicine. Accessed 29 July 2017
24. Fees and funding. BioMed Central Medicine web site. http://bmcmedicine.biomedcentral.com/submission-guidelines/fees-and-funding. Accessed 29 July 2017
25. The American Journal of Medicine open access option. Elsevier web site. https://www.elsevier.com/journals/the-american-journal-of-medicine/0002-9343/open-access-options. Accessed 29 July 2017
26. CMAJ Open. Canadian Medical Association Journal Open web site. http://cmajopen.ca/site/misc/about.xhtml. Accessed 29 July 2017
27. Deutsches Arzteblatt International web site. https://www.aerzteblatt.de/int/about-us. Accessed 29 July 2017
28. MJA Open. Medical Journal of Australia web site. https://www.mja.com.au/open. Accessed 29 July 2017
29. Open access. Oxford Academic web site. https://academic.oup.com/journals/pages/open_access. Accessed 29 July 2017
30. BJGP editorial process & policies. British Journal of General Practice web site. http://bjgp.org/authors/bjgp-editorial-process-and-policies. Accessed 29 July 2017
31. OnlineOpen. Wiley Author Services web site. https://authorservices.wiley.com/author-resources/Journal-Authors/licensing-and-open-access/open-access/onlineopen.html. Accessed 29 July 2017
32. BioMed Central web site. https://www.biomedcentral.com/about. Accessed 29 July 2017
33. British Medical Journal Open web site. http://bmjopen.bmj.com/pages/about/. Accessed 29 July 2017
34. Medical Clinics of North America open access option. Elsevier web site. https://www.elsevier.com/journals/medical-clinics-of-north-america/0025-7125/open-access-options. Accessed 29 July 2017
35. Instruction for authors. International Journal of Medical Sciences web site. http://www.medsci.org/ms/author. Accessed 29 July 2017
36. Collins FS, Tabak LA (2014) Policy: NIH plans to enhance reproducibility. Nature 505:612–613
37. Sharing clinical trial data: maximizing benefits, minimizing risk - PubMed - NCBI. https://www.ncbi.nlm.nih.gov/pubmed/25590113. Accessed 18 Jan 2017
38. Grants. Alfred P. Sloan Foundation web site. https://sloan.org/grants/apply#tab-grant-proposal-guidelines/. Accessed 1 April 2017
39. Open access policy. Bill and Melinda Gates Foundation web site. http://www.gatesfoundation.org/how-we-work/general-information/open-access-policy. Accessed 1 April 2017
40. Ford Foundation expands Creative Commons licensing for all grant-funded projects. Ford Foundation web site. https://www.fordfoundation.org/the-latest/news/ford-foundation-expands-creative-commons-licensing-for-all-grant-funded-projects/. Accessed 1 April 2017
41. Data sharing philosophy. Gordon and Betty Moore Foundation web site. https://www.moore.org/docs/default-source/Grantee-Resources/data-sharing-philosophy.pdf. Accessed 1 April 2017
42. Dissemination and sharing of research results. National Science Foundation web site. https://www.nsf.gov/bfa/dias/policy/dmp.jsp. Accessed 1 April 2017
43. Krumholz HM, Waldstreicher J (2016) The Yale Open Data Access (YODA) project — A mechanism for data sharing. N Engl J Med 375:403–405
44. Krumholz HM, Ross JS (2011) A model for dissemination and independent analysis of industry data. JAMA 306:1593–1594
45. Academic Research Organization Consortium for Continuing Evaluation of Scientific Studies–Cardiovascular (ACCESS CV), Patel MR, Armstrong PW, Bhatt DL et al (2016) Sharing data from cardiovascular clinical trials—A Proposal. N Engl J Med 375:407–409
46. Gillies RJ, Kinahan PE, Hricak H (2016) Radiomics: images are more than pictures, they are data. Radiology 278:563–577
47. Herrick R, Horton W, Olsen T et al (2016) NeuroImage XNAT central: open sourcing imaging research data. NeuroImage 124:1093–1096
48. XNAT web site. https://www.xnat.org/about/. Accessed 13 April 2017
49. Clark K, Vendt B, Smith K et al (2013) The Cancer Imaging Archive (TCIA): maintaining and operating a public information repository. J Digit Imaging 26:1045–1057
50. Armato SG, McLennan G, Bidaut L et al (2011) The Lung Image Database Consortium (LIDC) and Image Database Resource Initiative (IDRI): a completed reference database of lung nodules on CT scans. Med Phys 38:915–931
51. Chen Y, Elenee Argentinis JD, Weber G (2016) IBM Watson: how cognitive computing can be applied to big data challenges in life sciences research. Clin Ther 38:688–701
52. Loder E (2013) Sharing data from clinical trials: where we are and what lies ahead. BMJ 347:f4794–f4794
53. Mello MM, Francer JK, Wilenzick M et al (2013) Preparing for responsible sharing of clinical trial data. N Engl J Med 369:1651–1658
54. Anderson BJ, Merry AF (2009) Data sharing for pharmacokinetic studies. Paediatr Anaesth 19:1005–1010
55. Gøtzsche PC (2011) Why we need easy access to all data from all clinical trials and how to accomplish it. Trials 12:249
56. Berlin JA, Morris S, Rockhold F et al (2014) Bumps and bridges on the road to responsible sharing of clinical trial data. Clin Trials 11:7–12
57. Peat G, Riley RD, Croft P et al (2014) Improving the transparency of prognosis research: the role of reporting, data sharing, registration, and protocols. PLoS Med 11:e1001671
58. Milia N, Congiu A, Anagnostou P et al (2012) Mine, yours, ours? Sharing data on human genetic variation. PLoS One 7:e37552
59. Lee ES, McDonald DW, Anderson N, Tarczy-Hornoch P (2009) Incorporating collaboratory concepts into informatics in support of

translational interdisciplinary biomedical research. Int J Med Inform 78:10–21
60. Antman E (2014) Data sharing in research: benefits and risks for clinicians. BMJ 348:g237
61. Sardanelli F (2017) Trends in radiology and experimental research. Eur Radiol Exp https://doi.org/10.1186/s41747-017-0006-5
62. Golay X (2017) The long and winding road to translation for imaging biomarker development: the case for arterial spin labelling (ASL). Eur Radiol Exp 3. https://doi.org/10.1186/s41747-017-0004-7
63. Grill JD, Holbrook A, Pierce A et al (2017) Attitudes toward potential participant registries. J Alzheimers Dis 56:939–946
64. Kasenda B, von Elm E, You J et al (2014) Prevalence, characteristics, and publication of discontinued randomized trials. JAMA 311: 1045–1051
65. Clarke MJ, Stewart LA (1997) Meta-analyses using individual patient data. J Eval Clin Pract 3:207–212
66. Phi X-A, Houssami N, Obdeijn I-M et al (2015) Magnetic resonance imaging improves breast screening sensitivity in BRCA mutation carriers age ≥50 years: evidence from an individual patient data meta-analysis. J Clin Oncol 33:349–356
67. Marinovich ML, Macaskill P, Irwig L et al (2015) Agreement between MRI and pathologic breast tumor size after neoadjuvant chemotherapy, and comparison with alternative tests: individual patient data meta-analysis. BMC Cancer 15:662
68. Retraction of articles from Springer journals. http://www.springer.com/gp/about-springer/media/statements/retraction-of-articles-from-springer-journals/735218. Accessed 12 March 2017
69. Qi X, Deng H, Guo X (2017) Characteristics of retractions related to faked peer reviews: an overview. Postgrad Med J 93:499–503
70. Rathi V, Dzara K, Gross CP et al (2012) Sharing of clinical trial data among trialists: a cross sectional survey. BMJ 345:e7570
71. Zarin DA (2013) Participant-level data and the new frontier in trial transparency. N Engl J Med 369:468–469
72. Farrar JT, Troxel AB, Haynes K et al (2014) Effect of variability in the 7-day baseline pain diary on the assay sensitivity of neuropathic pain randomized clinical trials: An ACTTION study. Pain 155: 1622–1631
73. Gabler NB, French B, Strom BL et al (2012) Validation of 6-minute walk distance as a surrogate end point in pulmonary arterial hypertension trials. Circulation 126:349–356
74. Gabler NB, French B, Strom BL et al (2012) Race and sex differences in response to endothelin receptor antagonists for pulmonary arterial hypertension. Chest 141:20–26
75. Bierer BE, Crosas M, Pierce HH (2017) Data authorship as an incentive to data sharing. N Engl J Med 376:1684–1687
76. Prasser F, Bild R, Kuhn KA (2016) A generic method for assessing the quality of de-identified health data. Stud Health Technol Inform 228:312–316
77. Barocas S, Nissenbaum H (2014) Big data's end run around anonymity and consent. In: Lane J, Stodden V, Bender S, Nissenbaum H (eds) Privacy, big data, and the public good. Cambridge University Press, New York, pp 44–75